JULY 1961

experimental mechanics

SEE PAGE 3

IN THIS ISSUE

PAGE

1 Model Investigations of Unstiffened and Stiffened Circular Shells

10 Damping Characteristics of Pipes Vibrating in Flexure and Filled with Various Materials

16 Structural Testing at High Temperatures

23 Twisting Stresses in Tape

33 Influence of Breadth in Bars with Reinforced Circular Holes Under Tension

39 On the Transverse-strain Sensitivity of Foil Gages

SESA JOURNAL OF THE SOCIETY FOR EXPERIMENTAL STRESS ANALYSIS

NEW!
BUDD FLEXAGAGE

(Pre-aligned double-deck pair of MetalFilm strain gages)

For the first time, a single gage that measures both bending and axial strain

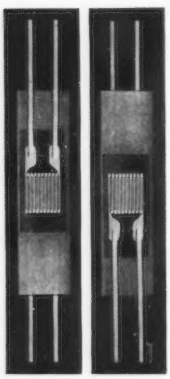

Mounts as a single, moisture-proof, calibrated gage *on one side of test surface.*

Eliminates difficult back-to-back gage mounting problems and need for pressure-proof lead wire installation, such as in pressure vessel analysis.

Makes possible bending strain analyses even on surfaces formerly considered inaccessible.

Separates bending strains from direct (tensile, membrane, hoop) strains . . . accurately measures both.

*Patent Pending

FOR FULL DETAILS, WRITE FOR NEW FLEXAGAGE BULLETIN

INSTRUMENTS Budd DIVISION

THE BUDD COMPANY • P.O. Box 245 • Phoenixville, Pa.

Consult your phone book for sales offices in: Atlanta, Ga.; Oak Park, Ill.; Detroit, Mich.; Seattle, Wash.; Dallas, Tex.; Los Angeles, Calif.

In Canada: Budd Instruments, Ltd., 170 Donway West, Don Mills, Ont.

Other Countries: Budd S.A., 10 Avenue de la Grande Armée, Paris 17e, France

Inaccessible interior? A single exterior-mounted Flexagage makes all your measurements!

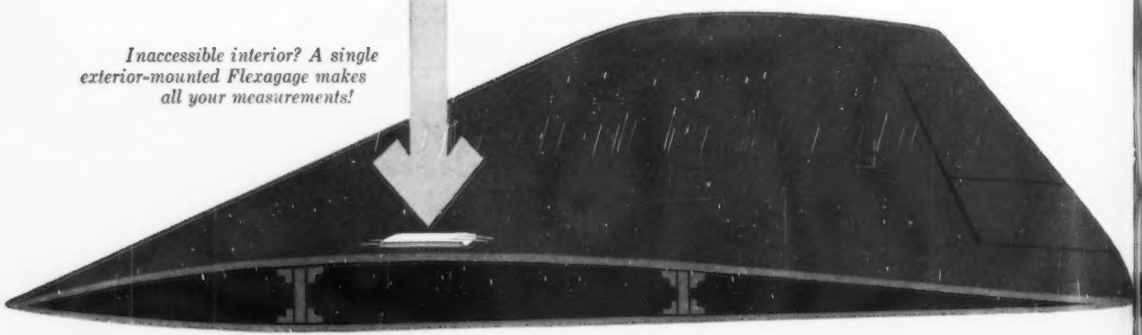

Other gages from Budd:

- MetalFilm electrical strain gages in a wide range of sizes, configurations and temperature compensations.
- PhotoStress Rosettes—the only gages that provide directly both orientation and separate magnitudes of principal strains.
- PhotoStress gages for unidirectional strain measurements, transducer applications, machine alignment and torque measurements.

For details, circle No. 1 on Reader Information Card

RNAL OF THE SOCIETY FOR EXPERIMENTAL STRESS ANALYSIS

experimental mechanics

VOLUME 1 • NUMBER 7 • JULY 1961

editor B. E. Rossi

asst. editor C. H. Willer

advertising D. L. Vidmark

art Gil Miller

OFFICERS AND EXECUTIVE COMMITTEE	JOURNAL ADVISORY COMMITTEE
D. C. Drucker, *president*	E. Wenk, Jr., *chairman*
I. Vigness, *vice-president*	D. C. Drucker
W. W. Soroka, *vice-president*	R. Guernsey, Jr.
W. M. Murray, *treasurer*	B. J. Lazan
B. E. Rossi, *executive secretary*	W. M. Murray
F. C. Bailey	C. C. Perry
B. J. Lazan	F. B. Stern, Jr.
J. C. New	I. Vigness
C. E. Taylor	
E. Wenk, Jr.	

ublished monthly by the Society for Experimental Stress Analysis. ublication office, 20th and Northampton Streets, Easton, Pa. Editorial nd general offices, 21 Bridge Square, Westport, Conn. Subscription 0.00 per year in the United States and Canada; foreign countries 2.00. Single copies, nonmembers $1.50; members $1.00. Second-class ostage paid at Easton, Pa. Copyright 1961 by the Society for Experimental Stress Analysis. The Society is not responsible for any statement made or opinion expressed in its publications. Permission is given to reprint any article after its date of publication provided credit is given and provided the copies are not intended for sale.

this month

TABLE OF CONTENTS

page

1 Model Investigations of Unstiffened and Stiffened Circular Shells
by W. T. Skene

10 Damping Characteristics of Pipes Vibrating in Flexure and Filled with Various Materials
by A. Ezzat

16 Structural Testing at High Temperatures
by L. Young

23 Twisting Stresses in Tape
by C. Mylonas and D. C. Drucker

33 Influence of Breadth in Bars with Reinforced Circular Holes Under Tension
by H. Shimada

39 On the Transverse-strain Sensitivity of Foil Gages
by J. H. Meier

3A Experimentally Speaking

4A Tracking Station

6A Personnel in the News

7A New Products

14A New Literature

17A Reader Information Card

18A Index to Advertisers

21A SESA News

25A Section Reports

26A From the Campus

SOCIETY FOR EXPERIMENTAL STRESS ANALYSIS
21 Bridge Square, Westport, Connecticut

SESA PUBLICATIONS

PROCEEDINGS OF THE SOCIETY FOR EXPERIMENTAL STRESS ANALYSIS

The PROCEEDINGS are a series of bound volumes comprised of the technical papers presented at National Meetings. These contain the results and descriptions of analytical and experimental investigations, as well as techniques for the measurement of mechanical strain. Published twice annually, they include up-to-date information on various phases of instrumentation. Currently available:

Volume III, No. 2
Volume IV, No. 1
Volume IV, No. 2
Volume V, No. 1
Volume XI, No. 2
Volume XII, No. 1
Volume XII, No. 2
Volume XIII, No. 1 (limited)
Volume XIII, No. 2 (limited)
Volume XV, No. 2
Volume XVI, No. 2
Volume XVII, No. 1
Volume XVII, No. 2

CUMULATIVE INDEX—PROCEEDINGS

Thirty-four books of the PROCEEDINGS have been published to date. This Index has been prepared to serve as an easy reference to any one of the 546 papers which have been published in the first thirty books. It consists of three parts: (1) chronological index, (2) author index, (3) topical index. It represents a "master reference file" to all PROCEEDINGS published, from Vol. I, No. 1 through Vol. XV, No. 2.

HANDBOOK OF EXPERIMENTAL STRESS ANALYSIS

This book opens with a thorough presentation of mechanical properties. It presents practical, usable information on: mechanical, electrical and optical gages, brittle coatings, photoelasticity, X-rays, service fractures, analogies, vibration measurements, theory of elasticity and precision of measurements. Stiff cloth binding—contains 1060 pages of text.

MANUAL ON EXPERIMENTAL STRESS ANALYSIS TECHNIQUES

For those who are new to the field of experimental stress analysis, the MANUAL introduces the fundamentals of experimental stress analysis in terms easily understood by the novice. It contains detailed instructions and, with the aid of illustrations and charts, elaborates on the application of three particular methods for determining stress: (1) SR-4 bonded wire strain gages, (2) stresscoat (brittle lacquer) and (3) photoelasticity.

STRAIN GAGE TECHNIQUES

Twenty-three chapters of lectures and laboratory experiments of special summer programs presented at leading universities, covering such topics as: fundamental concepts, selection of gages, basic considerations in strain-gage instrumentation, electrical and mechanical aspects of the gage system, the potentiometric circuit, the wheatstone bridge, amplitude modulation, fundamentals of measuring systems, some commercial systems and rosette analysis. Approximately 680 pages.

CATALOG OF EQUIPMENT USED IN EXPERIMENTAL STRESS ANALYSIS

The Catalog contains references to manufacturers of equipment, hardware and instrumentation used in the measurement of strain.

EXPERIMENTAL MECHANICS

Official monthly journal of the SESA. Includes technical papers and news items of interest to SESA members and to industry.

ORDER FORM

Publication	Author/s or Editor/s	Members' Price	Bulk Orders*	Price per Copy (Non members)	Postage and Handling (Add for Each Copy) U. S.	Postage and Handling (Add for Each Copy) Foreign	State Volume Number	Specify Quantity	Total
Proceedings of the Society for Experimental Stress Analysis	Mahlmann, CV and Murray, WM	$ 6.00	$ 6.00	$ 7.00	25¢	50¢	_____	_____	$_____
Handbook of Experimental Stress Analysis	Hetenyi, M.	16.75	16.75	17.75	Included	85¢		_____	$_____
Manual on Experimental Stress Analysis Techniques	Perry, CC and Bean, WT	2.00	1.25	3.00	Included	10¢		_____	$_____
Strain Gage Techniques	Murray, WM and Stein, PK	12.00	12.00	13.00	Included	85¢		_____	$_____
Catalog of Equipment	Hofmeister, WF	2.00	1.25	3.00	Included	10¢		_____	$_____
Cumulative Index		2.00	1.25	3.00	Included	10¢		_____	$_____
EXPERIMENTAL MECHANICS**	Monthly Journal	1.00		1.50	Included	20¢		_____	$_____

*Bulk Orders—10 or more copies of a *single book* (for *PROCEEDINGS*—10 or more copies of a single volume and number).
**Annual Subscription (including postage)—Domestic, $10; Foreign, $12.

Send books to:

_____

_____

_____

_____

Send bill to:

_____

_____

_____

_____

Total.....$_____
Remittance Enclosed ☐ Bill me ☐
PAYMENT MUST ACCOMPANY ORDERS FOR LESS THAN $5.00
Order Number_____
Order Issued by_____
Date_____

Experimentally Speaking

WHAT'S AHEAD

With a rapidly increasing labor force and with a current unemployment problem, there exists in varying degrees a feeling of concern for the future. Without underestimating the problem, I would like to point out a positive factor which seems to be not well understood. While it is generally known that expenditures for research and development (R&D) are increasing year by year, the rate of increase has been such that *we have spent as much for R&D in the last five years as in all the preceding years* (see bar diagram). The second important point is that *an average of about five years is required for R&D to manifest itself in the form of commercial products.* This means, that, if we imaging a sudden cessation of all R&D, we would still have a flow of new and improved products resulting from the vast amount of R&D work carried out in the past recent years. (About 10% of 1960 sales were in products not on the market in 1956). But instead of our imaginary cessation, there is every indication that R&D expenditures will continue at an increasing rate in the years ahead. An estimate of a 20% increase of R&D in four years has been made, with a new products ratio of total sales increasing from 10% to roughly 15%. Such an achievement would be expected to have a profound influence on our economy and our daily lives.

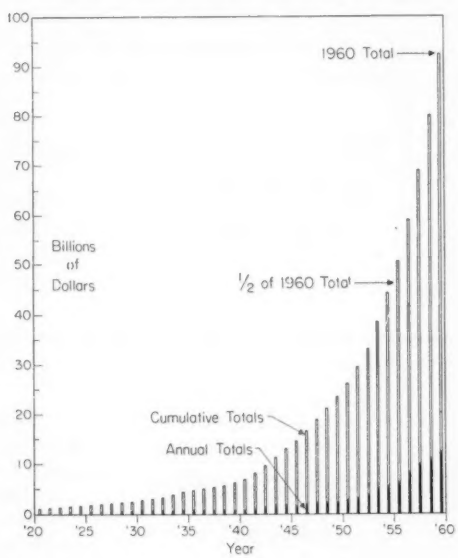

Might I also add that, for SESA and our journal EXPERIMENTAL MECHANICS, the above trend indicates an exciting potential for the future, since new apparatus, techniques and methods should be forthcoming at an increasing rate.

R. E. Peterson
PAST PRESIDENT, SESA

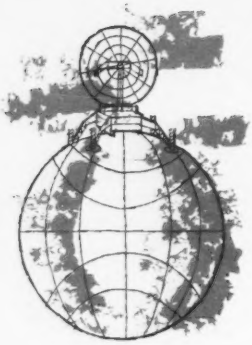

tracking station

the industry in focus

NOL Develops Portable Drop-tester

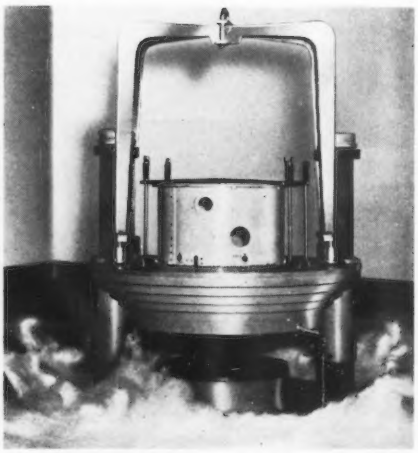

A relatively inexpensive portable drop-tester may replace permanent drop-tower facilities now used for shock testing at the Naval Ordnance Laboratory, Silver Spring, Md. A prototype model consists of a 900-lb anvil base on which a captive carriage is slide-mounted by means of two short pipe columns. A lightweight lifting yoke is attached to the carriage and isolated by glass-bead shock mitigators.

In operation, the device, with the test component mounted on the carriage, is lifted to the desired height by a mobile crane, the carriage separating from the anvil. When dropped, the base strikes first, embedding itself in the sand. A split-second later the carriage strikes the anvil and transmits the shock to the test object. In the experimental stage is an 8000-lb model capable of carrying a payload of 1000 lb or heavier.

Rapid Growth in Space Market Predicted

The growth of the space market in the 60's will double the skyrocketing growth of the electronics market of the 50's, according to General Electric Co.

The company predicts that the space market will increase from one billion dollars per year in 1960 to eight billion dollars per year in 1970. By comparison the booming electronics industry experienced only a four-to-one growth rate during the last decade.

General Dynamics Creates Five New Divisions

General Dynamics Corp. has announced the creation of five new operating divisions, two major organizational groups, and a realignment of corporate executive responsibility.

The continued increase in the size and complexity of the corporation was given as the reason. The changes are designed to provide a higher degree of managerial control and at the same time give greater flexibility to the individual divisions which serve essentially different markets and technologies.

The new divisions, all formerly components of the Convair Division, are: G-D/Astronautics (San Diego, Calif.), G-D/Fort Worth (Tex.), G-D/Pomona (Calif.), G-D/San Diego (Calif.), G-D/Daingerfield (Tex.).

Rocket-engine-thrust Test Stand

Towering 250 ft above the Mojave Desert floor is one of three huge stands designed to test the 1,500,000-lb thrust of Rocketdyne's F-1 engine. The F-1 is a single-chambered engine to be used as a building-block booster for manned space-flight vehicles.

Each of the stands in the $15,000,000 NASA complex will relay thousands of bits of information to an underground concrete control center. Data will then be transmitted by cryptographic teletype to a computer center where it will be processed and immediately returned to test site engineers.

NCR Expands Computer Marketing Facilities

A major expansion of marketing facilities for NCR electronic data processing systems was announced by The National Cash Register Co., Dayton, Ohio. The expansion will result in coast-to-coast coverage of business, industry and government in the marketing of NCR's 304 electronic data processing system and the recently announced 315 system which features the new NCR Card Random Access Memory (CRAM).

Polarad Acquires Federal Scientific

The acquisition of Federal Scientific Corp. of New York by Polarad Electronics was recently announced. Federal Scientific, which will continue to be operated by its present management, has been engaged in the research and development of advanced electronic equipment.

FUTURE MEETINGS

SESA

NOVEMBER 1–3. First International Congress on Experimental Mechanics. Hotel New Yorker, New York, N. Y.

1962 Spring Meeting, Dallas, Tex.

● Related Conference:

OCTOBER 29–31. International Symposium on Photoelasticity. Illinois Institute of Technology, Chicago, Ill

ASA

NOVEMBER 9–11. Meeting of the Acoustical Society of America. Cincinnati and Dayton, Ohio

IAS

OCTOBER 23–24. Institute of the Aerospace Sciences. Joint meeting with Canadian Aeronautical Institute. Quebec, Que., Can.

NRL

OCTOBER 10–12. The 30th Symposium on Shock, Vibration and Associated Environments. Detroit, Mich. Classified. Address: Code 4021 U. S. Naval Research Laboratory, Washington 25, D. C.

OSR

JULY 31–AUGUST 4. Conference of Air Force Office of Scientific Research and Martin's Research Institute for Advanced Studies. Differential Equations in Nonlinear Mechanics. Air Force Academy, Colorado Springs, Colo.

SAE

SEPTEMBER 11–15. Society of Automotive Engineers. National Farm, Construction and Industrial Machinery Meeting. Milwaukee Auditorium, Milwaukee, Wis.

OCTOBER 9–13. National Aeronautic Meeting. Ambassador Hotel, Los Angeles, Calif.

personnel
in the news

BAILEY NAMED PRESIDENT

Lessells and Associates, Inc., of Boston, Mass., announced the election of Fred C. Bailey as president. Professor John M. Lessells, founder of the firm and former president, became chairman of the board and a consultant to the company.

Mr. Bailey graduated from MIT in 1948 and received his master's degree from the same institution in 1949. After graduation, he served successively as a research engineer with the Caterpillar Tractor Co., and technical secretary, assistant, and then acting technical director of the Committee on Ship Structural Design of the National Research Council. His association with Lessells commenced in 1955, where he has served as project engineer, senior project engineer and executive vice president.

Professional and technical affiliations include the American Society of Mechanical Engineers, The American Welding Society, and the Society for Experimental Stress Analysis, which he serves as a member of the Executive Committee.

GALLANT APPOINTED LABORATORY DIRECTOR

Appointment of Raymond A Gallant as director of the engineering laboratory at the Chevrolet Engineering Center was recently announced by H. F. Barr, chief engineer.

Mr. Gallant, who has served as assistant director of the laboratory since February, joined Chevrolet in 1955 when the Engineering Center was opened. He helped organize the instrumentation department and served as its head until February.

In his new post he will be responsible for all laboratory testing of passenger car and truck components, and for the building of engines, axles and transmissions at the Engineering Center.

A native of Plattsburg, N. Y., and a graduate of Rensselaer Polytechnic Institute, Mr. Gallant began his career with General Motors in 1950 as a college graduate in training with the Research Staff. He was awarded a master's degree in engineering mechanics from the University of Michigan in 1954 and spent the following year on educational leave of absence doing graduate work, research and teaching at Rensselaer before joining Chevrolet.

Mr. Gallant is a member of the Society of Automotive Engineers, American Society of Engineering Education, Instrument Society of America, and a past chairman of the Detroit Section of the Society for Experimental Stress Analysis.

CONNER JOINS ORMOND

Ralph N. Conner has joined Ormond Instrumentation Center, Santa Fe Springs, Calif., and will serve in the capacity of general sales manager. Mr. Conner has had 21 year's experience with Baldwin-Lima-Hamilton and was formerly district manager for that firm.

Fred C. Bailey

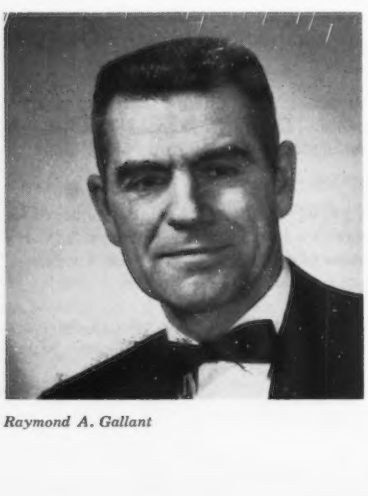

Raymond A. Gallant

RICHARDSON APPOINTED TO RESEARCH STAFF

Trans-Sonics, Inc., announced the appointment of Allyn S. Richardson to its research staff. Mr. Richardson will be concerned with research and the preliminary development of new devices and systems for the Burlington, Mass., firm.

Holder of a degree in chemical engineering from the University of British Columbia, Mr. Richardson received his masters degree from Harvard in 1949. He subsequently spent six years at Harvard in post-graduate work.

SCHIAVONE MADE DIRECTOR

Daniel C. Schiavone, has been named director of reliability on the corporate engineerng staff of The Martin Co.

Dr. Schiavone came to Martin from Bell Aerosystems Co., where he was assistant chief engineer of the Rockets Division. Before that, he was manager of propulsion system design for the Chrysler Corporation's Missile Division.

While with Chrysler, Dr. Schiavone worked with Dr. Wernher von Braun's group on the Army's Redstone and Jupiter ballistic missile programs. A native of Minneapolis, Minn., he received his Ph.D. degree in mechanical engineering from the University of Minnesota in 1951.

NEULAND NAMED MANAGER

Joseph G. Neuland has been named western district field engineering manager for the Systems Division of Beckman Instruments, Inc., Anaheim, Calif.

Mr. Neuland will be responsible for sales of the company's proprietary data systems in the western United States.

With Beckman since 1953, he was at one time manager of engineering and has participated in the development of data-processing systems for military, space and industrial programs.

MORGAN APPOINTED APPLICATION ENGINEER

Melvin L. Morgan has joined Datex Corp., Monrovia, Calif., as an application engineer in the Sales Department. Mr. Morgan attended Rensselaer Polytechnic Institute and was formerly development engineer with Lycoming Division of Avco Manufacturing in Stratford, Conn.

He will be responsible for the preparation and costing of technical proposals.

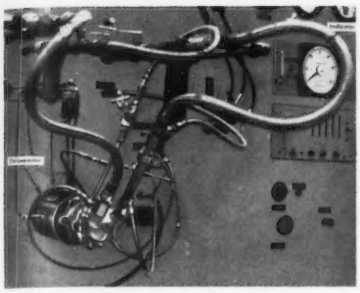

PAD-TYPE TORQUOMETER

The pad-type "Torquometer," manufactured by B & F Instruments, Inc., 3644 N. Lawrence St., Philadelphia 40, Pa., and used in production tests to evaluate hot fluid hydraulic pumps, is constructed with inherent strength needed to support the pump. Pad-type couplings, in accordance with AND standard specifications, are used on the drive end for strength and proper mating characteristics. For high-temperature operation, all components are designed to withstand 500° F; and 700° F solder is used on brushes. High-temperature Torquometers are guaranteed to 350° F operating and 400° F nonoperating. Standard temperature compensation maintains sensitivity constant to 1% or better per 100° F temperature change.

Standard models cover torque ranges from 1.0 lb-in. full scale to 30,000 lb-in. full scale and speed ranges up to 50,000 rpm. **53**

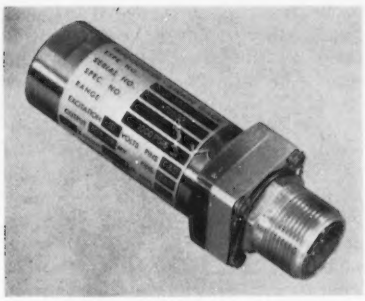

TRANSDUCER

A new pressure transducer, Type 4–350, has been announced by Consolidated Electrodynamics Corp., a subsidiary of Bell & Howell Co., 360 Sierra Madre Villa, Pasadena, California.

Over-pressure performance is specified as 10 times the rated pressure or 10,000 psi (whichever is less) and when applied for 3 min will not cause a zero set to exceed 1.0% of full range output, according to manufacturer.

The instrument also features a high sensitivity of 50 mv, low residual unbalance, and a combined figure of ±0.35% for linearity and hysteresis. Pressure ranges are from 0–100 to 0–5000 psi absolute and gage. The operable temperature range is from −320 to +300° F.

The 4-350 utilizes the unbonded strain gage principle with a four-active-arm spring-type sensing element and a diaphragm force summing area. **57**

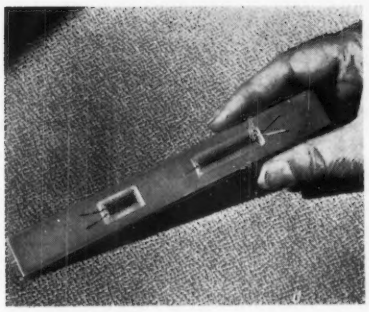

WELDABLE, STABILIZED STRAIN GAGES

A new line of weldable strain gages—designed to provide electrical stability from cryogenic through 750-deg. temperatures—has been developed by Electronics & Instrumentation Division of Baldwin-Lima-Hamilton Corp., 42 Fourth Ave., Waltham 54, Mass.

Small and rugged, the gages afford ease of installation, operation over an extremely wide range of temperatures, and high linearity over the complete temperature range, the manufacturer states.

The new gages are fully stabilized by heat treating, cutting over-all installation time from days or hours to minutes, through elimination of the need for curing and stabilizing after the gages are installed on a testpiece.

Incorporating special SR-4 foil gages bonded to 0.005-in. thick stainless-steel shim stock, the weldable gages are made in two basic types: (1) Phenolic-bonded Constantan foil, for temperatures to 500° F; (2) ceramic-bonded Nichrome V foil, for temperatures to 750° F continuous, or 1000 deg short-term. **58**

new products

For more details regarding these products, circle item number on Reader Information Card

STRAIN GAGES

Micro Systems Inc., a subsidiary of Electro-Optical Systems, Inc., 319 Agostino Rd., San Gabriel, Calif., has announced the extension of the present Micro-Sensor product line from two principal types to 29 types. The expanded line will include strain gages with both positive and negative gage factors. Lengths as short as 0.080 in. and resistance ranges of 120 to 1000 ohms are available. Temperature range of the expanded line is from −320 to +650° F. The gages are available with or without adhesive backings.

A particular feature of the new gage models will be an "in-line gage" which is characterized by the direct line placement of the sensor contacts with the silicon element, thus enabling the user to trim the width of the gage backing for limited area applications. Gage factor on all new gages will remain at 120. **55**

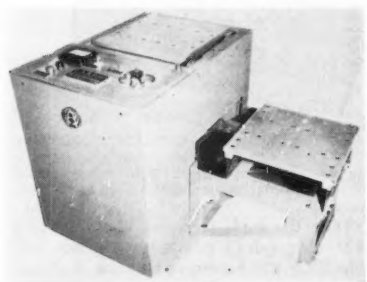

VIBRATION MACHINE

The L. A. B. Corp., 501 Onondaga St., Skaneateles, N. Y., announces a new, compact, low-cost reaction-type vibration machine, designed and constructed for use in quality control, environmental testing and general engineering and research laboratories. The Type RVP-16-50 has a 50 lb test load capacity and a 15 g maximum acceleration rating. Operating in the frequency range from 5 to 60 cps with

A thermal-dynamic

MATERIALS TESTING SYSTEM

PROGRAMS
Load or Strain
and Temperature
Simultaneously

RECORDS
Load vs. Time
Temperature
vs. Time
Strain vs. Time
Load vs. Strain

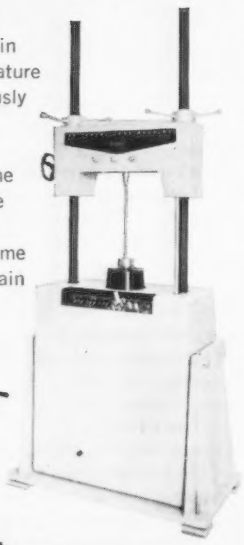

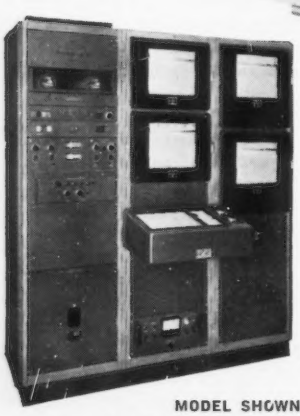

MODEL SHOWN
Loading Capacity: ± 10,000 lbs.
Loading Rate: ± 5,000 lbs./second
Ram: Hydraulic actuated, 8" stroke
Heating Power Capacity: Up to 130 KVA

Take the high response characteristics of electro-hydraulic servo valves and loading mechanisms, add the convenience of pencil-line program plotting, apply the precision of electronic load and temperature control and recording techniques, and you have the basis of this new testing system designed with just one thought in mind — to advance the art of materials testing.

RI RESEARCH INCORPORATED

Write Dept. SJ, Box 6164, Minneapolis 24, Minn.
For details, circle No. 2 on Reader Information Card

total excursions up to 0.100 in. maximum, the machine will meet a wide range of military specifications and commercial vibration testing requirements, the manufacturer reports.

A single reaction vibrator generator of special design utilizes only the vertical force component to produce simple harmonic motion at the primary table. Because the reaction generator produces force over a full 360 deg on each revolution, the horizontal force components may be employed to drive one or two additional tables attached to the sides of the machine to allow simultaneous testing of multiple test objects in both the vertical and horizontal directions. The side tables are available as separate items and can be added in the field. **59**

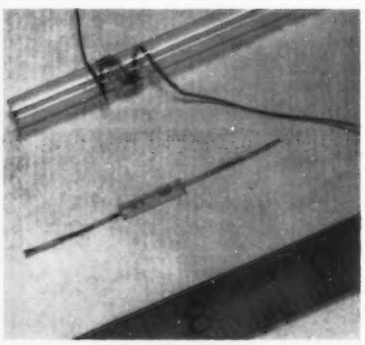

SEMICONDUCTOR STRAIN GAGES

An entire new line of solid state strain gages, effective June 1, was announced by Kulite-Bytrex Corp., 50 Hunt Street, Newton 58, Mass.

The manufacturer reports that it has completely revamped its product line to provide higher working strain levels, increased flexibility, better handling characteristics, and smaller sizes than were previously available. Its current line of DA and DAN gages has been discontinued with the introduction of the new DB Series gages.

The improved characteristics of the new gages are said to result from technological advances and field application data derived on earlier gages. The product line described includes matched gages for a variety of materials, gages for dynamic measurements which provide 50 times greater output at one-third the "apparent strain" of conventional high-output wire gages, small gages for limited space requirements (0.1 gage length) and gage factor from minus 140 to plus 170. The gages are incorporated in a new highly flexible epoxy matrix and are available in resistance ranges of 120 to 5,000 ohms. **60**

Use Reader Information Card!

TRANSISTORIZED, CALIBRATED FIELD-INTENSITY RECEIVER

Polarad Electronics Corp., 43-20 34th Street, Long Island City 1, N. Y., has developed a mobile, transistorized, calibrated field-intensity receiver, covering the 1000 to 10,000 mc frequency range. The entire complement of equipment consists of a basic unit, four interchangeable RF tuning units, an impulse calibrator, five antennas and a tripod.

Model CFI microwave field-intensity receiving system is designed to perform the tests prescribed by the latest military specifications covering RF leakage and interference in electronic and associated equipment, according to manufacturer. In addition, such measurements as operational field intensity data, propagation studies, RF signal analysis and general communications can be made under the conditions of precise measurement since the equipment has a built-in impulse calibrator which covers the entire frequency range at a high degree of stability. The Model CFI is also said to be capable of accurately determining the shielding effectiveness and harmonic or spurious output of transmitters. **61**

ACCELEROMETER

The development of the Model 410 accelerometer, having a sensitivity rating of 750 mv/g maximum, has just been announced by Columbia Research Laboratories, MacDade Blvd. & Bullens Lane, Woodlyn, Pa. The Model 410 is a true compression sensing device having the highest sensitivity of any accelerometers in Columbia's standard line. Applications for this type of accelerometer

include vibration meters, vibration limiters, safety devices, burglar alarms and other systems where high output is essential to trigger or operate various switching mechanisms and readout instruments.

Frequency response of the Model 410 is flat within ±5% from 0.5 cps to 2 kc over an extended acceleration range of 0.0016 g to 1000 g. Resonant frequency is 15 kc, maximum cross sensitivity is 5% and nominal capacity of 750 μμf. Temperature range is from −65 to +350° F for standard units and −65 to +500° F for high temperature units with less than ±10% variation in sensitivity throughout both ranges.

The Model 410 accelerometer has a stainless-steel case 1.5 in. high with a $^3/_4$-in. hexagon base. The unit weighs just 2 oz. **63**

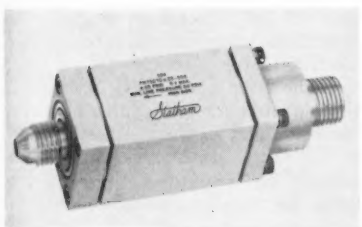

HIGH-TEMPERATURE PRESSURE TRANSDUCER

A new series of high-temperature gage and differential pressure transducers, the P732, that measure pressures over a wide variety of ranges and under extreme environmental conditions have been introduced by Statham Instruments, Inc., 12401 W. Olympic Blvd., Los Angeles 64, Calif. The small and lightweight P732 pressure transducers, of stainless-steel construction, are temperature compensated for continuous operation to +600° F.

Ambient temperature limits on the P732 are from −320 to +650° F. Pressure ranges on the gage and unidirectional differential models are from 0–2 psi through 0–5000 psi. The bidirectional differential model operates in ranges from ±1 through ±100 psi.

The Statham P732, was designed for aero-space, nuclear or industrial pressure measurement applications. **65**

ELECTRONIC CONTROL SWITCH

An electronic relay that will switch up to 15 amp with a 1.8 microamp or less control signal has just been marketed by Central Scientific Co., a division of Cenco Instruments Corp., 1700 Irving Park Rd., Chicago 13, Ill.

The switch, designed to operate

solenoids, heaters, regulators, instruments, contact meters, etc., has relay contacts that will handle a maximum of 15 amp at 115 v, 60 cycle ac (noninductive load) when triggered by anything from a short circuit, or zero ohms, to 10 megohms resistance.

This current is amplified by a vacuum-tube circuit which, in turn, energizes the control relay. The single-pole double-throw relay contacts are wired to control the two "normally closed" and two "normally open" three-terminal grounded female outlets. A built-in signal light goes "on" when the switch is energized.

The entire unit is encased in a steel housing. **67**

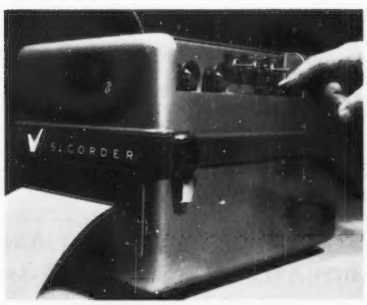

LOW-COST OSCILLOGRAPH

The Heiland Division of Minneapolis-Honeywell, 5200 E. Evans Ave., Denver 22, Colo., has introduced a low-cost direct-recording oscillograph designed for use in normal laboratory testing and evaluation.

Known as the 1406 Visicorder, the new model produces instantly readable records of up to six channels of scientific and test data simultaneously, the company said.

It is the fourth member of the firm's Visicorder family of direct-recording oscillographs. Previously introduced models have recording capacities of 14, 24 and 36 channels.

The model 1406 Visicorder may be ordered with a choice of galvanometers and record drive speeds, and is available with or without grid line and/or timing systems. It records variables from 0 to 200 cps. **69**

LA

OVER 185 YEARS OF CUMULATIVE EXPERIENCE IN THE AREAS OF

stress analysis
fatigue analysis
vibration analysis

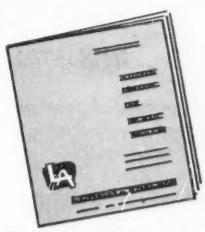

• Bulletin R describes our capabilities.

LESSELLS AND ASSOCIATES, INC.
engineers
916 Commonwealth Avenue
Boston 15, Massachusetts

LA

For details, circle No. 3 on Reader Information Card

TUMBLE-RATE TEST STAND

Kearfott Division, General Precision, Inc., 1150 McBride Ave., Little Falls, N. J., has announced the production of the CO5 6452 008 tumble-rate test stand, a highly precise unit used to test gyros and other devices requiring precise orientation or rotation. This unit features: rotary table locking arrangement to permit selection of 0, 90, 180 and 270 deg static angular positions; tapered roller bearings to provide low-friction, accurate turntable mounting; 30 heavy-duty, low-noise slip rings to provide for signal and power-transfer requirements; two-motor drive system to assure system stability and freedom from backlash, high gear reduction and large-diameter bull gear mounted directly on table stand to enable high torque-to-voltage gradient, and leveling jacks, with hold-down bolts and azimuth adjusting locking device, to insure proper level and polar alignments. 71

ARC SWITCH

A new arc switch, designed to facilitate the controlled discharge of stored electrical energy in laboratory and production applications, has been announced by MHD Research, Inc., P.O. Box 1815, Newport Beach, Calif.

Designated Model AS-25, the new arc switch is rated for 7–20 kv operation, with a capacity of 2500 joules. It is actuated by spark ejection, generated by the Model ASE-10 arc-switch trigger electronics. In operation, a capacitor is charged to the desired potential; then, at the convenience of the operator, a secondary high-voltage discharge ionizes the switch spark gap, causing it to conduct, discharging the capacitor.

The jitter (uncertainty in the exact time of discharge) is approximately 1 microsecond. As this discharge occurs in an inert atmosphere, long component life is assured. Provision is made for four co-axial conductors to connect to the switch. 73

For free Information and Literature Use Reader Information Card See Page 17A

Experimental Stress Analysis for Missiles and Space Craft

STRAIN GAGE TECHNIQUES and INDUSTRIAL PHOTOELASTICITY

Three Short Intensive Courses on EXPERIMENTAL STRESS ANALYSIS
At the Dept. of Engineering, University of California at Los Angeles

STRAIN GAGE LECTURES . . . . . August 21-25, 1961
STRAIN GAGE LABORATORY . . August 28-September 1, 1961
INDUSTRIAL PHOTOELASTICITY . . . . . September 5-9, 1961

Under Joint Sponsorship of Engineering Extension, Dept. of Engineering—University of California at Los Angeles and Society for Experimental Stress Analysis.

For additional information, please write to Engineering Extension, Engineering Bldg., Unit 11, Rm 6266, University of California, Los Angeles 24, Calif. Phone: BRadshaw 2-6161 or GRanite 3-0971, Ext. 369.

STAFF

William T. Bean, Jr.
Consulting Engineer
Detroit, Michigan

Ward B. Brewer
Engineering Research Department
Lockheed Aircraft Corporation
Burbank, California

Jerome Catz
Department of Mechanical Engineering
Massachusetts Institute of Technology
Cambridge, Massachusetts

Edward W. Larson, Jr.
Rocketdyne Division
North American Aviation, Inc.
Canoga Park, California

David J. Leeds
Department of Engineering
University of California
Los Angeles, California

Milton M. Leven
Research Laboratories
Westinghouse Electric Corporation
East Pittsburgh, Pennsylvania

William M. Murray
Department of Mechanical Engineering
Massachusetts Institute of Technology
Cambridge, Massachusetts

Joseph C. Sanchez
Micro Systems, Inc.,
San Gabriel, California

Clarence R. Smith
Structures and Materials Laboratories
Convair
San Diego, California

Peter K. Stein
Editor, Strain Gage Readings
Phoenix, Arizona

Leon J. Weymouth
Electronics & Instrumentation Division
Baldwin-Lima-Hamilton Corporation
Waltham, Massachusetts

Felix Zandman
Instruments Division
The Budd Company
Phoenixville, Pennsylvania

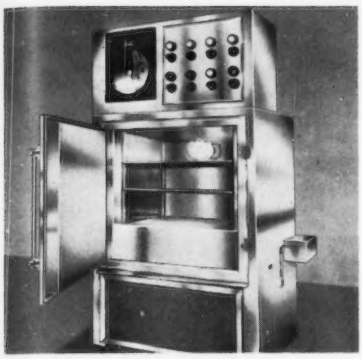

TEMPERATURE-HUMIDITY CHAMBER

Hudson Bay Co., environmental division of Labline, Inc., 3070 W. Grand Ave., Chicago 22, Ill., announces the addition of a 4-cu ft upright chamber to its present line of temperature-humidity test cabinets. This unit has a temperature range of 0 to 200° F with a control tolerance of ±2° F and a humidity range of 20 to 95% RH within ±5%.

The "Environ-Cab" has wide usage for environmental testing of chemicals, electronic components, paints, plastics, packaging, protective coatings, etc., and for JAN & MIL specifications.

An oversized 1/4 hp continuous-duty, motor-driven blower supplies air circulation throughout the chamber to eliminate temperature gradients The hermetically sealed, air-cooled compressor uses F-12 refrigerant. Heat transfer is achieved with a copper tube, aluminum-finned cooling coil. **75**

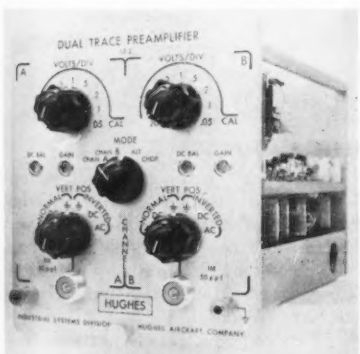

PREAMPLIFIER FOR MEMO-SCOPE

The development of a dual trace preamplifier for its Memo-Scope oscilloscope model 105, a high frequency storage oscilloscope with a writing speed of 1,000,000 ips, has been announced by Hughes Aircraft Co., Industrial Systems Division, P.O. Box 90904, Airport Station, Los Angeles 45, Calif.

The preamplifier, which the company said is now in production, is designated model 05-2. It employs a blanked writing beam during switching time when operated in the chopped mode. It can provide chopped displays of both Memo-Scope channels simultaneously, alternate displays of both channels or single operation of either channel. The unit has a pass band of direct current to 10 megacycles, a chopping rate of 270 kc and a sensitivity of 0.05 v per division. **77**

PHOTOELECTRIC TAPE READER

Data Stor division, Cook Electric Co., 2700 Southport Ave., Chicago 14, Ill., announces the development of its Model 90 photoelectric tape reader which provides a total punched-tape capacity of approximately 500,000 bits of information.

The Model 90 is supplied with a Cook Electric Co. photoelectric reading system.

This photoelectric tape reader is suitable for "on-line" service in computer, communication and control applications. Data, in the form of coded hole sets, are photoelectrically read from pre-punched tape and transformed to electrical output pulses.

The photoelectric reading head is designed to accommodate standard 5, 6, 7 and 8 level codes punched 10 holes per inch along and across the tape. **79**

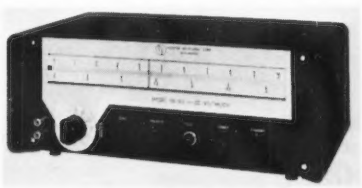

DC SERVO VOLTMETER

Model HV-160 d-c servo voltmeter provides very high-input impedance on all scales, according to its manufacturer, Houston Instrument Corp., P.O. Box 22234, Houston 27, Tex. Input is potentiometric (over 100 megohms) on ranges from 3 millivolts to 1 v, and is 10 megohms on ranges from 3 to 300 v. Servo gain is automatically adjusted for each scale by the range switch. Accuracy is 0.15% on eleven selectable scales. Double regulated zener reference eliminates reference cell replacement and standardization problems. Indication is provided by knife-edge pointer on 14-in. mirror scale. Hardware is provided for rapid conversion from case to rack mounting or vice versa.

Loading errors are said to be substantially eliminated by the use of the HV-160 voltmeter in millivolt measurements. **80**

High Performance
Low Price

PORTABLE STRAIN INDICATOR

MODEL HW-1 (PATENT APPLIED FOR)

The Only Indicator Insensitive
To Long Lead Wire Capacitance

Price $495

PATENTED by STRAINSERT
INTERNALLY GAGED
TRANSDUCERS:

STRAINSERT BOLTS

for Ultimate Reliability and
Precision In Bolt Tension
Load Measurement

Force and Pressure Transducers
and True Miniature Transducers

PORTABLE BOLT TESTER
& TORQUE WRENCH
CALIBRATOR

Special Internal Gaging
and Instrumentation
for Overload Protection
and Danger Warning Devices

STRAINSERT COMPANY

the inside line of strain gage devices

24 Summit Grove Avenue
Bryn Mawr, Pennsylvania

For details, circle No. 5 on Reader Information Card

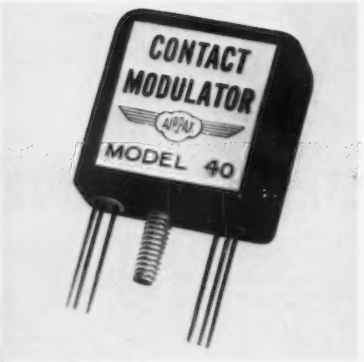

MIDGET CHOPPER

Model 40 low-noise chopper, designed for 400 cps drive, withstands 100 g shock and vibration in any direction equivalent to sinusoidal vibration at an amplitude of 0.060 in. total travel over a frequency of 10 to 55 cps and 15 g from 55 to 2500 cps, according to an announcement by Airpax Electronics Inc., Cambridge Division, Cambridge, Md.

Chopper noise has been brought to an irreducible minimum. At one megohm load, 400 cps, noise is down in the random noise level. Unit is hermetically sealed and continuous operation is maintained over a temperature range of −65° C to +100° C. Rated life exceeds 2000 hr.

This miniaturized electro-mechanical chopper weighs 9 g. Dimensions are $^{21}/_{32}$ in. x $^{21}/_{64}$ in. x $^{5}/_{8}$ in. **81**

POWER SUPPLY

Tektronix, Inc., P.O. Box 500, Beaverton, Ore., announces that its latest product, the Type 132 power supply, provides an easily portable housing for any Tektronix A-to-Z plug-in unit—thus enabling the many plug-ins to be used with or without an oscilloscope in a wide variety of applications.

The compact unit powers an internal amplifier and one Tektronix "letter-series" plug-in.

Internal amplifier of the Type 132 has a frequency response of dc to 22 megacycles, rise-time of 15 nanosec., noise level less than 0.5 millivolts, peak-to-peak (referred to internal amplifier input). Front-panel terminals permit push-pull or single-ended + or −input. **85**

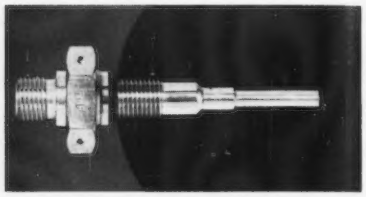

SHEATHED HIGH-SPEED PROBE

RdF Corp. (formerly Arthur C. Ruge Associates), Hudson, N. H., announces the development of a new high-speed probe with a CP platinum sensor hermetically sealed and protected in a 316 stainless-steel sheath.

This new RdF probe has a response speed of less than 300 msec for one time constant.

Compatible with liquid oxygen, the Type 3255 sheathed and sealed probe can also be used with corrosive media.

The temperature range of the RdF Type 3255 resistance probe is from −423° F (liquid hydrogen) to 400° F, according to the manufacturer. **91**

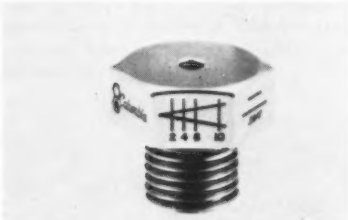

RETICLE ADAPTOR

A quick on-the-spot calibration device that enables direct visual calibration of vibration equipment over a 30 to 200 cps range has just been announced by Columbia Research Laboratories, MacDade Blvd. & Bullens Lane, Woodlyn, Pa.

Two different reticle patterns are engraved on the adaptors. One is the CRL Wedge, which provides measurement of 20, 40, 60 and 100 mils double amplitude, and the other is the CRL Para-Line, which is a series of parallel lines spaced 0.0647 in. apart to measure ±10 g at 55 cps, a requirement of many MIL specs.

The calibration reticle adaptors are hexagon-shaped devices that can be provided with standard size studs or bores to fit thread sizes of the various types of shaker tables and accelerometers commonly in use. **92**

SESA

invites all manufacturers of engineering and scientific equipment used in experimental mechanics to exhibit at

1961 EXPOSITION

held in conjunction with

FIRST INTERNATIONAL CONGRESS ON EXPERIMENTAL MECHANICS

Hotel New Yorker, New York City
November 1, 2, 3, 1961

Lively, working exhibits doing something and telling your story are the best way to talk to engineers and scientists. This is your opportunity for best results.

For details, write to

SESA, 21 Bridge Square, Westport, Conn.,
or Circle No. 20 on Reader Information Card

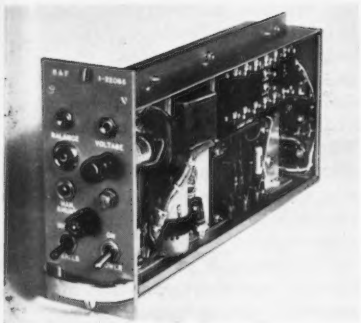

STRAIN GAGE AND TRANSDUCER CONDITIONER

B & F Instruments, Inc., 3644 N. Lawrence St., Philadelphia 40, Pa., announces a new universal input conditioning unit for data-acquisition systems work with the inherent flexibility to meet most typical applications. It is a single-channel module with an integral floating power supply. It may be used with 1, 2 or 4 arm bridges, and will adapt to any input wiring technique, including 8 wire bridge inputs. The shields are carried through the unit. The individual internal power supplies may be adjusted between 1 and 15 v dc.

Calibration may be achieved via the single- or double-shunt technique. Sequential and simultaneous calibration is available for four step or single step plus and minus values. Six modules are packaged in an $8^3/_4$-in. panel suitable for standard 19-in. relay rack mounting. **93**

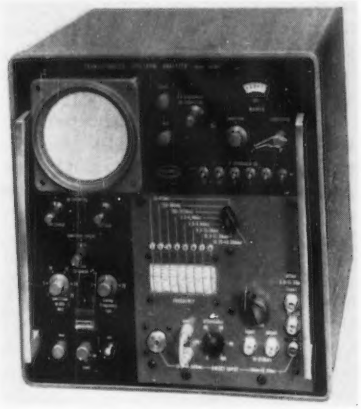

MICROWAVE SPECTRUM ANALYZER

Polarad Electronics Corp., 43-20 34th St., Long Island City 1, N. Y., has developed a mobile, transistorized, microwave spectrum analyzer. The Model SA-84T spectrum analyzer covers the frequency range from 10 mc to 40,880 mc.

The instrument is said to be capable of a number of operations, including spectral measurements, detection and identification of spurious signals, countermeasures analysis, measurement of the frequency difference of two RF signals, testing microwave oscillators (magnetrons, klystrons, etc.) for pulling, double-moding and other types of malfunctions, checking the tracking of radar components, and measurement of spectral characteristics of pulse-modulated and FM signals.

This spectrum analyzer is particularly suited to mobile operation because of its light weight (70 lb), its extensive transistorization and its acceptance of either standard 12-v automobile battery power or 115 v a-c powers. **97**

FOR FREE INFORMATION AND LITERATURE USE READER INFORMATION CARD
See Page 17A

MEMBERSHIP IN SESA

In the space age, measurements of stresses, forces and accelerations must be made to check calculations and to obtain information that cannot be calculated.

The Society for Experimental Stress Analysis is **the forum for work and workers in the experimental mechanics field.**

How you can join the Society and take advantage of its many benefits is explained in descriptive literature available.

For further details write to:

SOCIETY FOR
EXPERIMENTAL STRESS ANALYSIS
21 Bridge Square, Westport, Conn.

PHOTOELASTIC STRESS ANALYSIS WITH POLAROID* FILTERS

Standard Equipment or Special
Complete Apparatus or Components

Point Light Sources
White Light and Monochromatic (546 or 589 line)

Matched Quarter Wave Plates to 17″ diameter

Polaroid Polarizers to 17″ diameter
Cemented Glass Laminations #6/006

Straining Frames

Recording Cameras

* T. M. Reg. U. S. Pat. Off. by Polaroid Corporation

THE POLARIZING INSTRUMENT COMPANY, Inc.
IRVINGTON-ON-HUDSON, NEW YORK

For details, circle No. 6 on Reader Information Card

To obtain free literature, circle item number on Reader Information Card

Testing Machines

A new brochure describes the complete line of equipment made by Steel City Testing Machines, Inc., 8817 Lyndon Ave., Detroit 38, Mich. Brinell hardness testing machines, Penetrascopes, ductility testers, tensile and compression testing machines, transverse testers, hydrostatic and pneumatic testing machines, proving rings and calibration presses, and special testing machines are discussed.

Printed in two colors and containing four pages, Bulletin G-361 also contains information on the background, experience, and distribution facilities of the company. **101**

Strain-gage Wiring Terminals

A line of strain-gage wiring terminals is described and illustrated in bulletin No. 4340 published by Electronics & Instrumentation Division, Baldwin-Lima-Hamilton Corp., 42 Fourth Ave., Waltham 54, Mass.

The four-page, two-color bulletin includes photographs and drawings of the terminals, characteristics and specifications, features, types, dimensions and curves of typical leakage resistance vs. temperature for high-temperature terminals.

These terminals provide convenient strain-relief junctions for integral strain gage leads and heavier instrumentation lead wires. Configurations are available for both single and rosette gages.

All terminals can be installed on flat or curved surfaces, and are available in five basic types for maximum operating temperatures from 500 to 1200° F. **103**

Temperature Recorders

A new 8 1/2 by 11, 12-page illustrated booklet entitled "Temperature Recording from Platinum Resistance Sensors" is now available from Brush Instruments, division of Clevite Corp., 37th & Perkins, Cleveland 14, Ohio.

The booklet describes and illustrates how a Brush Universal Carrier Amplifier and a platinum resistance sensor are applied to provide a combination for recording temperatures from −320 to +2000° F. This recording technique displays temperature deviations of $^1/_{100}$ of 1 deg.

Basic setup procedures, temperature compensation, bridge circuits, calibration charts and recording accuracy are also described. **105**

Beckman Bits

Beckman Bits, a new magazine published by Systems Division of Beckman Instruments, Inc., is now available for distribution from Beckman Systems Technical Publications Department, 325 Muller St., Anaheim, California.

This first edition of the new quarterly contains 14 pages of articles, illustrations and application information about data processing equipment, amplifiers and systems management personnel and techniques. Among the features is a documented report on exhaustive test results on the Model 210 data-processing system. **107**

Cryogenic Temperature Sensors

Trans-Sonics, Inc., Burlington, Mass., offers a new eight-page bulletin, No. 2000, describing its platinum-resistance temperature transducers. Specifically designed for use with cryogenic fluids, such as liquid hydrogen and "Lox," the sensors are suitable for airborne or ground-based applications.

As described in Technical Bulletin 2000, the temperature transducers may be calibrated in Trans-Sonics, Inc.'s own pressure cryostat against an NBS calibrated reference thermometer. The accuracy of such elements is ±0.1° F at temperatures as low as −435° F. Units containing trimming networks to insure interchangeability to ±0.1° F are also described.

In addition to describing Trans-Sonics cryogenic temperature transducers, the bulletin discusses the company's background and facilities. **109**

Metal Fasteners and Corrosion Resistance

Various kinds of corrosion and the different metals suited to resist them are given a thorough review in "Harper Corrosion Guide," a 24-page illustrated brochure published by The H. M. Harper Co., Morton Grove, Ill., maker of metal fasteners.

Written to help manufacturers build corrosion resistance into their products and properties, the guide analyzes the seven basic types of corrosion and shows what specific kinds of metals best resist them. These include brass, naval bronze, silicon bronze, nickel and high-nickel alloys, stainless steels, aluminum, copper, monel metals and high-temperature alloys.

A corrosion guide chart lists 136 types of corrosive agents that engineers and maintenance people may be troubled by and shows how well each of eight types of metals resist each of these agents. **111**

Engineering-article Writing Guide

Brief "Primer on Technical Articles for Engineers" gives an easy-to-understand language instructions on how to write technical articles for professional journals and trade magazines. Seven chapters describe major types of articles wanted by editors, how to organize and write them, how to criticize the finished manuscript, and how to work with editors.

Some "tricks-of-the-trade" of professional writers are included in chapters on psychology of writing production and on assuring reader interest. A sample editorial inquiry letter and a checklist are included.

Available from American Industrial Writing Institute, P.O. Box 5453, Pasadena, Calif., $1 per copy, postpaid.

Miniature Thermocouples

A new line of microminiature thermocouples is described in a new bulletin, No. 4336, published by Electronics & Instrumentation Division of Baldwin-Lima-Hamilton Corp., 42 Fourth Ave., Waltham 54, Mass.

The six-page, two color bulletin covers the design, construction, applications and operating characteristics of these thermocouples, which have a probe diameter of only 0.014 in. and operate in a temperature range from cryogenic environments to 3000° F.

The bulletin includes drawings and photographs; circuit sketches; curves showing radiation error, time constant and response times; a listing of types and model numbers, and temperature ranges.

The thermocouples are intended for use in such applications as missiles and high-speed aircraft, surgery and medicine, temperature measurements in rocket fuel, jet-engine exhaust, moulding and casting, and turbine operation. Other uses are found in the instrumentation of atomic piles, shock tubes and wind tunnels, and gas chromatography. **113**

Power Supplies, Current Indicators and Amplifiers

Elcor Inc., subsidiary of Welex Electronics Corp., 1225 W. Broad St., Falls Church, Va., announces the release of three recently revised catalogs dealing with its complete line of products.

Catalog No. 3-361 deals with isolated power supplies and isolated isoformers. Catalog No. 4-361 describes current indicators and integrators, and current source. Catalog No. 5-361 gives complete information on d-c amplifiers, wide-band d-c amplifiers, and high-voltage amplifiers. **115**

Tapered Tubing

Straight and reverse-tapered tubing, in size from 0.080-in. to 1.500-in. OD, is described in Data Memorandum No. 29 just published by Superior Tube Co., 1976 Germantown Ave., Norristown, Pa.

Recently introduced by Superior, the tapered tubing features close tolerances and freedom from cracks on the inside diameter, making it most attractive for use as rocket engine thrust chamber tubes, according to the memorandum. It further states that reverse-tapered tubing eliminates much of the severe forming and fabrication previously required to reduce the diameter of tubing in the throat area of the engine's exhaust chamber. **117**

Transducer for Sea-water Temperature Measurement

Trans-Sonics, Inc., of Burlington, Mass., announces the availability of its Type T-4005 sea-water temperature transducer.

Having an accuracy and interchangeability of 0.09° C, the unit is designed for indefinite immersion in sea water, according to manufacturer. The T-4005 transducer contains its own bridge circuit, eliminating the need for additional circuit construction by the user. Calibration is expressed as mv/v vs. temperature over the unit's range of −5 to 30° C. Complete construction and operating characteristics are given in Trans-Sonics Special Product Note 4005. **119**

Special Instruments

"Special Instruments" is the title of the latest booklet released by Tektronix, Inc., P.O. Box 500, Beaverton, Ore.

Written in catalog style, the colorful 12-page booklet gives a detailed presentation of Tektronix special-purpose test instruments. These include a direct-reading L-C meter, an indicator unit, a waveform generator, 2 pulse generators and 2 power supplies.

The booklet contains specifications, performance characteristics, pertinent illustrations for various measurement applications. **123**

Portable Potentiometer Indicator

Thermo Electric Co., Inc., Saddle Brook, N. J., has released a revised edition of a 4 page, illustrated Catalog 64-1, on their "Minimite," portable potentiometer indicator. The $3^1/_2$ lb instrument, and a special adaptation called "'Airline' Minimite," are described in detail. Included are specifications, applications information, accessories such as a flange for flush-mounting in panels, switching facilities and carrying case. The portable "'Airline' Minimite" is a modification of the basic instrument, used to ground-check jet-engine exhaust-gas temperatures and calibrate cockpit indicators.

Photographs are used liberally to indicate relative size, show rugged construction details, ease of application and maintenance. **127**

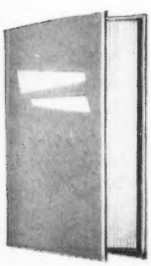

Helpful McGraw-Hill books for your professional library

THEORY OF PLATES AND SHELLS

Covers the general theory of bending of plates under lateral load, with applications to circular and rectangular plates, and with numerous tables simplifying the calculation of deflections and stresses in plates. Provides a treatment of combined bending and tension or compression of plates, with applications to thin plates. **By S. Timoshenko, Stanford Univ.; and S. E. Woinowsky-Krieger, Université Laval, Quebec, Canada. 2nd Ed., 580 pp., 280 illus. $15.00**

THEORY OF ELASTICITY

For engineers concerned with calculating stresses in engineering structures and machine parts—here is essential knowledge of the theory of elasticity, together with the solution of engineering problems of practical importance. The book discusses approximate and experimental methods of solving elastic problems which have proved useful in the study of complicated cases of stress distribution. **By S. Timoshenko and J. N. Goodier, Stanford Univ. 2nd Ed., 506 pp., 266 illus., $11.50**

FORMULAS FOR STRESS AND STRAIN

A compact and readily usable summary of important formulas, facts, and principles pertaining to strength of materials. This reliable reference for engineers provides helpful formulas for stress analysis and elasticity. All experimental data and empirical formulas are in line with current information. New material has been added, ensuring complete coverage of stress and strain. **By Raymond J. Roark, Univ. of Wisconsin. 3rd Ed., 381 pp., $8.25**

THE STRAIN GAGE PRIMER

What the bonded wire resistance strain gage can do in solving problems in experimental stress analysis is explained in this practical book. All phases are covered—from selecting the proper commercial gage through preparing surface of the test member, cementing, damage-proofing, and wiring the gage—to selecting the proper instrument to record the strain gage data, and interpreting readings in terms of significant stresses. **By C. C. Perry and H. R. Lissner, Wayne Univ. 280 pp., 180 illus., $6.00**

THE TESTING AND INSPECTION OF ENGINEERING MATERIALS

A practical approach to the principles and methods of materials testing, with full details on types of tests in use. Describes modern testing equipment and covers effects of variables on test results. Includes information on micro-hardness testers, non-destructive tests, low-temperature impact tests, and more. **By H. E. Davis, G. E. Troxell, Univ. of Calif.; and C. T. Wiskocil, formerly, Univ. of Calif. 2nd Ed., 431 pp., 171 illus., 42 tables, $7.50**

APPLIED ENGINEERING MECHANICS

Emphasizes the use of reasoning rather than complicated mathematics for solving engineering problems. Employing only simple mathematics, the book proceeds from easy to difficult phases of engineering mechanics, clarifying the principles advanced with numerous illustrations. Takes you step-by-step through the solutions of scores of technical problems. **By Alfred Jensen, formerly, Univ. of Washington; assisted by Harry H. Chanoweth, Univ. of Washington. 2nd Ed., 409 pp., 746 illus., $6.50**

SEE THESE BOOKS 10 DAYS FREE

McGraw-Hill Book Co., Dept. EXM-6, 327 W. 41st St., N. Y. 36, N.Y.

Send me book(s) checked below for 10 days' examination on approval. In 10 days I will remit for book(s) I keep, plus few cents for delivery costs, and return unwanted book(s) postpaid. (We pay delivery costs if you remit with this coupon—same return privilege.)

- ☐ Roark—**Formulas for Stress & Strain, $8.25**
- ☐ Perry & Lissner—**The Strain Gage Primer, $6.00**
- ☐ Davis et al.—**Testing and Inspection of Engr. Materials, $7.50**
- ☐ Jensen & Chenoweth—**Applied Engr. Mechanics, $6.50**
- ☐ Timoshenko & Woinowsky-Krieger—**Theory of Plates and Shells, $15.00**
- ☐ Timoshenko & Goodier—**Theory of Elasticity, $11.50**

Name..... Address.....

City..... Zone.... State.....

Position..... Company.....

For price and terms outside U.S., write McGraw-Hill Int'l. EXM-6

DC to 5000 cycles over an amplitude of 4″ peak to peak

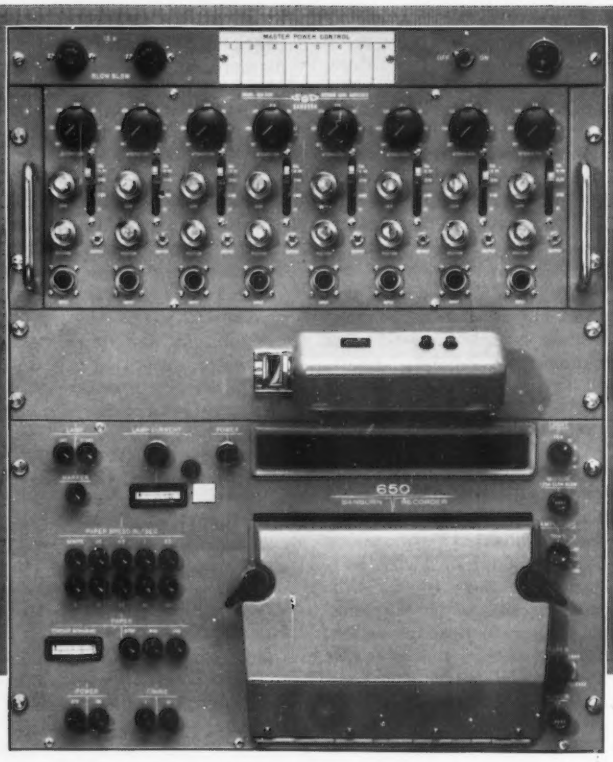

NEW SANBORN "650" SYSTEM OFFERS DIRECT READOUT, 8 TO 24 CHANNELS, ALL SOLID STATE CIRCUITS, FOR RACK MOUNTING OR INDIVIDUAL CASES.

Here's the *one* system that lets you record inputs from DC to 5 KC within 3 db at 4″ peak-to-peak amplitudes, without changing galvanometers. The "650" system consists of an 8-channel medium gain, general purpose amplifier unit driving a high speed, high resolution optical oscillographic recorder. It can be easily built into your system, packaged in a mobile cabinet or housed in individual cases. The single-chassis, 7″ high amplifier module has 8 separate channels, *complete from floating and guarded inputs to galvanometer outputs;* each channel comprises a front end modulator and input transformer, carrier amplifier, demodulator, filter and driver amplifier. Power Supply and Master Oscillator Power Amplifier are built-in. All amplifier elements are plug-in transistorized units for easy servicing.

Immediately readable recordings are made on 8″ wide daylight-loading ultra-violet-sensitive charts which require no chemical development. Features of the 12¼″ high recorder unit include 9 electrically controlled chart speeds from ¼″ to 100″/sec; calibrated monitoring screen; automatic trace identification and timing lines at 0.01 or 0.1 sec. intervals; amplitude lines spaced 0.1″ apart which can be blanked from ¼, ½, ¾ or all of chart. Recorder is available with an 8-, 16- or 24-channel galvanometer block which is then equipped with the number of galvanometer elements desired by the customer. Both the Recorder and Amplifier are also available as individual units for use with other equipment.

SENSITIVITY 20 mv input gives 8″ deflection; 12 attenuator steps to X5000, smooth gain control.

INPUT RESISTANCE 100,000 ohms all ranges, floating and guarded; DC source resistance must be kept below 1000 ohms on mv ranges only.

COMMON MODE PERFORMANCE Rejection at least 140 db at DC, tolerance to ±500 volts, max.

GAIN STABILITY Better than 1% to 50° C. and for line voltage variation from 103 to 127 volts.

LINEARITY 1½% of full scale (8 in.)

NOISE 0.02″ peak-to-peak, max.

MONITOR OUTPUT On front panel; provides ±1v full scale across 100,000 ohm load

POWER REQUIREMENTS 103-127 volts, 60 cycle AC, 625 watts

Contact your Sanborn Sales-Engineering Representative for complete specifications and applications engineering assistance. Offices throughout the U. S., Canada and foreign countries.

SANBORN COMPANY
INDUSTRIAL DIVISION
175 Wyman St., Waltham 54, Massachusetts

For details, circle No. 7 on Reader Information Card

Model Investigations of Unstiffened and Stiffened Circular Shells

Test techniques used in evaluation of the effect of internal pressure on stability of shells used in modern aircraft and missiles are described; also, conclusions derived from the results are presented and discussed

by L. A. Harris, H. S. Suer and W. T. Skene

ABSTRACT—In 1951, an extensive review of the literature indicated that only a limited amount of test data was available to evaluate the effect of internal pressure on the stability of unstiffened and stiffened circular cylindrical shells. In addition, data on the postbuckling strength of stiffened cylinders were also limited. Because of the importance of the cylindrical shell in missile construction, an extensive investigation was initiated to provide such data. The present paper includes a description of the test techniques used in these investigations and some conclusions derived from the results.

Nomenclature

A = total sheet area ($2\pi rt$).
A_s = area of all stringers.
E = modulus of elasticity.
G = shear modulus.
L = length of cylinder.
R_p = ratio of internal pressure to critical external pressure (p/p_0).
R_s = ratio of critical shear stress with internal pressure to critical shear stress under torsion alone (τ/τ_0).
T_{cr} = panel buckling torque.
a = spacing of ring stiffeners.
b = spacing of stringers.
p = internal pressure.
p_0 = critical external pressure (considered negative).
r = radius of cylinder.
t = thickness of cylinder.
t_s = thickness of stringer material.
θ = angle of buckles with longitudinal axis of cylinder.
μ = Poisson's ratio.
σ_1 = longitudinal sheet stress.
σ_a = average axial stress (total end pressure load divided by area of skin and stringers).
σ_s = stringer stress.
τ = critical shear stress with internal pressure.
τ_0 = critical shear stress under torsion alone.

Introduction

In modern aircraft and missiles, extensive use is made of pressurized, unstiffened and stiffened circular cylindrical shell structures. Even though these shells may not be pressurized for structural purposes, systems requirements often dictate the use of internal pressure. Because internal pressure materially increases the buckling stress of circular shells, a considerable weight saving can be achieved by taking advantage of this increase in buckling strength.

When the experimental investigation described herein was initiated in 1951, test data on the effect of internal pressure on the stability of circular cylindrical shells were limited. The available data for both unstiffened and stiffened shells did not encompass the parameter ranges likely to be encountered in modern aircraft and missile structure. It was apparent that empirical data were required to obtain reliable design information. As a consequence, an extensive investigation of model circular cylindrical shells was initiated to provide some of these data.

A test jig was developed to apply axial compression, bending, torsion and external pressure, either singly or in combination. The jig also allowed the application of internal pressure. By proper dimensional scaling, model cylinders could be selected that were parametrically equivalent to full-scale structures. This equipment permitted the use of low-cost models in lieu of full-scale structure.

Initially, the unstiffened shells were fabricated from fiberglass or Mylar sheet. However, shortly after the beginning of the program, foil-gage aluminum and stainless steel became available and these materials were used in the majority of tests. Many of the specimens were fabricated with a single longitudinal, adhesive-bonded lap joint. Some of the later unstiffened cylinders were seam welded, which proved to be a satisfactory technique. Adhesive bonding was also used in the fabrication of the ring and stringer reinforced test shells. Unfortunately, the stiffened cylinders could not be used to study the ultimate strength of the shell because pre-

L. A. Harris is Supervisor, Structural Mechanics, Space and Information Systems Division, North American Aviation, Inc.; H. S. Suer is Section Head, Ground Systems Dynamics, Space Technology Laboratories, Inc. (formerly Senior Structures Engineer, S&ID); and W. T. Skene is Manager, Applied Research, Space and Information Systems Division, North American Aviation, Inc.
Paper was presented at 1959 SESA Spring Meeting held in Washington, D. C., on May 20–22.

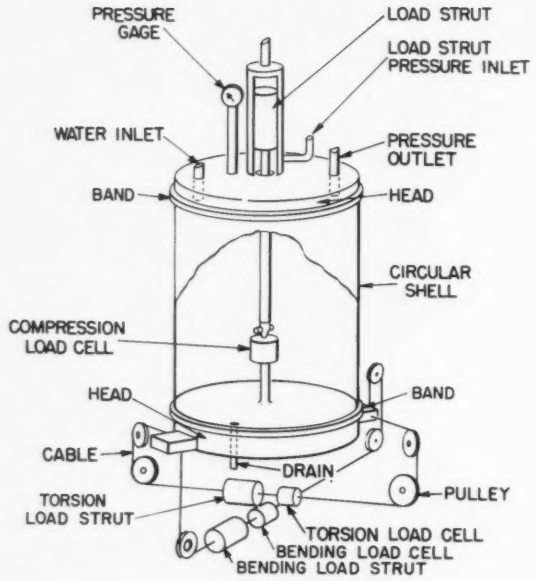

Fig. 1—Test-jig schematic

mature failure was induced in the bond between the skin and the stringers.

The present paper includes a description of the test techniques used in these investigations and presents the results of some of the tests.

Unstiffened Cylinders

Test Specimens

At the initiation of the investigation, metal foil was not available in large sizes and, as a result, the first specimens were fabricated from fiberglass or mylar with a single longitudinal, adhesive-bonded lap joint. Although the fabrication and testing of these specimens were satisfactory, it was found that the mechanical properties of these materials varied from specimen to specimen and consistent results were difficult to obtain. Early in the program, foil-gage 2S-H-18 aluminum alloy and 18-8 half-hard stainless steel became available in rolls up to 36 in. wide, and these materials were used to fabricate the specimens for the remaining tests.

Over 200 test cylinders were fabricated from stainless steel and aluminum-alloy foils. The cylinders were fabricated with a $^3/_8$-in. wide longitudinal lap joint bonded with Epon VI adhesive which was cured under pressure at 200° F. Use of adhesive bonding had the advantage that residual stresses were reduced. The bonded joint did not appear to interfere with the buckle pattern in any of the specimens. Some of the later test specimens were fabricated by seam welding, which proved to be a faster and simpler technique. Although some wrinkling occurred at the seam of the welded cylinders, no appreciable difference could be noted between the buckling stresses of the bonded and of the welded cylinders.

The test cylinders were fabricated from 0.005-inch-thick aluminum foil and 0.0032-, 0.004- and 0.0087-in. stainless-steel foil. These sheet thicknesses were the averages of a number of micrometer measurements, and the maximum variation in thickness from the mean was less than 10%. The cylinders were tested with unsupported lengths of 9.5 and 22.5 in. The length of the cylinder was perpendicular to the direction of rolling of the sheet material. Sample specimens of the foil were regularly tested to determine the modulus of elasticity and the compressive yield strength of the aluminum and steel. The modulus of elasticity used in evaluating the test data was 10.5×10^6 and 27.0×10^6 psi, respectively, for the aluminum and stainless-steel foils.

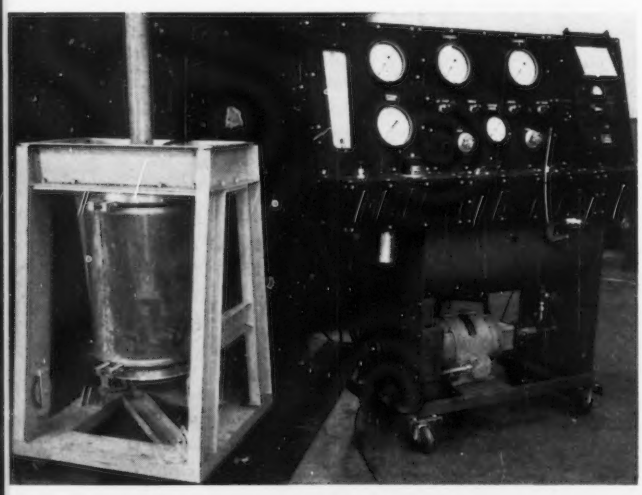

Fig. 2—Test apparatus with Mylar cylinder in position for test

Fig. 3—Ripples in pressurized torsion specimen prior to buckling

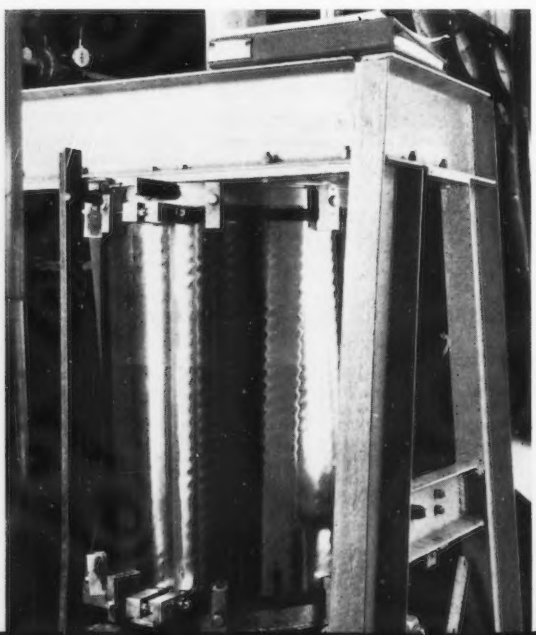

Test Apparatus and Procedures

A jig was developed to test circular cylinders $18^1/_2$ in. in diameter and of variable lengths. A schematic drawing of the jig is shown in Fig. 1, and a mylar cylinder is shown in position for testing in Fig. 2.

The test cylinders snugly fitted the lower and upper 3-in. aluminum heads of the test jig. The cylinders were pressed carefully onto these heads. The cylinder was placed on the lower head, and the internal strut and load cell were connected. The lower head was raised slowly by hydraulic pressure and, at the same time, the cylinder was guided on to the upper head of the jig. The cylinder was stabilized by a small internal pressure to prevent damage as it slipped over the upper head. As the lower head continued to rise, the position of the cylinder on the heads was carefully measured and the lower head was guided to keep the cylinder square on the heads.

Each cylinder was firmly clamped to the heads with rubber-lined steel bands which were tightened with bolts to a predetermined torque. To hold the cylinder more tightly to the heads, eight lugs were screwed against each band. The bands prevented slippage and leakage between the heads and the cylinder.

Compressive, bending and torsion loads were applied to the cylinder with hydraulic struts and were measured with Baldwin type U-1 SR-4 strain indicators. The axial strut and the load cell for compression are visible through the transparent mylar cylinder in Fig. 2. The bending moment or torque was applied to the bottom head by two cables which were activated by a hydraulic strut. The pulley-cable loading system for applying these loads is shown schematically in Fig. 1. Heavy-duty ball-bearing aircraft pulleys and $^1/_4$-in. steel cables were used to apply these loads. A check test indicated that the friction in the pulley system was negligible, which assured equal loads in both cables. Internal pressurization was pneumatically applied and was varied from 0 to about 24 psi. External pressure was applied by partially evacuating the cylinders.

The control console shown in Fig. 2 was used to regulate the strut pressures. The loads were measured by SR-4 load cells. Internal or vacuum pressure was generally measured by a 5-ft mercury manometer reading to 0.1 in. A Wallace-Tiernan dial manometer with a least reading of 0.05 in. of water was used to read low pressures.

Before applying any other load, a compressive force equal to the dead weight of the lower head of the test jig was applied to the specimen. In the bending and torsion tests, an additional compressive load could also be applied to the lower head to balance the longitudinal tension force applied by the internal pressure. For combined loadings, the order of application of loads had no effect on the magnitude of the critical stresses.

When the internal pressure exceeded 2 psi, the test cylinders were partially filled with water for safety purposes and the average internal pressure reported. The dead weight of the water was balanced by the central load strut.

The buckling loads of the test specimens were determined visually. For most specimens, a visual determination of the buckling load was relatively simple because the buckles often snapped in position. Occasionally buckles appeared to grow out of relatively large initial irregularities. Incipient buckling of a pressurized cylinder was often indicated by the formation of circumferential ripples. Although initially very shallow, these ripples could be seen easily in the reflected surface of the cylinder, as shown in Fig. 3 for torsion. The load at which buckles with well-defined longitudinal and transverse wave lengths

Fig. 4—Typical buckle pattern for unpressurized cylinder in compression

Fig. 5—Typical buckle pattern for pressurized cylinder in compression

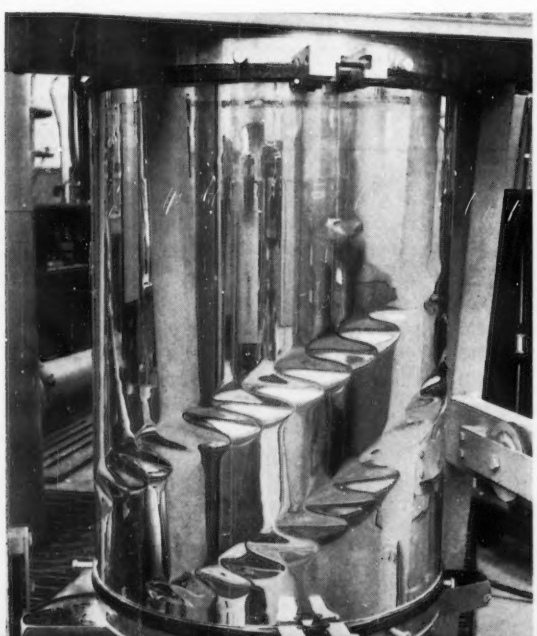

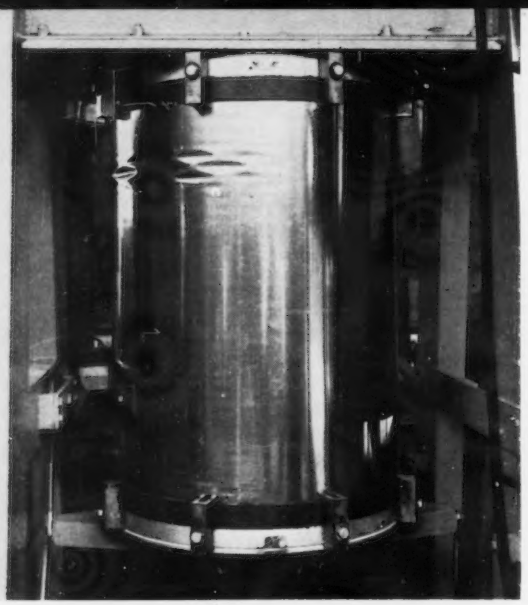

Fig. 6—Typical buckle pattern for pressurized cylinder in bending

Fig. 7—Typical buckle pattern for hydrostatic pressure

formed was always within 10% of the initial rippling. Just prior to buckling, the ripples often extended over the entire length of the cylinder.

The final buckle pattern extended only over a portion of the cylinder. In the case of pressurized cylinders, generally only one or two series of buckles occurred. The buckles appeared to be elastic and visually disappeared upon removal of the load. Some of the cylinders were retested with equal or larger internal pressure. Slightly lower values of critical stress were often obtained with equal pressure, indicating that some permanent distortion of the shell had occurred during the previous test.

Test Results

For the unstiffened cylinders, five loading conditions have thus far been studied: pressurized cylinders in compression, bending and combined compression and torsion; combined external pressure and torsion; and pressurized cylinders in torsion. The analysis of the data and recommended design curves for the first four of the loadings have been reported in previous papers.[1-4] Typical buckle patterns for these loading conditions are shown in Figs. 4 through 10. The results of the tests of pressurized cylinders in torsion are presented below.

The effect of internal pressure on the torsional buckling stress has been considered in two previous papers. Crate, Batdorf and Baab[5] developed a semi-empirical interaction formula, $R_p + R_s^2 = 1$, for combined pressure and torsion based on a limited series of tests. Hopkins and Brown[6] derived a small deflection theoretical analysis by modifying Donnell's original analysis for unpressurized cylinders. Their theoretical calculations generally agreed well with the experimental results of Reference 5 and sub-

TABLE 1—RESULTS OF TESTS OF UNSTIFFENED CYLINDERS IN TORSION
18-8 half-hard stainless steel, $E = 27 \times 10^6$ psi, r = 8.75 in., L = 22.5 in.

Specimen No.	r/t	p, psi	τ, psi	θ, deg	Specimen No.	r/t	p, psi	τ, psi	θ, deg
				Unpressurized					
112-1	1006	0	2162	..	95-1	2734	0	569	..
114-1	1006	0	2256	18	223-1	2734	0	250	10
94-1	2734	0	487	..	..	..	..	..	..
				Pressurized					
204-1	1006	4.4	7407	30	109-1	2734	2.4	4688	45
205-1	1006	4.4	7168	..	105-1	2734	4.4	6173	..
203-1	1006	8.4	9582	45	106-1	2734	8.4	10559	..
206-1	1006	8.4	9295	..	266	2734	8.4	9542	70
202-1	1006	16.4	14600	45	267	2734	8.4	9502	70
207-1	1006	16.4	12903	45	268	2734	8.4	9542	65
217-1	1006	20.4	14409	50	107-1	2734	16.4	14620	..
218-1	1006	20.4	14791	55					

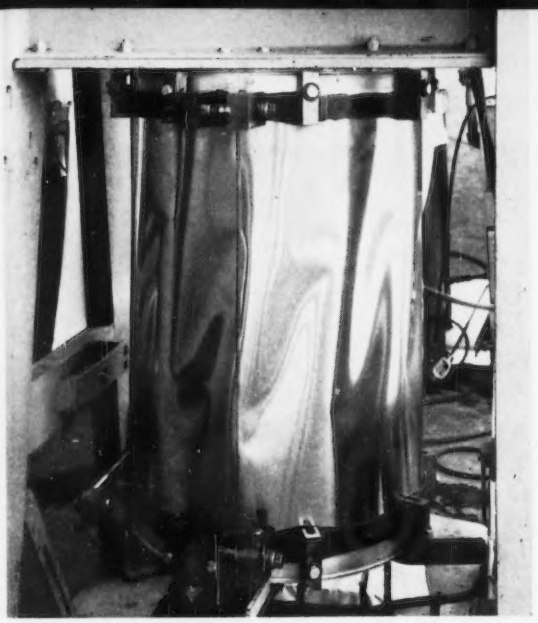

Fig. 8—Typical buckle pattern for combined torsion and external pressure

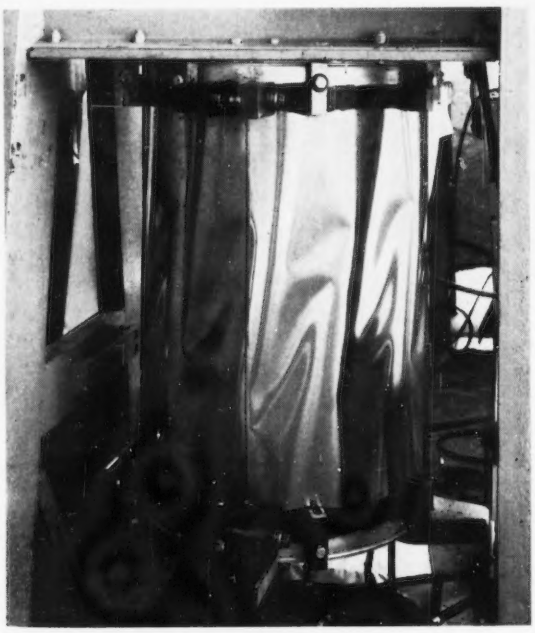

Fig. 9—Typical buckle pattern for unpressurized cylinder in torsion

Fig. 10—Typical buckle pattern for pressurized cylinder in torsion

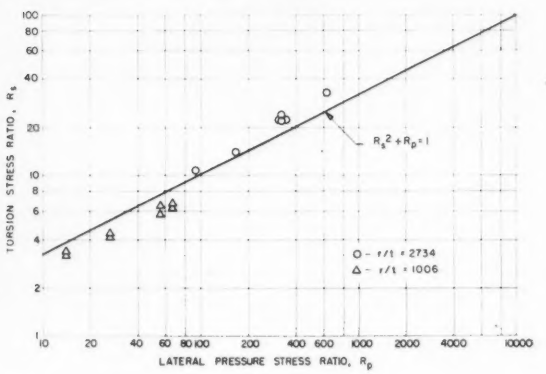

Fig. 11—Interaction curve for cylinders in torsion with lateral internal pressure

stantiated the semi-empirical interaction curve. The present investigation was made to extend the test data to the range of internal pressures and radius to thickness ratios of current interest in missile and aircraft design.

A total of 5 unpressurized and 15 pressurized model circular cylinders were tested in torsion. For the internally pressurized specimens, the longitudinal tensile stresses induced by pressure were balanced by a compressive load. The geometry of the cylinders and the test data are given in Table 1. A photograph of a typical buckle pattern for an unpressurized cylinder is shown in Fig. 9 and for a pressurized cylinder in Fig. 10. As expected, the angle which the buckles made with the axis of the cylinder increased as the ratio of the internal pressure to the torque increased (refer to Table 1).

In Fig. 11, the test data are compared to the interaction curve of Reference 5. In calculating the val-

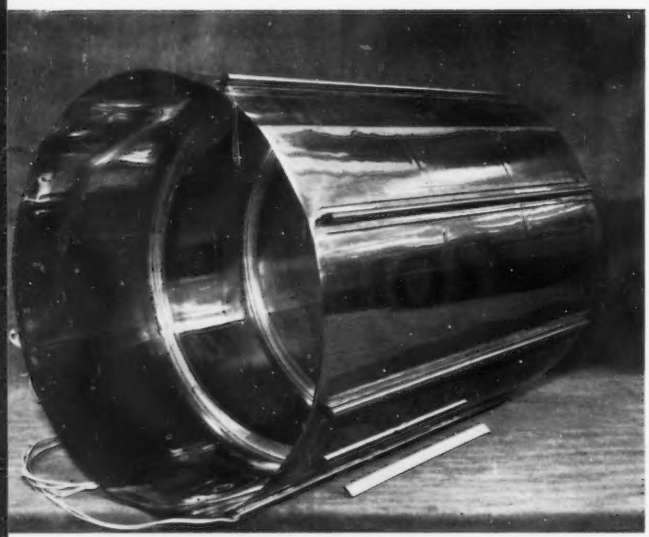

Fig. 12—Model stiffened cylinder

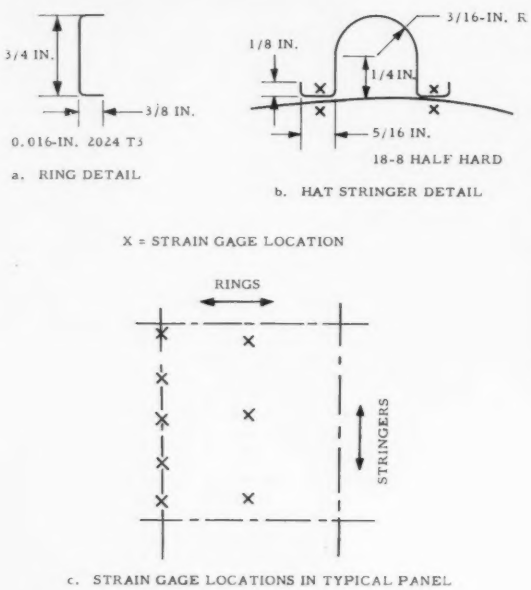

Fig. 13—Stiffener details and strain-gage locations

ues of R_s, the buckling stress for torsion alone has been defined as the average of the experimental values. In calculating the values of R_p, the buckling stress for external lateral pressure alone has been calculated from Reference 7. It may be seen in Fig. 11 that the interaction curve adequately describes the behavior of circular cylinders in torsion with internal lateral pressure. Based on the present data, the interaction curve of Fig. 11 is recommended for design within the range of parameters investigated.

It should be noted that the experimental data of Fig. 11 are for cylinders under lateral pressure only and, therefore, the data indicate the direct benefit of

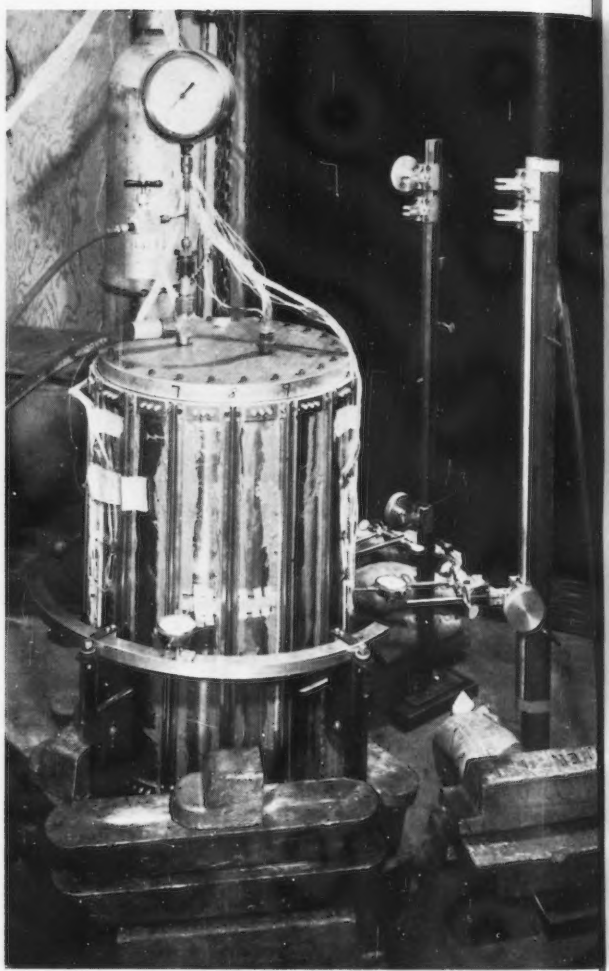

Fig. 14—Test setup for internal pressurization of stiffened cylinders

internal lateral pressure on the torsional buckling stress. If, in addition, the cylinder is axially pretensioned to a stress of $pr/2t$ by the internal pressure on the cylinder heads, an additional benefit would result. It can easily be shown by a Mohr's circle construction that a torsional stress of $0.707\ pr/t$ is required before compression is induced in the skin of a hydrostatically pressurized cylinder. At low values of pr/t, the benefit of the axial tension is relatively small but, at large values of pr/t, the effect of the axial stress induced by internal pressure would be expected to predominate.

Stiffened Cylinders

Whereas unstiffened cylinders can be scaled by reducing the thickness of the skin, radius and length, a proper scaling of stiffened cylinders requires also a scaling of rings, stringers and attachments. This has been difficult to accomplish inexpensively. Scaling of the attachments is especially difficult.

TABLE 2—RESULTS OF TESTS OF STIFFENED CYLINDERS

Specimen No.	t, in.	t_s, in.	p, psi	a, in.	b, in.	T_{cr}, kip-in.	θ, deg	G(psi) Before T_{cr}	G(psi) After T_{cr}
1	0.0087	0.0087	40.4	7.08	2.75	..	..	..	..
2	0.0087	0.0087	40.4	7.08	2.75	..	..	..	..
3S	0.0032	0.0032	3.7	7.08	6	10	45	11.0×10^6	[b]
4S	0.0032	0.0032	0	7.08	6	[b]	20	[b]	1.0×10^6
			1			3/5.5[a]	35	10.9×10^6	1.0×10^6
			2			6/9	40	8.6×10^6	1.0×10^6
5S	0.0032	0.0032	3.7	7.08	6	10/15	40	9.47×10^6	1.0×10^6
6S	0.0087	0.0087	0	14.7	6	7/7	15	[b]	1.2×10^6
7S	0.0087	0.0087	8.4	14.7	6	50[b]	40	9.5×10^6	[b]
8S	0.0032	0.0087	0	14.7	6	[b]	15	[b]	1.6×10^6
9S	0.0032	0.0087	3.4	14.7	6	10/13	35	8.7×10^6	1.8×10^6
10S	0.0087	0.0087	4.3	14.7	6	32/38	35	11.8×10^6	0.9×10^6
11S	0.0087	0.0087	4.3	14.7	6	31/39	30	10.3×10^6	0.8×10^6
								10.0×10^6 (average)	1.1×10^6 (average)

[a] The lower torque is the initial buckling and the high torque is obtained from the interaction of the load deflection curves in the unbuckled and the buckled states.
[b] Insufficient data.

The present tests were initiated to investigate the feasibility of fabricating small-scale models economically by adhesive-bonding techniques. In particular, the use of adhesive bonding considerably simplifies the attachment of the stiffeners to the shell.

Two problems were chosen for study in this pilot series: (1) the stress distribution in the stringers and skins of pressurized stiffened cylinders and (2) the tension-field behavior of unpressurized and pressurized stiffened cylinders. The data obtained were the stress distribution due to internal pressure and/or torsion, the panel buckling torques, and the effect of internal pressure on the torque-rotation relationship. It was intended to obtain data on the ultimate strength and mode of failure but premature failures of the adhesive bond occurred. Described herein are the fabrication of the model cylinders, the test equipment and procedures, and the test results.

Test Specimens

A photograph of a typical test specimen is shown in Fig. 12. The cylinders were fabricated from 0.0032- and 0.0087-in. thick, half-hard 18–8 stainless-steel foil. They had a length of $22^1/_2$ in., a radius of 8.75 in. and r/t ratios of approximately 1000 and 2730. The stringers were formed from the same material to the shape shown in Fig. 13. The ring stiffeners were formed from 2024-T3 aluminum alloy to the cross section shown in Fig. 13. The location of the internal rings and the number of external stringers were varied during the test program. Table 2 summarizes the important dimensions of the cylinders.

The fabrication sequence for the shells was as follows: (1) the longitudinal seam of the shell was bonded, (2) the hat-section stringers were bonded to the outside surface of the shell and (3) the aluminum rings, which were split to allow a reduction in diameter for insertion inside the cylinder, were then bonded in place. Rings, stringers and cylinders were bonded under temperature and pressure with Epon VI adhesive.

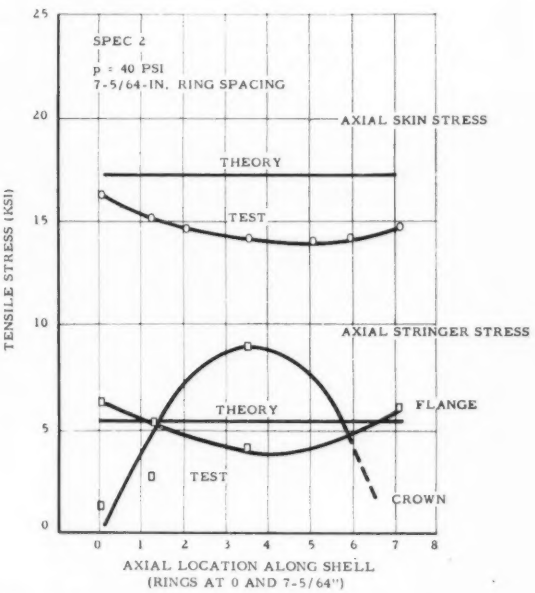

Fig. 15—Stress distribution from internal pressure

Test Apparatus and Procedures

For the tests to investigate the stress distribution under pressure alone, both the sheet and the stringers were bolted to 1-in.-thick heads, as shown in Fig. 14.

Doubler strips and fittings were used at the ends to provide sufficient contact area. The test jig used for the torsion tests of stiffened cylinders was the same as that described for unstiffened shells, with clamps to bolt the stringer ends to the top and bottom heads. The clamps were required to transfer the high-tension-field stringer loads to the heads.

Strain rosettes were placed back-to-back on the skin panels, and six axial gages were mounted across sections of the stringer between rings. A typical strain-gage layout is shown in Fig. 13. One of the strain gages was located on the inside of the hat section and becomes inaccessible during subsequent fabrication of the shell. As a consequence, this gage was mounted and the wires were attached and insulated before assembly of the test specimen. For most specimens, strain gages were located at five sections along the stringers between rings.

For the torsion specimens, dial indicators were used to measure the rotation of the movable lower head of the jig with respect to the upper fixed head. These measurements were used to establish the torque-rotation relationships.

Fig. 16—Buckle pattern for pressurized stiffened cylinders in torsion

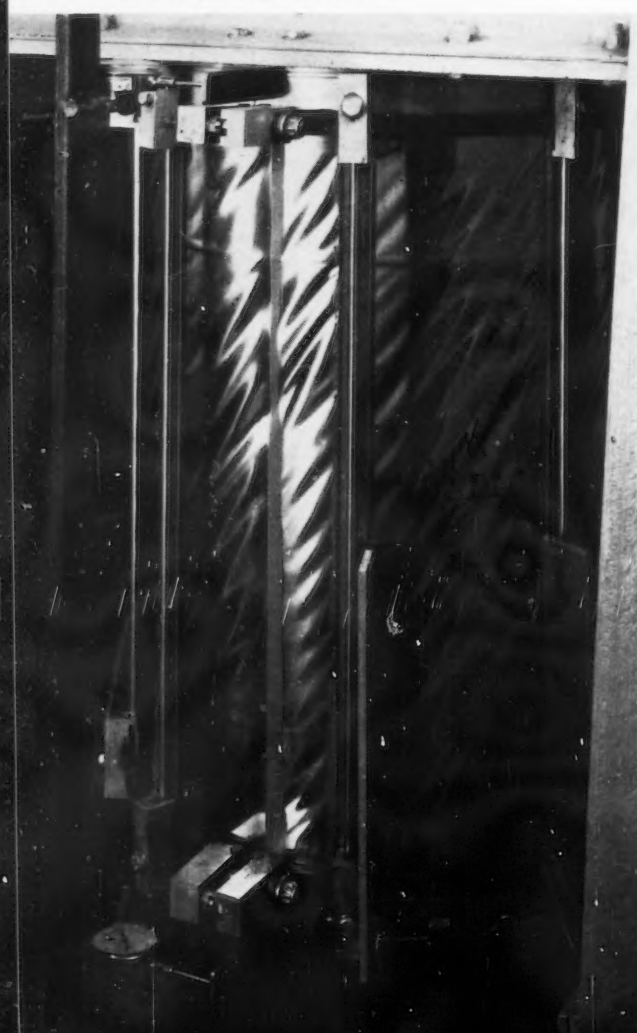

Test Results

STRESSES INDUCED BY INTERNAL PRESSURE—A comparison between theory and test is shown in Fig. 15 for a typical specimen. The data shown are the relationships between the axial sheet and stringer stresses as a function of the distance between rings. Crown and flange stresses are shown for the stringer. Internal pressure causes an outward bowing of the stringers between rings as indicated by the crown and flange stresses.

Theoretical predictions of the longitudinal sheet and average stringer stresses, neglecting stresses induced by compatibility of strains between stringers, rings and sheet, are shown in Fig. 15. The analysis[8] is based on equal axial deformations for the sheet and the stringers which gives

$$\sigma_1 = \sigma_a\left\{1 + 2\frac{A_s}{A}\right\}$$
$$\sigma_s = \sigma_a(1 - 2\mu)$$

Note that the average longitudinal sheet and stringer stresses are not equal. This inequality is a result of the Poisson's ratio effect which occurs in the sheet under biaxial tension but is absent in the longitudinally stressed stringers.

Good agreement was found between test and theory for the midspan average stringer stress, but the stresses adjacent to the rings are significantly different than predicted. The experimentally determined axial skin stress is a maximum of about 25% less than predicted.

TENSION-FIELD BEHAVIOR—For this series of specimens, the torque was applied after the cylinder had been pressurized. A photograph of highly developed tension-field buckles in a typical specimen is shown in Fig. 16.

The torsional rigidity of the prebuckled and postbuckled cylinders was studied by measuring the rotation of the lower end of the cylinder with respect to the upper fixed end. Table 2 summarizes the data from the cylinders under torsion. Plots of the torque-rotation data for one configuration are shown in Fig. 17. It is significant to note that the torsional ridigities of both the unpressurized and the pressurized shell are approximately the same after, as well as before, panel buckling. The torque at which buckling occurs is increased, of course, as the internal pressure is increased (refer to Table 2). The shear modulus of the unbuckled shells averaged 10.0×10^6 psi for all the specimens, whereas the theoretical value, $G = E/2\ (1 + \mu)$, would be 10.5×10^6 psi. The shear rigidity calculated from the postbuckling portion of the curve averaged 1.1×10^6 psi and appeared to be the same as for the unpressurized shell at pressures up to 3.7 psi.

The stringer stress distribution caused by diagonal tension is shown in Fig. 18 for a cylinder with a 0.0032-in.-thick skin, 0.0087-in.-thick stringer material and an aspect ratio of about 2. The effect of torque on the stringer stress is negligible until sheet buckling occurs. Then, diagonal tension in the sheet significantly increases the stringer axial stresses and

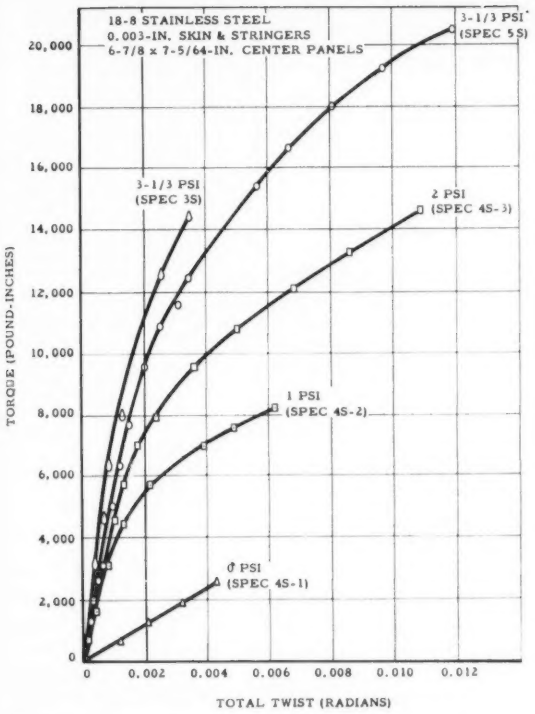

Fig. 17—Typical torque-rotation results for stiffened cylinders

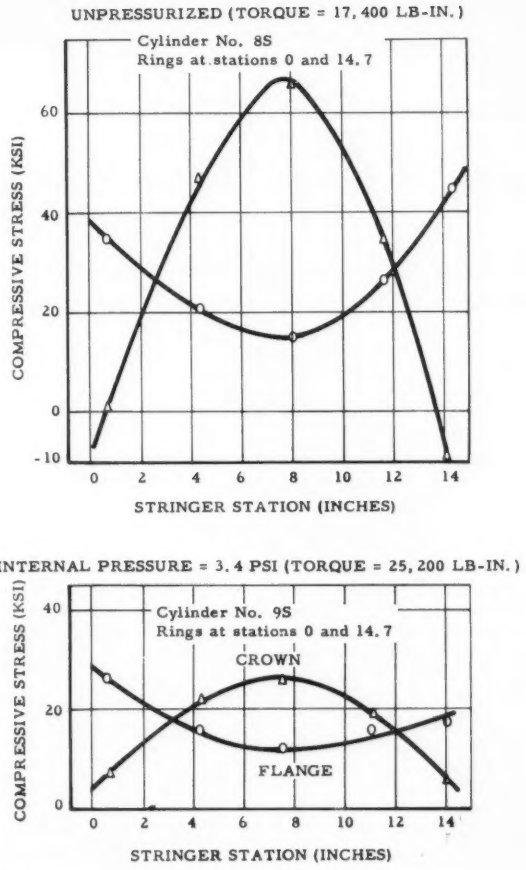

Fig. 18—Typical diagonal tension stringer stresses

applies an inward radial load which causes bending in the stringer. In Fig. 18 are shown graphs of stringer stresses induced in unpressurized and pressurized cylinders by tension-field action. Note that the distribution of the bending stress caused by torsion of the unpressurized cylinder is similar to that caused by internal pressure, but is of the opposite sign. As a consequence, the diagonal tension stringer axial and bending stresses are partially relieved by the internal pressure axial and bending stresses, as indicated in Fig. 15. This partial balancing of stresses may have important beneficial effects in those cases in which forced crippling of the compression side of the stringer precipitates ultimate failure of the stiffened shell.

It was intended that the test specimens should provide data on the ultimate strength as well as the stringer and skin stress distribution before and after buckling of the panels. However, most of the specimens failed prematurely either in the longitudinal seam or as a result of buckles forcing their way under the stringers and destroying the adhesive-bonded joint. Although difficulties of this kind were encountered, it is nevertheless believed that proper design of the test specimen and the use of the proper adhesive would make the specimens useful for studies of ultimate failures.

Acknowledgment

The authors gratefully acknowledge the assistance of the personnel of the Missile Division Laboratory.

References

1. Harris, L. A., Suer, H. S., Skene, W. T., and Benjamin, R. J., "The Stability of Thin-Walled Unstiffened Circular Cylinders Under Axial Compression Including the Effects of Internal Pressure," Jnl. Aero. Sci., 24, No. 8, 587–596 (August 1957).

2. Suer, H. S., Harris, L. A., Skene, W. T., and Benjamin, R. J., "The Bending Stability of Thin-Walled Unstiffened Circular Cylinders Including the Effects of Internal Pressure," Ibid., 25, No. 5, 281–287 (May 1958).

3. Harris, L. A., Suer, H. S., and Skene, W. T., "The Effect of Internal Pressure on the Buckling Stress of Thin-Walled Cylinders Under Combined Axial Compression and Torsion," Ibid., 25, No. 2, 142–143 (February 1958).

4. Suer, H. S., and Harris, L. A., "The Stability of Thin-Walled Cylinders Under Combined Torsion and External Lateral or Hydrostatic Pressure," Jnl. Appl. Mech., 81, series E, No. 1, 138–140 (March 1959).

5. Crate, H., Batdorf, S. B., and Baab, G. W., "The Effect of Internal Pressure on the Buckling Stress of Thin-Walled Circular Cylinders Under Torsion," NACA L4E27, May 1944.

6. Hopkins, H. C., and Brown, E. H., "The Effect of Internal Pressure on the Initial Buckling of Thin-Walled Circular Cylinders Under Torsion," British Aeronautical Research Council, R&M No. 2423, January 1950.

7. Batdorf, S. B., "A Simplified Method of Elastic-Stability Analysis for Thin Cylindrical Shells," NACA Report 874, 1947.

8. Martin, V. I., and Smith, N. Y., "Relation Between Stringer Stress and Longitudinal Sheet Stress in a Reinforced Cylindrical Shell Under Internal Pressure," Aerophysics Laboratory Report PDM-8, North American Aviation, Inc., October 1950.

Damping Characteristics of Pipes Vibrating in Flexure and Filled with Various Materials

Tests indicate that, in general, filling a pipe in flexure with any material, liquid or solid, increases its damping characteristics

by Ahmed Ezzat

ABSTRACT—Tanks and pipes vibrating in flexure and filled with various materials have been a problem in power plants, factories, airplanes and tankers. The present experimental investigation was carried out on a pipe vibrating in flexure and filled with various materials, both liquid and solid. The tests showed that, in general, filling a pipe in flexure with any material, liquid or solid, increases its damping characteristics. An increase in the kinematic viscosity of the filling liquid, or a decrease in the size of the particles of the filling solid, will result in a corresponding increase in the equivalent damping factor of the system.

General Objective of Work

Vibrating tanks and pipes are frequently encountered in every-day engineering practice. In power plants and factories, as well as in airplanes and tankers, vibrations are transmitted to pipes and tanks which are filled with various fluids. The main objective of this work is to study experimentally the effect on the damping characteristics for flexural vibrations of filling a pipe with various materials.

Experimental Equipment

The experimental equipment comprises a 5-lb Calidyne shaker connected to a power supply and a variable frequency oscillator. An aluminum alloy pipe $1^5/_8$ in. diam, 36 in. long and 2.4 lb in weight was supported on two swivel bearings mounted on a rigid steel frame. One end was closed and the other end was fitted with a screw plug which permitted filling it with various materials. The pipe was centrally placed over the shaker plate which was fitted with an aluminum T section. This was fixed in such a position that its web would be normal to the axis of the pipe and just touching its lower part. The function of the web of the T-section was to strike the pipe at its center, thus transmitting the vibrations from the shaker plate to it. A sensitive millivoltmeter was used to register the voltage output of the shaker pickup coil which is proportional to the velocity of the shaker plate. The assembly of the experimental equipment is shown in Fig. 1.

Shaker Equipment

The shaker and the associated power supply and the variable frequency oscillator have been matched to provide sinusoidal mechanical excitation over a wide range of frequency. The control cabinet associated with the shaker contains three chassis units comprising the complete power supply system for the shaker. The top chassis contains the d-c field supply for the shaker, and the field current is maintained constant throughout the whole range of testing. The bottom chassis contains the variable frequency signal source, a Hewlett-Packard 202D oscillator having a frequency range from 2 to 70,000 cps. The shaker amplitude and frequency were controlled from the panel of this chassis. The middle chassis contains the model 8 S power amplifier, the output of which is coupled to the shaker-armature connection through a Variac (a constantly variable auto-transformer) and an armature-current indicator.

Shaker

This is a model 6 Calidyne shaker with an armature suspended on strap flexures to maintain the alignment of the armature coil in the air gap. The electrical connection of the shaker to the control cabinet is made by means of five-conductor cable. The cable supplies both the d-c field and the a-c armature current and also a ground connection. The shaker is mounted on a concrete block which is held by four stiff springs and eight rubber pads to a steel framework. The velocity of the armature is established by a voltage generated by a special coil, designed for this purpose, which moves in this magnetic field.

Experimental Procedure, Results and Discussion

The pipe was mounted in its proper position over the shaker plate, touching the top end of the T-

Ahmed Ezzat is Associate Professor, Faculty of Engineering, Cairo University, Cairo, Egypt.

Paper was presented in 1958 at SESA Spring Meeting held in Cleveland, Ohio, May 14–16.

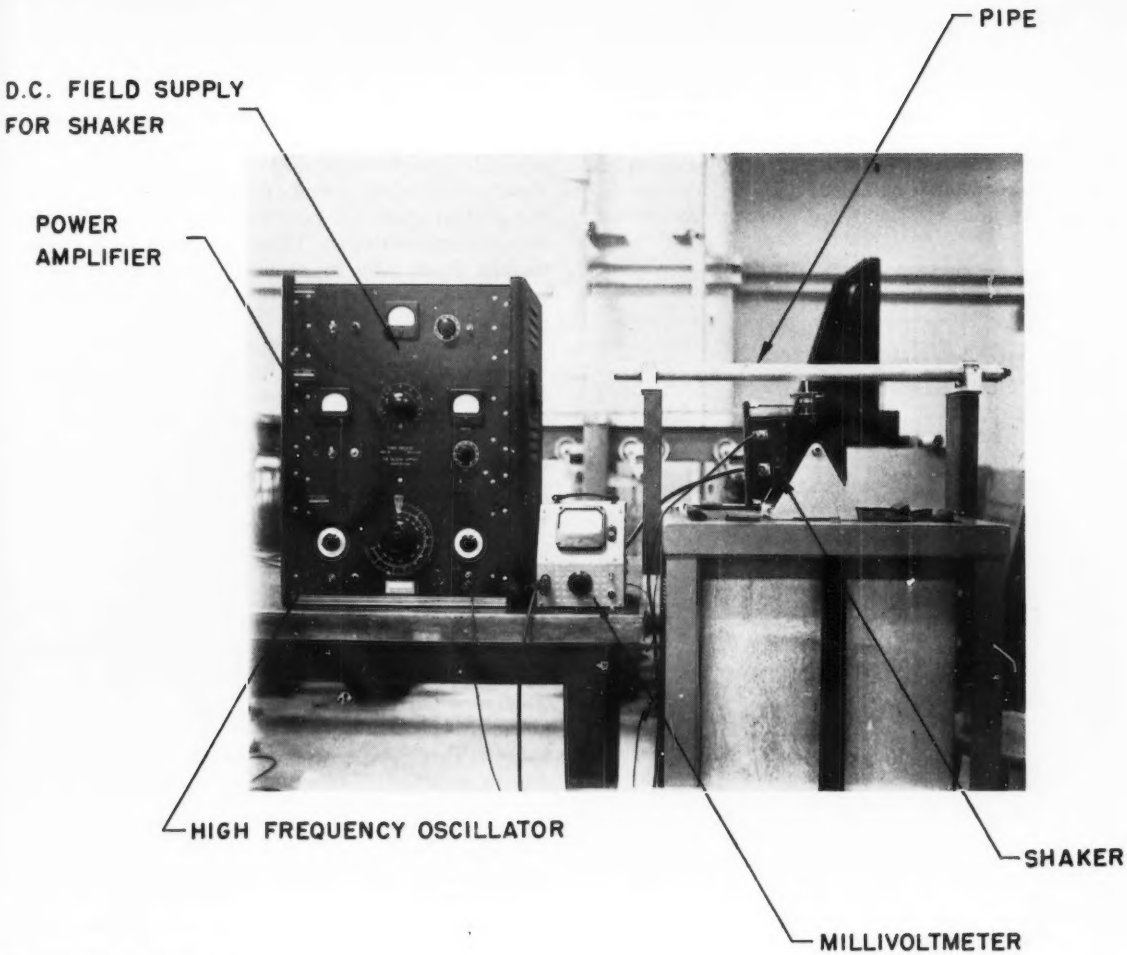

Fig. 1a—Experimental equipment

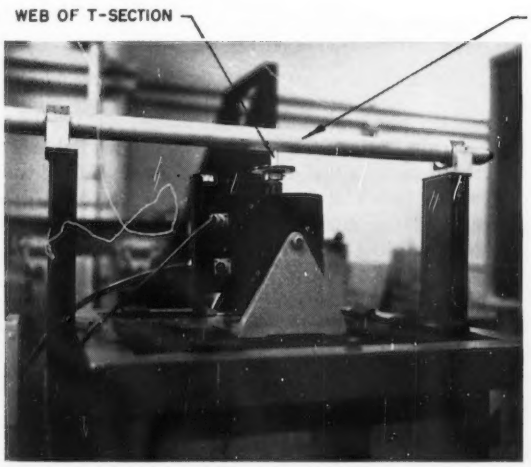

Fig. 1b—Close-up of pipe and shaker

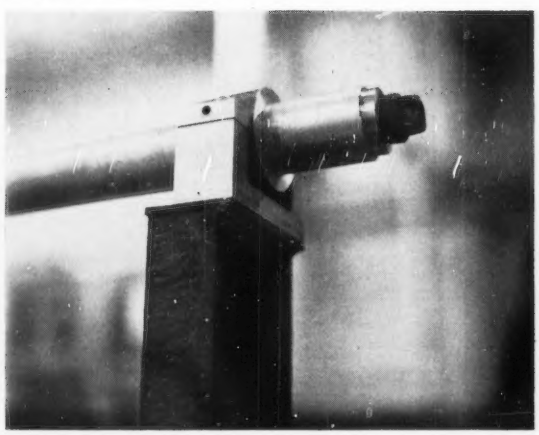

Fig. 1c—Swivel support

section web and the equipment was adjusted to have maximum power amplification together with optimum conditions of operation. The amplitude was adjusted to a certain suitable value and the frequency was increased. The values of the shaker output voltage in volts were recorded at each corresponding frequency setting. This was repeated both on increasing and decreasing frequencies to detect for the consistency and repeatability of the recorded values.

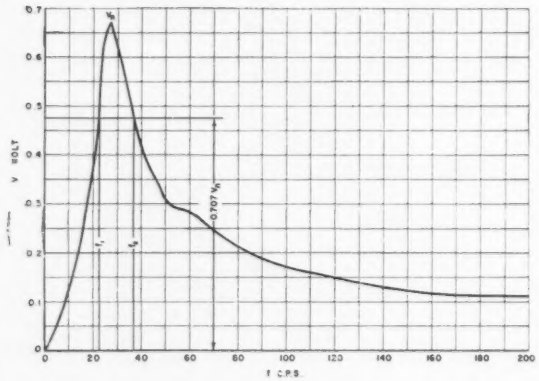

Fig. 2—Tests with pipe empty

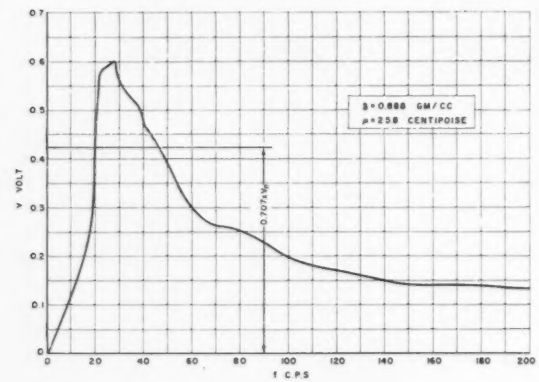

Fig. 3—Tests with pipe full of light lubricating oil

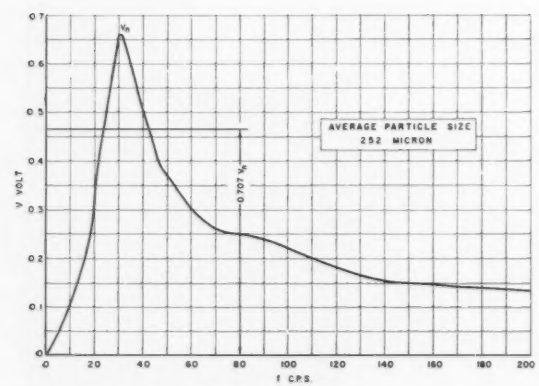

Fig. 4—Tests with pipe full of C-109 sand

In the neighborhood of the apparent maximum readings, very small increments in frequency were provided to define the resonant frequencies with an error of less than 0.5 cps.

This procedure was carried out with the pipe empty and in a similar way it was repeated with the pipe full of various materials. It is to be noted here that, on the whole range of experiments covered in the present work, the pipe was supported at hinged ends (swivel bearings) This condition was preferred mainly to be able to keep the end conditions as similar as possible when dismantling and returning the pipe in position.

A variety of materials was used to fill the pipe. To determine the effect of liquids upon its damping characteristics, the pipe was filled with liquids of different densities and viscosities, namely, water, fuel oil, light lubricating oil and heavy lubricating oil. The effect of solid substances in its damping characteristics was determined by packing the pipe with $^3/_8$-in. granite gravel and two different grades of Ottawa sand (C-190 and C-109, respectively).

The curve correlating the frequency to the voltage output of the shaker coil was drawn for each case. Figures 2, 3, and 4 show three typical curves representing three tests carried out (1) with the pipe empty, (2) with the pipe filled with light lubricating oil (δ = 0.888 g/cc and μ = 258 centipoise) and (3) with the pipe filled with C-109 Ottawa sand. For each case the value of ζ_e = the equivalent damping factor of the system is computed by using the formula:

$$\zeta_e = \frac{f_2 - f_1}{2f_n}$$

where f_2 and f_1 are the frequencies at $0.707V_n$, f_n is the resonant frequency of the system; $\zeta_e = C_e/C_{c_e}$ and V_n = the volt reading, at resonance, of the shaker coil; C_e is the equivalent damping coefficient of the system and C_{c_e} is its equivalent critical damping coefficient.

If K_e is the equivalent spring constant of the system, then

$$f_n = \frac{1}{2\pi}\sqrt{\frac{K_e}{m}}$$

and $K_e = 0.1025\ W\ f_n^2$ lb/in.

$$C_e = 2m\ \zeta_e\ \omega_n = 0.0325\ W\zeta_e f_n, \text{ lb/in. per sec.}$$

From the previous relations the values of C_e, C_{c_e} and K_e were also calculated and tabulated in Table 1.

From Figs. 2, 3 and 4 it is seen that, on filling the pipe with either a liquid or a solid, the value of V_n decreases and the curve flattens. Both changes contribute to an increase in the value of the equivalent damping factor ζ_e of the system.

In Figs. 5 and 6, the values of the gain in the equivalent damping factor of the system $\Delta\zeta_e$ are drawn on a semilogarithmic basis, against the viscosity for filling fluids and against particle size in case of solid substances.

In the former case, it is obvious that a steady uniform increase in $\Delta\zeta_e$ is obtained with increase in the viscosity of the filling fluid.

TABLE I—RESULTS OF TESTS WITH EMPTY PIPE AND WITH FILLED PIPE

Description	μ, Centipoise	δ, gm/cc	ν, in. sec $\times 10^{-6}$	f_n, cps	V_n, volts	f_2, cps	f_1, cps	ζ_e	W, lb.	C_e, lb/in. ps	C_{ce}, lb/in. ps	K_e, lb/in.	$\Delta\zeta_e$	ΔC_e, lb/in. ps	ΔC_{ce}, lb/in. ps	ΔK_e, lb/in.	$\Delta K_e \cdot \delta$ lb^2/in.^{4}
Empty pipe	...	...	...	28	0.67	37	23	0.25	2.4	0.55	2.2	193	0	0	0	0	0
Pipe full of:																	
Water	1	1	48.2	24	0.60	41	21	0.406	4.7	1.485	3.65	277	0.156	0.935	1.45	84	3.13
Fuel oil	11.4	0.84	650	27	0.59	44	20	0.445	4.35	1.70	3.82	325	0.195	1.15	1.62	132	4.01
Light lubricating oil	258	0.888	14,000	27	0.60	46	20	0.482	4.44	1.88	3.90	330	0.232	1.33	1.72	137	4.38
Heavy lubricating oil	740	0.904	39,400	27	0.54	48	20	0.522	4.51	2.09	4.00	338	0.272	1.54	1.8	145	4.75
Pipe full of:	Particle size, mm, average																
Granite gravel	9.55	1.56	...	28	0.67	42	26	0.286	6.0	1.56	5.45	484	0.036	1.01	3.25	291	16.4
C-190 Ottawa sand	0.59	1.72	...	31	0.62	42	23	0.306	6.35	1.96	6.4	625	0.056	1.41	4.2	432	27.0
C-109 Ottawa sand	0.252	1.69	...	31	0.67	43	22	0.338	6.30	2.15	6.35	620	0.088	1.60	4.15	427	26.1

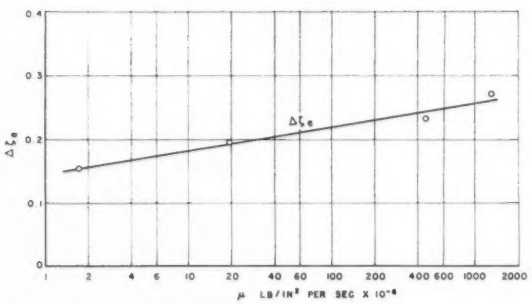

Fig. 5—Change in equivalent damping factor, ζ_e, due to change in viscosity of filling liquid

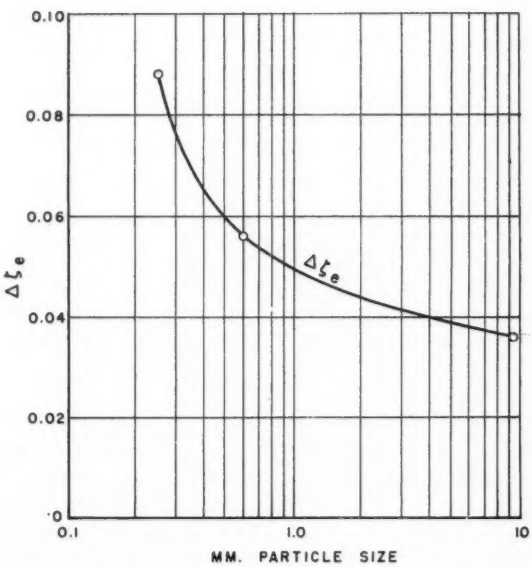

Fig. 6—Rate of change of equivalent damping factor with particle size of filling solid material

It was thought that the density δ of the fluid might have an effect and hence Fig. 7 was drawn on a semilogarithmic basis showing the changes in $\Delta\zeta_e$ with the kinematic viscosity* for the filling fluid ν. It is noticed that the two curves are almost similar in behavior which might suggest, to some extent,

* *Kinematic viscosity is the ratio of viscosity to density.*

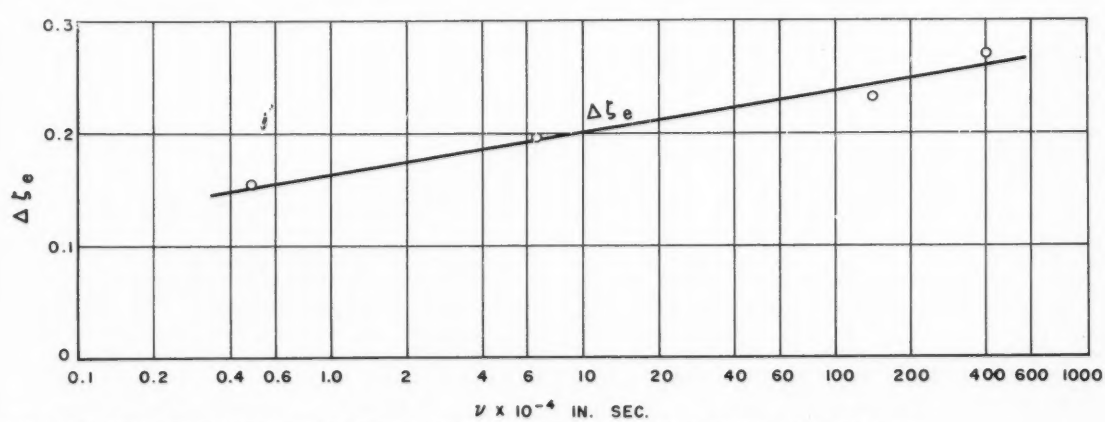

Fig. 7—Change in equivalent damping factor, ζ_e, due to change in kinematic viscosity, ν, of filling liquid

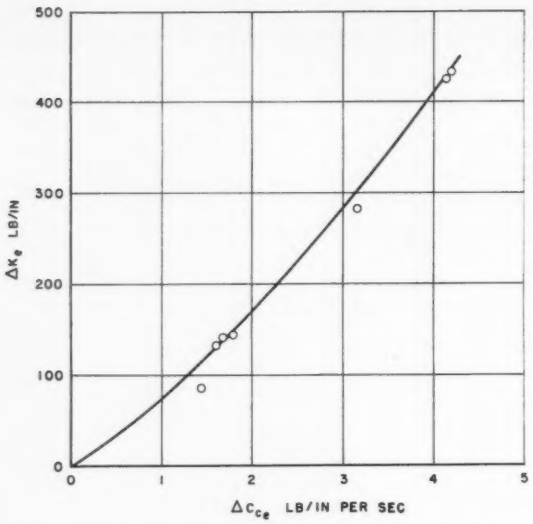

Fig. 8—Change in equivalent critical damping coefficient, C_{ce}, accompanying change in equivalent spring constant, K_e, of system, owing to filling the pipe with liquid or solid material

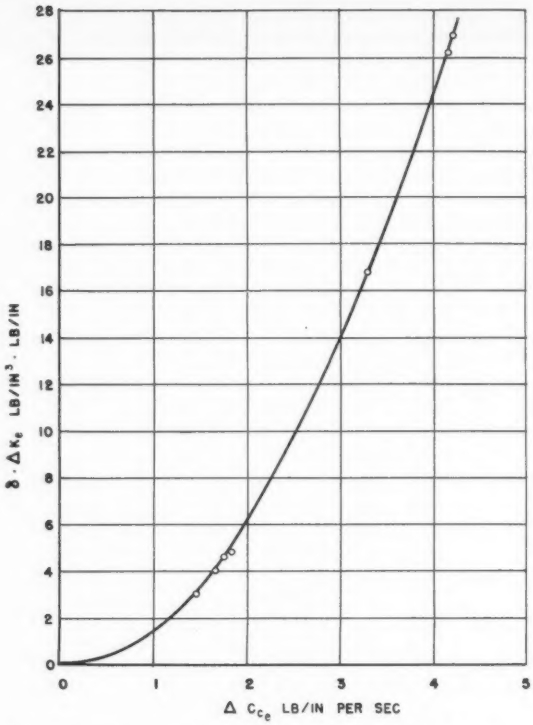

Fig. 9—Change in equivalent critical damping coefficient, C_{ce}, with joint change in equivalent spring constant, K_e, and density, δ, of filling material

the independence of $\Delta\zeta_e$ of δ. However, it is recalled that

$$\zeta_e = \frac{C_e}{C_{c_e}}$$

and that

$$C_{c_e} = 2m\cdot\omega_n \quad \text{or} \quad C_{c_e} = 2\frac{W}{g}\sqrt{\frac{gK_e}{W}}$$

and hence $C_{c_e} = A\sqrt{W.K_e}$ which points out that ζ is indirectly affected by the density of the fluid, through its effect upon C_{c_e}.

This favored the plotting of the changes in the equivalent critical damping coefficient ΔC_{c_e} against ΔK_e in Fig. 8 and against the product $\delta\cdot\Delta K_e$ in Fig. 9. It can be seen that the increase in the equivalent spring constant ΔK_e is necessarily accompanied by a slight increase in the equivalent critical damping coefficient ΔC_{c_e} (Fig. 8). On the other hand, it is perceived that to obtain a big increase in C_{c_e}, a large increase in the product $\delta\cdot\Delta K_e$ is essential.

Plotting the change in both C_e and C_{c_e} against the kinematic viscosity ν revealed the fact that they both behave in an almost similar manner, resulting in a steady increase in $\Delta\zeta_e$ with increase in the kinematic viscosity of the filling fluid. ΔC_{c_e} and ΔC_e both increase with increasing kinematic viscosity but it seems that the rate of increase in C_e is more than that noticed with C_{c_e}. Since the fluids used change considerably in viscosity while the change in their densities is very small, it seems reasonable to state that the equivalent coefficient of damping C_e is dominantly affected by the change in viscosity, while C_{c_e} is affected by the change in density.

In the case of filling the pipe with solid material, it can be concluded that the increase in the particle size decreases the gain in ζ_e and C_e of the system. This might be due to the fact that the smaller the particles are, the more is the friction and consequently the better is the damping characteristic of the system.

Conclusions

1. In general, the filling of a pipe in flexure with any material, liquid or solid, increases its damping characteristic. In other words, the equivalent damping factor ζ_e, the equivalent critical damping coefficient C_{c_e} and the equivalent damping coefficient, C_e, all increase in magnitude.

2. The equivalent spring constant of the system K_e increased on filling the pipe with liquid or solid material. However, the rate of increase in K_e, when the pipe is filled with a liquid, increases with the increase in the kinematic viscosity ν up to a certain value after which it begins to be hardly affected with further increase in ν (Fig. 12).

3. Generally speaking, the equivalent critical damping coefficient of the system C_{c_e} increases as the product $\delta\cdot\Delta K_e$ increases, but a large increment in $\delta\cdot\Delta K_e$ is necessary to effect a noticeable increase in C_{c_e} (Figs. 8 and 9).

4. The increase in kinematic viscosity of the filling liquid results in a corresponding increase in the

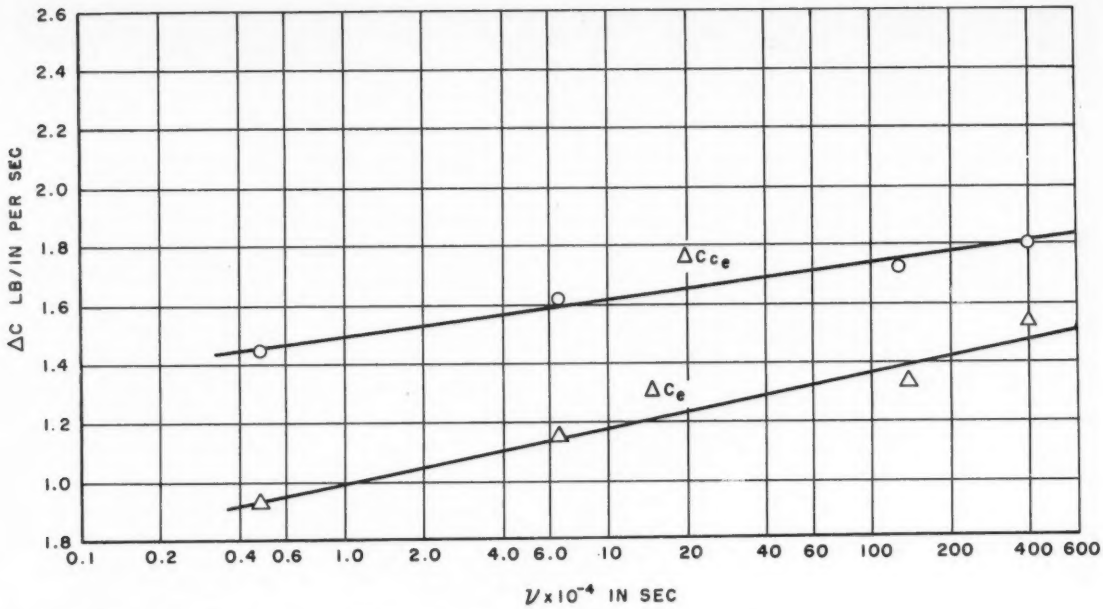

Fig. 10—Effect of change in kinematic viscosity, ν, of filling liquid on the rate of change of both equivalent critical damping and damping coefficients, C_{ce}, and, C_e, of the system

equivalent damping factor of the system ζ_e (Fig. 7). Moreover, a decrease in the size of the particle of the filling solid material increases, as well, the value of ζ_e (Fig. 6).

5. The rate of increase in the equivalent damping coefficient C_e and that in the critical damping coefficient C_{c_e} increases with either increasing kinematic viscosity of fluid or with decreasing particle size of filling solid. However, in case of liquids, it seems that C_e is more affected by changes in ν than is C_{c_e}. On the other hand, in case of solid material, the change in the particle size affects C_{c_e} more than it does C_e (Figs. 10 and 11).

Acknowledgment

The writer wishes to express his thanks to the staff of the Engineering Department at University of California, Los Angeles, Calif., for the cooperation he received. He is grateful to Prof. William T. Thomson for his valuable guidance.

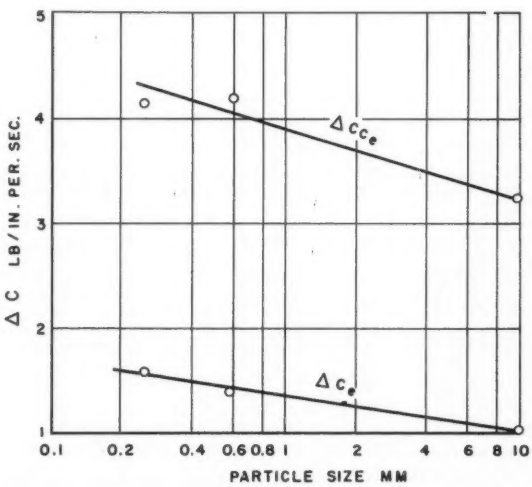

Fig. 11—Rates of change of both equivalent critical damping and damping coefficients with particle size of filling solid material.

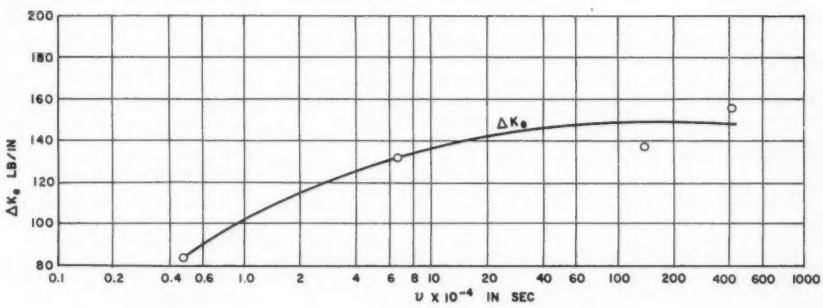

Fig. 12—Effect of variation in kinematic viscosity of filling liquid on rate of increase in equivalent spring constant, K_e, of the system

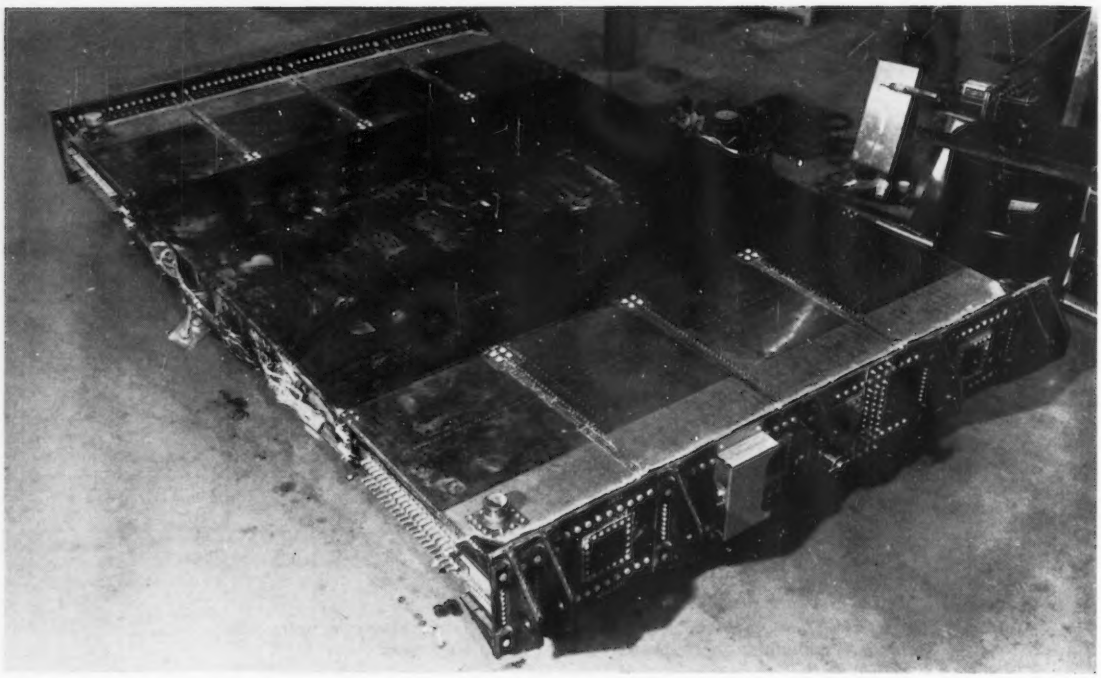

Fig. 1—Test specimen

Structural Testing at High Temperature

Equipment, techniques and methods developed during the course of the tests, as well as some of the special problems that were introduced in simulating fuel conditions, are described and discussed

by Louis Young

ABSTRACT—This paper describes the equipment and procedures used in testing a large multicell box beam under various combinations of applied loading and transient heating. Data are presented on the performance of radiant-heat lamps when enclosed by aluminum reflectors and powered by automobile-type batteries. In addition, solutions are given to the following special problems introduced by simulating fuel conditions: (1) sealing the specimen without disturbing the normal paths for heat flow; (2) protecting strain gages and thermocouples from the simulated fuel.

Introduction

Tests were conducted at Lockheed Aircraft Corp. on a large box beam for the purpose of securing two types of information under simulated conditions of structural loading and transient heating. One was data on the structural behavior of the beam, either when empty or containing fuel. The other was to develop equipment, techniques and methods for duplicating external loading and aerodynamic heating. This paper is concerned only with the equipment, techniques and methods that were developed during the course of the tests and with some special problems that were introduced in simulating fuel conditions.

Test Program

The tests were conducted under the following conditions:

Louis Young is Structures Engineer, Lockheed Aircraft Corp., Burbank, Calif.
Paper was presented at 1960 Spring Meeting held in Indianapolis, Ind., on May 18-20.

Types of tests:

(*a*) Room temperature with load.

(*b*) High temperature without load.

(*c*) High temperature with load.

Types of loading:

(*a*) Constant moment.

(*b*) Constant shear.

(*c*) Pure torsion.

Types of fuel conditions:

(*a*) Empty.

(*b*) Half full.

Box Beam

The outlined test program was for the 150-in.-long four-celled rectangular box beam of 420 stainless steel in Fig. 1 that had a length-to-width ratio of approximately 3 to 2. Of the total length, only a little more than the central third was actually used as the heated test specimen. The outside or end portions acted principally as jigs for supporting, loading and restraining the central portion.

Sealing

Because of simulated fuel conditions that were involved in some of the tests, the box beam had to have all its joints, external rivets and other openings sealed in order to prevent the make-believe fuel from leaking out. The internal strain gages and thermocouples also had to be protected from possible detrimental effects of the simulated fuel. In addition, the sealants had to withstand temperatures up to approximately 600° F.

Selection of sealants and sealing techniques to meet the above requirements involved extensive investigations and trials. After these investigations, the external skin panel rivets were sealed with Silastic dispersion S-6-128, while Silastic sealant S-2007 was applied over all skin and stringer splices, rib-to-skin attachments, internal strain gages and some of the thermocouples.

The panel joints at the internal spars were sealed by applying Silastic between external sealing strips and the skin-panel joints. This procedure eliminated any insulating effects of the sealant between the skin and spars and permitted the latter to function as heat sinks. The joints at the outside spars were sealed with the aid of U-shaped sealing strips that extended around the edge of the joint. Here too, good thermal contact was maintained by having no sealant between the skin panels and spar. After application of the sealant, the Silastic was vulcanized in a large aging oven.

Thiokol PRC 5501 was used for sealing the specimen's end assemblies. This sealant required no heating to effect a cure, but it could be used only in cool regions where room temperature was not exceeded appreciably.

Copper tubes were used to keep the electrical leads of the internal strain gage and thermocouple dry. These tubes were brought out of the box beams through its outside spars and the end assemblies. Kirksite was poured over these tubes at their exit ports in the spars while Thiokol PRC 5501 was used to seal their exits in the end assemblies.

Inside strain gages were installed and sealed as shown in Fig. 2. For outside gages, the second layer of cement and some varnish completed the installation.

The internal thermocouples were sealed in a manner which was similar to that used to seal the strain gages. They were placed, however, in direct contact with the skin and had only the second layer of cement and the sealant that were used in the strain-gage installation.

Simulated Fuel

Some of the box-beam tests were made in order to simulate thermal conditions with the beam half full of JP-5 fuel. To eliminate the fire hazard, a nonflammable substitute for JP-5 was sought that would carry the same amount of heat away from the skin and internal structure as JP-5 does at a given temperature. One way of depicting the rate at which a fluid convects heat away from a surface is by the convective heat-transfer modulus, ϕ, which is defined in Fig. 3.

Experimental investigations showed that a nominal mixture of 2% carboxy-methyl-cellulose (CMC) in water most nearly simulated the thermal properties of JP-5 fuel over the temperature range from 80 to 230° F. While the 2% CMC and water mixture duplicated the heat transfer properties of JP-5 fuel reasonably well, it did not duplicate the boiling point. JP-5 fuel boils at a temperature between 325 and 375° F, while the 2% CMC in water mixture boils at 230° F. However, matching both the convective properties and the boiling point was virtually impossible.

It was originally thought that the thermal properties of sloshed JP-5 fuel should be duplicated in order

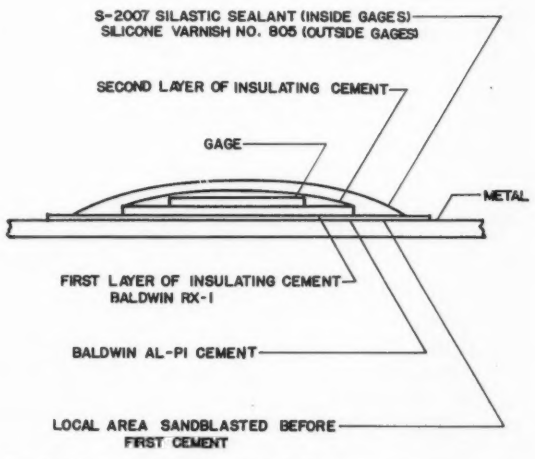

Fig. 2—Typical strain-gage installation

to simulate better the fuel conditions existing in a flying aircraft. Tests, however, showed that the convective heat-transfer modulus in Fig. 3 was extremely sensitive to small changes in the amount of agitation of the fuel, and that the effects of fuel sloshing could be accounted for only if some standard amount of sloshing could be agreed upon. The difficulties involved in accounting for these factors led to selecting a slightly higher value of ϕ for the simulated fuel than what would be appropriate for unsloshed JP-5 fuel.

Since the simulated fuel is quite viscous, approximately like honey, special equipment had to be designed for storing and transferring it to and from the specimen.

Supporting, Loading and Restraining Systems

A loading beam, suspended above the specimen by four posts, was used to support the test item, to act as a loading or jack platform and to support the upper surface radiant heating lamps and some heat reflectors. One side of the loading beam was tied into a concrete block house in order to prevent lateral motion of the loading beam and to eliminate all side loads on the posts.

Support or connection of the specimen to the loading beam was provided by whiffletrees or tie rods at the ends of the specimen, depending on whether the end reactions were tension or compression. Since specimen loading was possible outside the heated zone of the specimen, standard hydraulic jacks were used. Normal provisions for restraint prevented lateral and longitudinal motion of the specimen without restriction of vertical deflection or surface slope under thermal or externally applied loads.

Heating System

The purpose of the heating system was to apply heat to the upper and lower surface of the box beam in modes and at rates corresponding to those expected in flight. At an early date, radiant lamps were selected to provide the heat as they provided a very efficient transfer of electrical energy into thermal energy. Sixty-five percent efficiency was more than feasible as opposed to a maximum efficiency of approximately 15% for hot air systems. A battery-powered direct-current system was also decided on because it was inexpensive and all necessary components were immediately available.

The General Electric 1000 T3 radiant-heat lamp was selected as the heat source. This lamp is a $^3/_8$-in. outside diam, clear-quartz tube that is approximately 12 in. long and is rated at 220 v. It may be used at considerably higher voltages. The characteristics of this lamp under direct current are shown in Fig. 4. Note that the lamp's wattage in this figure varies approximately as the 1.5 power of the voltage, and at 365 v, the lamp draws 5.6 amp of current with an output of 2 kw.

The lamp holders, in Fig. 5, were designed with highly polished aluminum reflectors. Their surface dimensions were 10 by 24 in., with heating lamps placed at a center-to-center spacing of 0.55 in. or any multiple thereof. This spacing permits mounting up to 18 lamps on each half of the lamp holder with a resulting output of 60 Btu per square foot per second at 450 v. With six lamps per lamp holder, 48 of these lamp holders were supported by the loading beam above the specimen and, below, a similar amount were mounted in a mobile cart that could be moved for removal of the specimen.

Power for the heating system was supplied by 490 six-volt automobile storage batteries. These batteries were located in a specially ventilated battery room near the test area. Because the batteries required some charging between each test, it was not possible to conduct more than two tests a day. The arrangement of the batteries is best understood from study of the schematic for a typical power unit in Fig. 6. Each such unit contained 70 batteries arranged in sub-banks of 14 batteries. The complete

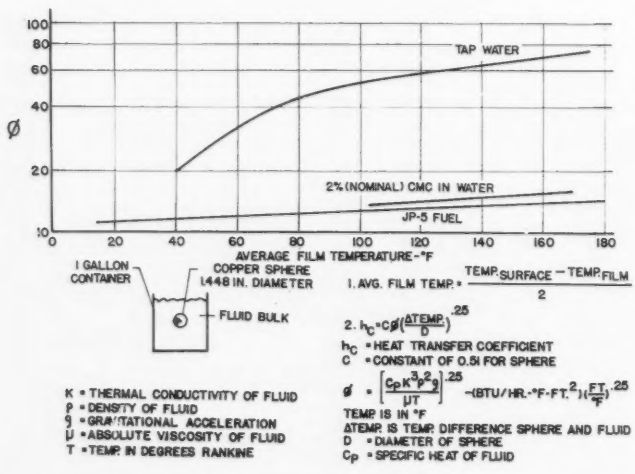

Fig. 3—Convective heat-transfer modulus for fluids

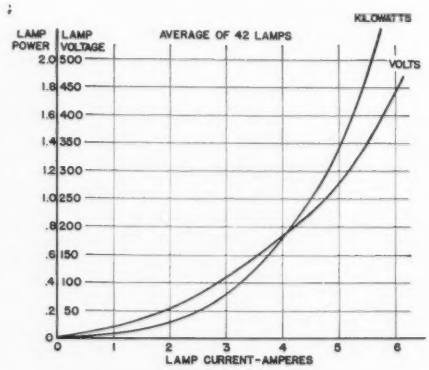

Fig. 4—Lamp characteristics for General Electric 1000 T3 clear-quartz lamp under d-c power

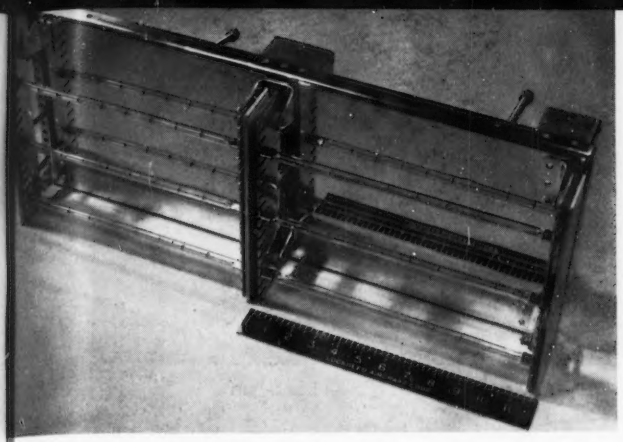

Fig. 5—Lamp holder with six lamps

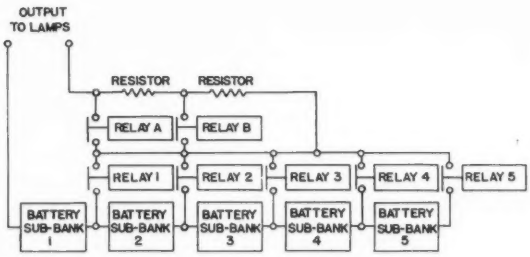

Fig. 6—Schematic of a typical power unit

installation consisted of seven such units and included circuit breakers, switches to charging generators, voltmeters and other electrical elements that were aligned against two walls of the battery room.

The two 26-position switches on the control panel of Fig. 7 provided manual control for the battery-lamp circuit in independently heating the upper and lower surfaces of the specimen. These switches had thirteen different power settings with alternate positions breaking the circuit. The different power settings are given in Table 1.

Besides these power settings, the power to the lamps could be varied by connecting the lamp holders in parallel or series arrays.

TABLE 1—THE RELAYS CLOSED AT EACH POWER SETTING
Relay designations refer to Fig. 6

Power setting	Battery sub-bank relays closed	Resistance relays closed
1	1	B
2	2	
3	2	A
4	2	B
5	3	
6	3	A
7	3	B
8	4	
9	4	A
10	4	B
11	5	
12	5	A
13	5	B

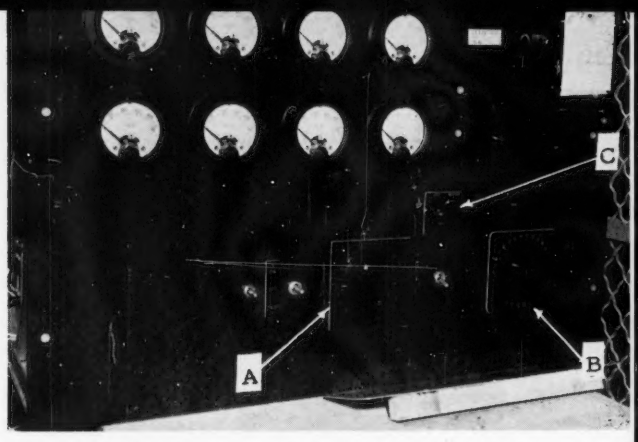

Fig. 7—Control panel. A, upper-surface program control switch. B, lower-surface program control switch. C, selector for master control or separate control

The two switches in Fig. 7 were originally intended to supply different power to the upper and lower surfaces of the box beam only in the half-full-of fluid tests. Because of higher convective losses, however, to atmospheric air on the upper surface, the lower-surface temperature was 30 to 60° F higher than the upper surface in tests with the empty specimen when the same power was used to heat both surfaces. Hence, separate switches were adopted for each surface in both the empty and the half-full-of fluid tests in order to better regulate the heat programs.

Preliminary calibration tests showed that the heated portion of the specimen had to be surrounded by aluminum reflectors in order to obtain a reasonably uniform heat distribution, along with acceptably high efficiency in the transfer of thermal energy from the lamps to the specimen. These reflectors, which are shown in Fig. 8, prevented direct viewing of the specimen's surface for checking possible buckles. To surmount this difficulty, a window

Fig. 8—Over-all setup for heating and loading the box beam showing reflectors in place

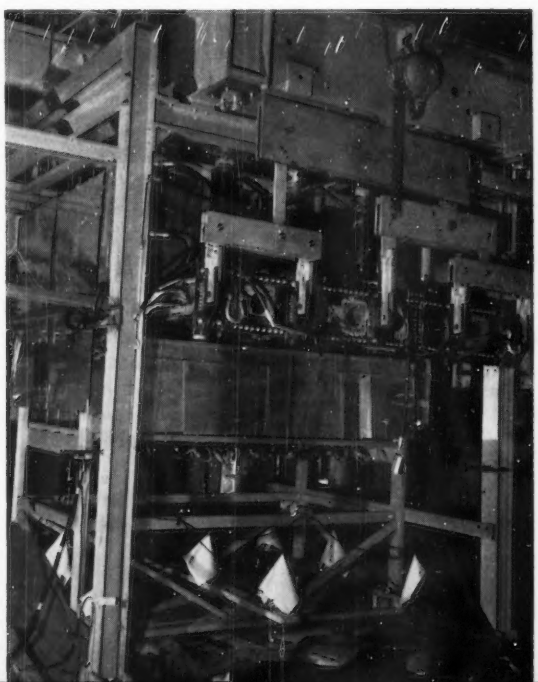

material was sought that would transmit light but reflect heat. A product manufactured by the Sierracin Corp. called "Sierracote" had the desired properties.

Sierracote is a high-vacuum vaporized metallic coating that can be applied to glass or plastic. When placed on glass, it could be used in viewing ports and windows for TV cameras and motion-picture projectors where visible light must be transmitted, but heat filtered out. The TV picture in Fig. 9 was through Sierracote.

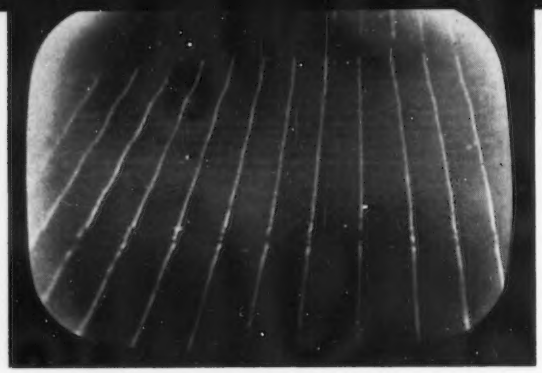

Fig. 9—TV view of buckled grid on box beam

Calibration Tests

In the main tests, the box beam had to be heated at prescribed time-temperate rates. To determine how these rates could be programmed, some calibration tests were made which afforded an opportunity to check on the uniformity of temperature distributions in the heated area of the specimen. While various lamp-to-specimen distances were checked during calibration, a distance of 23.25 in. was used in the actual tests in order to permit visual inspection of the surface of the heated specimen.

The results of calibration tests for lamp-to-specimen distances of 5.25 to 23.25 in. were as given below. (It should be noted that these results are for heat lamps powered by direct current and surrounded by aluminum reflectors.)

1. The heating rate to the test section of the specimen is independent of lamp-to-specimen distance for lamp voltages greater than 180 v and surface temperatures less than 400° F. Above 400° F, the heating rate to the test section of the specimen at a lamp distance of $23^1/_4$ in. is about 10% less than the heating rate for lamp distances of $5^1/_4$ and $14^1/_4$ in.
2. The thermal efficiency decreases as the specimen temperature increases.
3. The lower the lamp current, the greater effect the surface temperature has on thermal efficiency, as shown in Fig. 10.
4. The higher the specimen temperature, the more nonuniform is the heat distribution.
5. Even though the individual heat contours depend upon the distance between the lamps and the specimen, the amount of surface area within the 90% heating contours, in Fig. 11, is virtually independent of lamp distance. This is shown in Fig. 12.
6. There is no difference between the heat input to the surface directly under a lamp and the heat input to the surface between the lamps. No tests, however, were made with lamp-to-specimen distances less than lamp-to-lamp spacing.

The surface areas within the 90% heating contours in Fig. 11 are plotted in Fig. 12 to show the effects of surface temperature and lamp-to-specimen distance on heat distribution. Several ways to improve the heat distribution are listed below:

1. Using a more efficient heat reflector, such as gold.

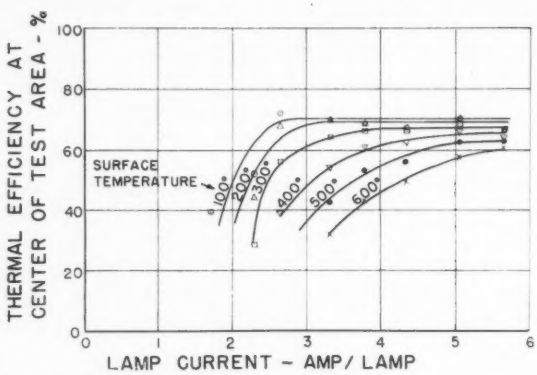

Fig. 10—The relation between thermal efficiency at center of test area and lamp current

2. Replacing side reflectors with lamp holders.
3. Increasing the power in heat lamps that are near the edges of the heated area.
4. Decreasing the lamp-to-lamp spacing near the edges of the heated area.
5. Heating an area which is much larger than the test area.

The most practical of these suggestions, in terms of economy, are listed in methods 2 through 4.

Instrumentation

The installation and operation of measuring and recording devices for strains, temperatures and deflections was complicated by the need for them to function accurately at high speeds, at high temperatures, in synchronization with each other, and in the case of some instruments, under liquid. The various sensing units also had to function over a wide temperature range and record in time synchronization to permit the cross plotting of data.

The strain gages that were used were of the etched-foil type and made of "Advance" metal by Baldwin-Southwark. These gages were grouped at right angles in pairs like shear gage pairs and active and dummy pairs for axial stresses. Some pairs of gages also were mounted back to back on the skin panels and in the webs of the spars in order to detect buckling.

"Advance" foil gages may be used up to 600° F by accounting for the strain due to the difference in

thermal expansion between the gage and specimen and to changes in gage resistance with temperature. Otherwise, the temperature limit is approximately 400° F. The temperature limitations on a strain gage do not mean that the gage cannot be used at a higher temperature; merely, that this is the maximum temperature at which the change in resistance per unit of strain divided by the gage resistance is a linear function of the strain and at which the gage will likely be in a reusable condition.

Strains were read on each gage and corrections to these readings were computed from the change in temperature of the gage. Changes in temperature for each cluster of strain gages, as well as for the specimen and for the simulated fuel, were measured with iron-constantan thermocouples.

Over 250 data signals from strain gages and thermocouples were recorded on six galvanometer channels of a 36-channel Miller oscillograph. Three of these channels were devoted to strain data and three to temperatures with signals being commuted through stepping switches that scanned all instruments every 10 sec. A seventh channel was connected to a pressure transducer to record a continuous trace of the externally applied loads from the hydraulic jacks. These seven channels were recorded on paper tapes that had to be developed photographically.

The deflection of the specimen was recorded at nine points. Invar rods, having an extremely small coefficient of expansion, connected the specimen at these points to ER 804 deflection boxes beneath the lower surface lampholders. These deflection boxes are a Lockheed development and were mounted on the lower lamp cart to convert deflections into electrical signals that could be recorded on a Brown recorder. Recording the start of the constant-speed paper drive in the Brown recorder permitted synchronization of the deflection readings with other recorded data.

Testing Procedures at High Temperature

The use of heat in structural testing complicates testing procedures in a number of ways. Some of the problems are listed below:

1. The thermal effects on an aircraft structure are transient in nature. To record the true nature of these effects, all instruments have to be read exceedingly rapidly. This problem was solved by the Miller oscillograph.

2. High temperatures along with heat reflectors made the specimen inaccessible for close observation during testing. This was solved by viewing the specimen visually or with TV and motion-picture cameras through ports in the reflectors.

3. High temperature affects the accurate operation of strain and deflection-measuring devices. This was solved by proper calibration.

4. The short duration of some tests plus the need to coordinate load application and thermal input made it exceedingly difficult to adjust techniques or

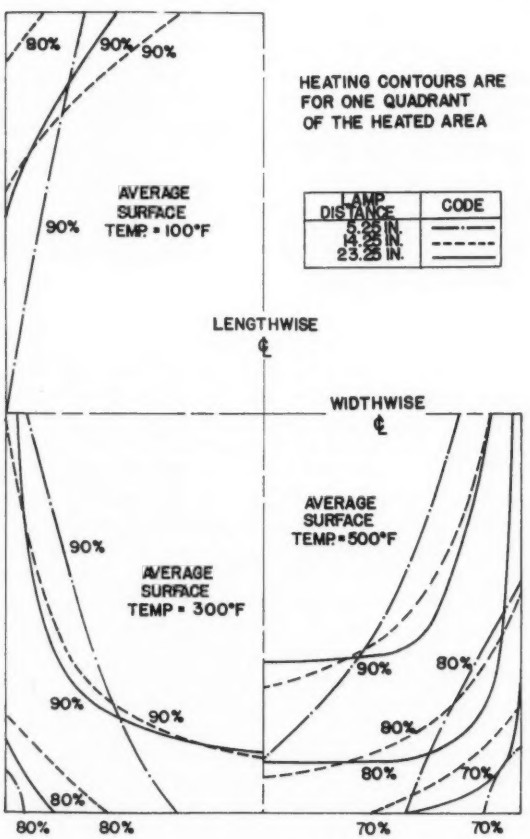

Fig. 11—Contours of heating rate as a percent of heating rate at center in calibration test

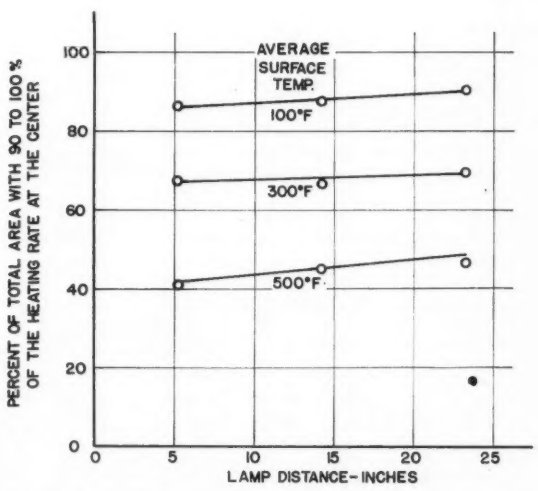

Fig. 12—Relation between the area with 90 to 100 percent of the heating rate at the center of the test area and lamp distance for different surfaces. Average lamp current is 3.80 amp per lamp

controls during a test in the manner commonly employed in static structural tests. Preliminary tests eliminated many such problems in the actual tests.

In addition to the problems listed above, a number of others peculiar to this particular program had to be met. These included:

1. The accumulation of great amounts of data because of the large number of strain gages and thermocouples that were used. This resulted in a major data-reduction problem.

2. The lag in data reduction made it impossible to correct test procedures each day for findings made on the previous day's run. Monitored sensing units alleviated this situation.

3. The effects of simulated fuel. For example, sealing of the internal strain gages and thermocouples made it necessary to have calibrations under both wet and dry conditions. These calibrations, which were made before each test, showed that the sealant had cracked in the course of testing on some of the strain gages and thermocouples to make them inoperative in the wet tests but still fully effective in the dry or empty tests.

The steps followed in the high-temperature tests are outlined below:

1. Preliminary checks were made of the specimen, jig, loading and heating system.

2. A heating schedule in the form of a disk was prepared and attached to a clock mechanism on the heating-system control panel. These disks start rotating at the beginning of a test. Markings on the disks showed the operator when changes in the power settings should be made to create the correct temperature rise on the specimen's surfaces.

3. All instrumentation was turned on simultaneously at zero time.

4. Load was applied in $2^1/_2\%$ increments every 15 sec, starting at 15 sec after zero time. This stepped-load input led to an almost linear loading rate that could be easily duplicated between tests. In the "heat alone" tests, this step was eliminated.

5. The power to the radiant-heat lamps was increased or decreased at the power control panel according to the setting on the heating-schedule disk. The disk started rotating at zero time while heating started at zero time plus 45 sec in all tests. Because of these timing disks, the heat program could not be changed during a test. Programming of the heat was a trial-and-error process, and required two or three preliminary tests before an acceptable heat program was obtained and placed on a disk.

6. All instrumentation was run continuously from zero time minus thirty seconds.

7. Critical strain gages and thermocouples, as well as all deflections, were monitored throughout each test.

These steps were used on all the high-temperature tests.

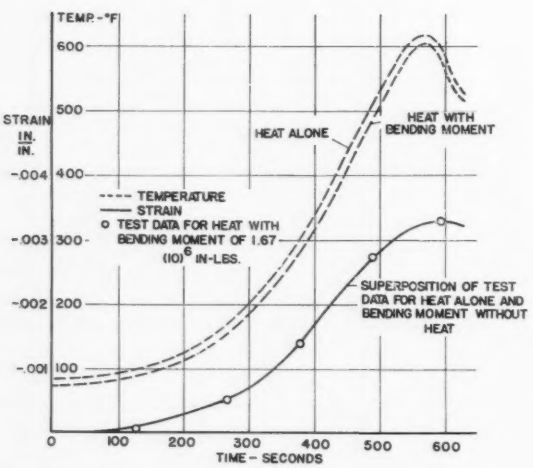

Fig. 13—Temperature and superposition of strains in "heat alone" and "load alone" tests for comparison with test data for combined heat and load

Duplication of Test Results

The equipment, techniques and procedures just described provided temperature- and load-versus-time programs that could be easily duplicated in succeeding tests. One way to show this is to superimpose elastic strains from "load alone" and "heat alone" tests for comparison with elastic strains obtained from a test conducted under similar but simultaneous conditions of heat and load. The favorable results of such a comparison are shown in Fig. 13. Also shown are the temperature-time curves for the "heat alone" and heat-with-load tests. Note that the separation between these two temperature curves is due to the difference in room temperature on the two days of testing. Another item evident from the superposition in Fig. 13 is that the hydraulic loading system is very effective in accurately reproducing load-time programs.

Conclusions

Experience gained from tests on the large steel box beam has been applied to other thermal tests and provides the basis for current high-temperature testing techniques at Lockheed Aircraft Corp.

The equipment, while flexible enough to use for providing different types of heat and load inputs to several sizes of specimens, has undergone some revisions. The revised heating system uses continuous heat control in place of the 13-step heat programs that were provided by the two stepping switches. In addition, the shape of the lamp holders has been changed in order to provide increased heating efficiency. The power for heating also has been changed from batteries to a large alternating current system that eventually will be capable of heating complete airplanes. Battery-powered heating systems, however, still provide a reasonable and economical approach to testing aircraft structures at high temperatures because of their low initial cost, ready availability of components and ease of construction.

Twisting Stresses in Tape

The stresses induced in a thin tape by bending over pulleys, by axial tension and by twisting of the tape when running between two out-of-plane pulleys, are analyzed

by C. Mylonas and D. C. Drucker

ABSTRACT—An analysis is presented of the stresses induced in a thin tape by bending over pulleys, by axial tension and by twisting of the tape when running between two out-of-plane pulleys. Analytical results are compared with some photoelastic tests on tape models made of epoxy resin. The weak retardation produced by the thin tape is multiplied by repeated light passage through the tape and is measured by a bent-beam compensator. The tests are of especial interest because the rate of rotation of the principal stresses is higher than had been encountered before. Surprisingly, the experimental results uncorrected for rotation are in good agreement with the calculated stresses.

List of Symbols

b = tape width.
b_1 = central width of tape equal to $b/\sqrt{3}$.
d = tape thickness.
f = depth of parabolic segment for entire width b of tape. The units of f are fringe orders.
f_1 = depth of parabolic segment for central width $b/\sqrt{3}$.
$f_A, \ldots, f_D$ = fringe order at various points of the tape.
m = mirror reflectivity.
r_i = light ray which has passed i times through specimen.
w = angle of twist over a length of tape equal to its width b. In the present report w is always less than 0.1π (twist of at most one revolution in a length equal to twenty widths).
w_{cr} = critical twist at which buckling occurs.
x = coordinate axis in direction of the thickness of the tape.
y = coordinate axis in direction of the width of the tape.
z = coordinate axis in direction of the length of the tape.

C. Mylonas and D. C. Drucker are Professors of Engineering, Division of Engineering, Brown University, Providence, R. I.

Paper was presented at the 1960 SESA Spring Meeting held in Indianapolis, Ind., on May 18–20.

The results discussed in this paper were obtained in the course of research sponsored by the International Business Machines Corp.

A_0 = original light intensity.
A_i = light intensity after i passages.
$A_{i,\,opt}$ = optimum light intensity after i passages.
C_σ = stress optical coefficient, a material fringe value with units of stress per fringe for a 1 in. thickness.
C_ϵ = strain optical coefficient, strain per fringe for a 1 in. thickness.
D = diameter of pulley.
E = Young's modulus.
F_2 = focal length of collector lens V_2.
G = shear modulus.
K = principal curvature of the helix in which longitudinal fibers twist.
L = arbitrary length of tape, length of untwisted fibers.
L' = length of twisted fibers when the end cross sections are held a fixed distance L apart.
N = relative retardation in wave lengths ($\lambda = 5461$ Å).
P = longitudinal force applied along axis of tape.
R = ratio of twice the rotation of principal stresses to the relative phase retardation over a light path.
S = $\sqrt{1 + R^2}$.
α = angle between partially reflecting mirrors.
ϵ = normal strain.
γ = shear strain.
θ = angle between maximum principal stress and tape axis.
ν = Poisson's ratio.
σ = normal stress.
σ_{cr} = critical buckling stress.
σ_p = longitudinal normal stress due to external pull P.
σ_z', ϵ_z' = longitudinal stress and strain when end cross sections are held at the same distance apart in the straight and the twisted tape.
σ_{z0}, ϵ_{z0} = longitudinal normal stress and strain in the absence of external loading.
τ = shear stress.
ψ = angle of twist of tape over length L.

Fig. 1—Twisting of tape between out of plane pulleys

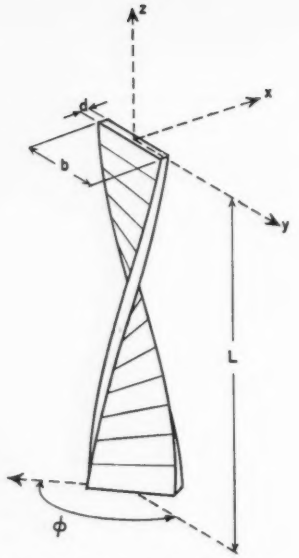

Fig. 2—Detail of twisted tape

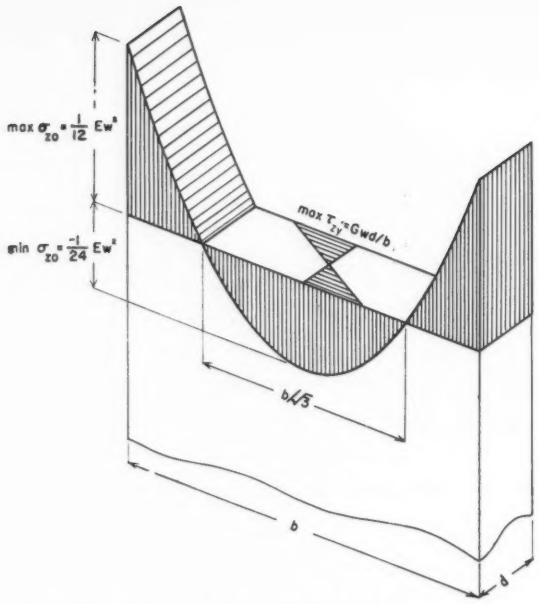

Fig. 3—Shear stresses and self-equilibrating normal stress distribution on the cross section of the tape

Introduction

The extensive use of recording tape in computers and the possible delays resulting from their damage by overstress led to this study of the permissible loading and stresses in tape. The tape may be subjected to bending over a pulley, to axial tension and to twisting between out-of-plane pulleys. The permissible intensity of each of these actions can be determined from the stresses which they produce. In general, the relative magnitudes of the various stresses depend strongly on the ratio b/d of width to thickness of the tape, as well as on the intensity of each loading action. The ratio b/d is always large, e.g., 25 for a typical steel tape (0.125/0.005 in.) and 250 for a typical plastic tape (0.500/0.002 in.). The extreme thinness of the tape allows large angles of twist or bend with only small strains. It is not too difficult to bend the tape over a 1-in. diam pulley or to twist it by a full turn in a length equal to 20 tape widths, without any apparent damage. Thus, in spite of the large deflections, it is possible to make a reasonably accurate analysis based on small strains with all the usual strength-of-materials assumptions.

Bending Stresses

A tape of cross section $b \times d$ and Young's modulus E, under tension P, running over a pulley of diameter D develops peak stresses σ at the extreme fibers:

$$\sigma = \frac{P}{bd} \pm \frac{Ed}{D} \tag{1}$$

The bending stresses alone may be very high, and their damaging effects may be accentuated by reversed bending. For steel tape of a thickness d = 0.005 in. and a 1-in. pulley, the bending stress is 150,000 psi. For a plastic tape 0.002 in. thick with $E = 3 \times 10^5$ psi, the corresponding stress is only 600 psi.

Twisting Stresses

The twisting of the tape between pairs of out-of-plane pulleys is shown in Fig. 1. A length L of twisted tape is shown in greater detail in Fig. 2. The relative angle of twist of the end sections is φ. As described in Reference 1, the twisting stresses in any section can be considered to consist of torsional shearing stresses τ_{zy} and of longitudinal stresses σ_z due to change of length of the longitudinal fibers during their helicoidal twisting. The shearing stresses τ_{zy} for this narrow rectangular section are quite accurately determined away from the edges as:

$$\tau_{zy} = 2Gx\frac{\varphi}{L} = Gw\frac{2x}{d}\Big/\frac{b}{d} = {}^1/_2\frac{E}{1+\nu}w\frac{2x}{d}\Big/\frac{b}{d} \tag{2}$$

$$\text{for } |x| \leq {}^1/_2\, d$$

where G and E are the shear and Young's moduli, ν is Poisson's ratio for the tape, and $\varphi/L = w/b$ is the angle of twist per unit length of tape, expressed also as a twist of angle w over a length equal to the width b. For $\nu = {}^1/_3$ the shear stress is

$$\tau_{zy} = {}^3/_8\, Ew\frac{2x}{d}\Big/\frac{b}{d} \tag{2'}$$

Figure 3 shows the linear variation of the shear stress from the mid-plane $x = 0$ to the faces $|x| = {}^1/_2\, d$ where the extreme values are:

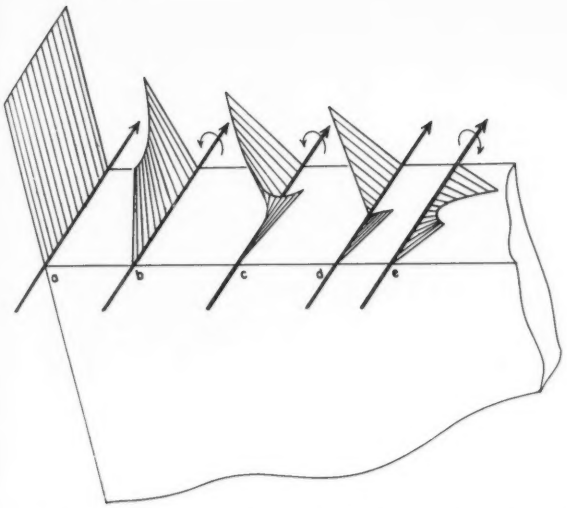

Fig. 4—Sketch of the variation of magnitude and direction of the principal tension over the tape thickness

$$\text{max, min } \tau_{zy} = \pm Gwd/b = \pm 3/8\, Ewd/b$$

The longitudinal strains produced by twisting can be calculated easily by considering first two cross sections held a constant distance apart during twisting. The fiber at the axis remains unstrained, but all others are deformed helicoidally and increase in length. The arc L' of a cylindrical helix of constant slope of original untwisted length L at a distance y from the axis is (Fig. 2):

$$L' = L[1 + (\varphi y/L)^2]^{1/2} = L\,[1 + (yw/b)^2]^{1/2}$$

The corresponding longitudinal strain is found as:

$$1 + \epsilon_z' = [1+(yw/b)^2]^{1/2}$$

or

$$\epsilon_z' = 1/2(yw/b)^2 - 1/8(yw/b)^4 + \ldots$$

But $y \leq 1/2\ b$ and $w < 0.1\pi$ (corresponding to a twist of one twentieth of a revolution in a length b). Even with the largest values of these variables, the higher order terms in ϵ' are less than 1% of the first and may be neglected. Therefore, very closely,

$$\epsilon_z' = 1/2(yw/b)^2 = 1/8(2yw/b)^2 \qquad (3)$$

and on the assumption of zero cross stress σ_y', the corresponding longitudinal stress is

$$\sigma_z' = 1/8\ E\ (2yw/b)^2 \qquad (3')$$

According to eq (3′), this longitudinal stress is always positive with a maximum value of $1/8\ Ew^2$ and an average value of $1/24\ Ew^2$. If now the length of the tape is allowed to change freely, the resultant force and the average stress will vanish. A uniform tensile stress will be subtracted from the parabolic distribution σ_z' so as to produce a self-equilibrating longitudinal stress distribution given by the parabola (Fig. 3)

$$\sigma_{zo} = 1/8\ Ew^2\ [\ (2y/b)^2 - 1/3] \qquad (4)$$

with a corresponding strain distribution ($\sigma_y = 0$)

$$\epsilon_{zo} = 1/8\ w^2\ [(2y/b)^2 - 1/3] \qquad (4')$$

Any applied force P will add a uniform stress σ_p, to make a total longitudinal stress

$$\sigma_z = \sigma_{zo} + \sigma_p = 1/8\ Ew^2\ [(2y/b)^2 - 1/3] + \sigma_p \qquad (5)$$

The highest longitudinal stress develops at the tape edges and the algebraic minimum at the axis

$$\begin{aligned} \max\ \sigma_z &= 1/12\ Ew^2 + \sigma_p \\ \min\ \sigma_z &= -1/24\ Ew^2 + \sigma_p \end{aligned} \qquad (5')$$

The stress in the tape is not given by σ_z and τ_{yz} alone. The tension in the longitudinal fibers, which are in a helicoidal shape, does give rise to a small compression σ_y in the direction of the width of the tape. The σ_y-trajectories are straight, and the σ_z-trajectories are helices—each of which has a curvature K. The differential equation of equilibrium in the stress-trajectories is:

$$\frac{d\sigma_y}{dy} + K(\sigma_y - \sigma_z) = 0 \qquad (6)$$

where

$$K = \frac{yw^2/b^2}{1 + y^2w^2/b^2} \qquad (7)$$

On the assumption that σ_y is small, it may be neglected in comparison with σ_z, and eq. (6) may be written as

$$\frac{d\sigma_y}{dy} = K\sigma_z \qquad (6')$$

Equation (7) can also be simplified because $y^2/b^2 \leq 1/4$ and $w^2 < (0.1\pi)^2$, hence

$$K \cong yw^2/b^2 \qquad (7')$$

Substitution of (7′) and (5) into (6′) gives

$$\frac{d\sigma_y}{dy} = y\,\frac{w^2}{b^2}\left\{\frac{Ew^2}{8}\left[\frac{2y^2}{b} - 1/3\right] + \sigma_p\right\}$$

which may be integrated directly between the limits y and $b/2$ to give

$$-\sigma_y = \frac{Ew^4}{384}\left[1 - 3\left(\frac{2y}{b}\right)^4 + 2\left(\frac{2y}{b}\right)^6\right] + \frac{\sigma_p w^2}{8}\left[1 - \left(\frac{2y}{b}\right)^2\right] \qquad (8)$$

The complete differential eq (6) with the exact value (7) of K give the same result (8), if the transcendental terms in the solution are expanded in power series and terms in w^6 or higher are neglected. Comparison with (5′) shows the magnitude of the maximum compressive cross stress σ_y to be less than $w^2/8$ times the maximum axial tensile stress σ_z. As $w^2/8 < 0.012$ for $w < 0.1\pi$, the assumption that σ_y is small is confirmed. When the axial force in the tape is zero, $P = 0$, the maximum value of σ_y is less than 0.003 times the maximum σ_z.

The strongest but still negligible photoelastic effect of σ_y will appear at points where σ_z is small or zero. In the worst case, the point with a stress dif-

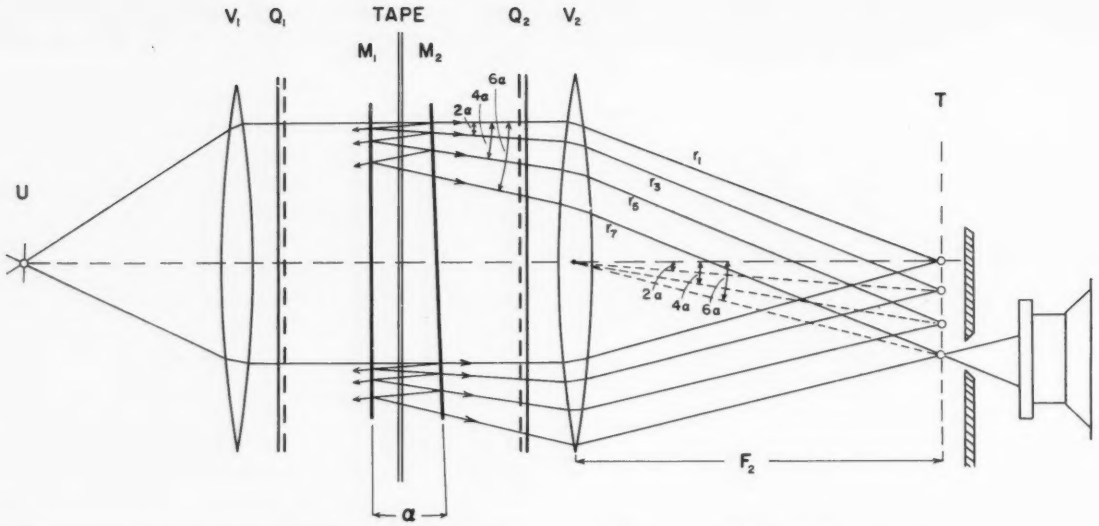

Fig. 5—Principle of the method of fringe multiplication with multiple light passages through the specimen

ference equal to zero will be displaced laterally by about two thousandths of the tape width.

With τ_{zy} variable linearly over the thickness d but constant across the width b (except at the edges), and with σ_z variable parabolically across the width b but constant over d (Fig. 3), it is obvious that the principal stresses vary in intensity and direction not only across the width but also through the thickness of the tape. The principal stresses, their difference, and their angle θ to the longitudinal axis are given by

$$\tan 2\theta = 2\tau_{zy}/\sigma_z \tag{9}$$

$$\sigma_1,\ \sigma_2 = {}^1/_2\sigma_z\ (1 \pm \sec 2\theta)$$
$$\sigma_1 - \sigma_2 = \sigma_z \sec 2\theta \tag{10}$$

The variations over the tape thickness at various distances from the axis are shown qualitatively in Fig

TABLE I—STRESSES IN TYPICAL TAPES

	Plastic			Steel
b	1.00 in.	0.705 in.	0.50 in.	0.125 in.
d	0.010 in.	0.0112 in.	0.002 in.	0.005 in.
b/d	100	63	250	25
φ/L	2π/20 in.	2π/20 in.	2π/20 in.	2π/20 in.
w, rad.	0.1π	0.075π	0.05π	0.0125π
E, psi	$\sim 3 \times 10^5$	3.75×10^5	3×10^5	30×10^6
G, psi	$\sim 1.15 \times 10^5$	1.4×10^5	1.15×10^5	$11.5 \times 10_6$
max τ_{yz}, psi	360	492	72	18,100
max ϵ_z	0.00821	0.00461	0.00205	0.00013
max σ_z, psi	2460	1730	615	3900
tan 2θ	0.292	0.569	0.233	9.28
max σ, psi	2510	1860	625	20,200
w_{cr}, rad.	0.164	0.260	0.065	0.65
σ_{cr}, psi	<330	<1040	<53	<53,000
D_0	1 in.	1 in.	1 in.	1 in.
σ_b, psi	3000	4160	600	150,000

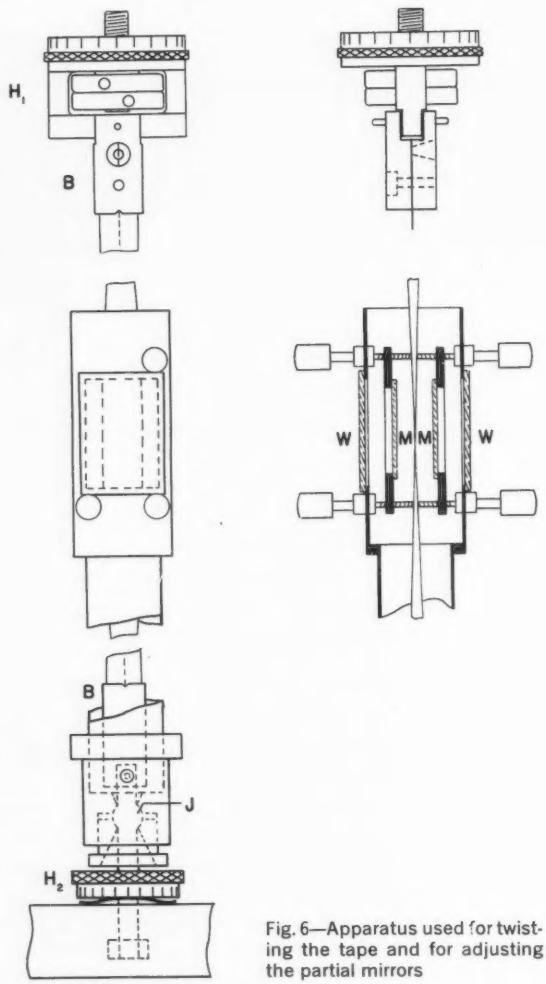

Fig. 6—Apparatus used for twisting the tape and for adjusting the partial mirrors

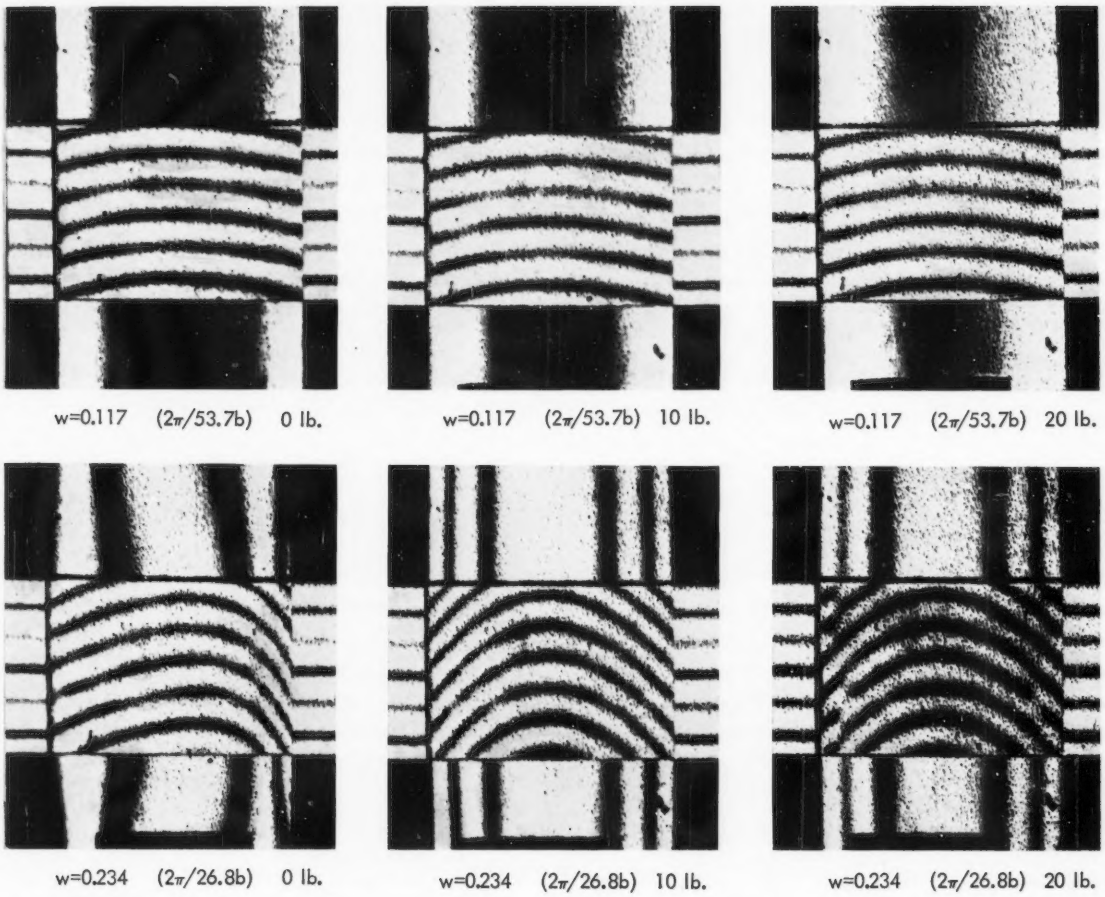

Fig. 7—Photoelastic photographs after 7 passages through tape. Thickness d = 0.0112 in.; width b = 0.875 in. b:d = 78

4. The ruled lines represent the maximum tension σ_1 in direction and magnitude. At the very edges, τ and θ are zero and σ_1 coincides with σ_z in intensity and direction. Just inside the edges τ_{zy} varies as in Fig. 3, but σ_z is strong and gives a small θ and a small amount of rotation. The rotation may also be small at the tape axis where the compressive stress σ_z may be relatively large (in the absence of axial pull). At intermediate points where σ_z is small the rotation may be severe. However, at points of pure torsional stress distribution ($\sigma_z = 0$), the principal directions do not rotate. (Mathematically speaking, they rotate instantaneously by 90 deg at the mid thickness of the tape, where their magnitude vanishes.) The principal stresses form a fixed angle of 45 deg to the tape axis and their magnitude varies linearly with the distance from the mid-plane. Regions with small stress σ_z and large rotations will also exist when an applied tension of the order of magnitude of min σ_{z0} is applied. But with very large axial pull, the stress σ_z is a substantial tension over the whole width of the tape, and the rotation will be everywhere negligible. The maximum stresses in typical tapes are shown in Table 1.

Buckling

In the absence of axial pull, a middle strip of the tape is in longitudinal compression of parabolic distribution (Fig. 3 and eq (4)) and may buckle. The exact treatment of this problem would be very complicated, so that results of plate theory will be used. On several counts the twisted tape does not fulfill the usual assumptions made in the buckling of plates: it is strongly bent in an anticlastic shape; it has no clearly defined points or type of support; and its in-plane loading is internal as produced by the twist and can be greatly altered by the buckling deflections. Furthermore, after the development of large buckling deflections, the tape appears to be bent in a series of alternating plane isosceles triangles whose equal sides form a constant angle with the tape edges. To some extent, this is also indicated by the antisymmetric shape of the photoelastic pattern of the buckled tape appearing in the left hand photograph of the second row in both Figs. 7 and 8. However, at the onset of buckling, the deflections are very small and the middle strip might well behave as a long plate in longitudinal compression, supported by the edge strips which are under tension. If the

edge strips were absolutely firm, they would afford a built-in edge restraint to the middle strip. But obviously the edge strips can easily rotate and deflect by small amounts. Probably, the equivalent width of a simply supported middle strip is well over the width $b/\sqrt{3}$ of the compressed region. In this approximate treatment, it will be assumed that strip continuity and low edge restraint balance out and that the problem is equivalent to an infinite plate of width $b_1 = b/\sqrt{3}$ (in the absence of any applied pull), subjected to longitudinal compression. Since the loading at mid-span is much more effective than near the supported edges, the compressive stress will be taken to be constant over b_1 and equal to the maximum compression at the tape axis. Then buckling according to this very crude theory will tend to occur in squares of side b_1 at a critical stress:[2]

$$\sigma_{cr} = -\frac{4\pi^2}{b_1^2 d}\,\frac{Ed^3}{12(1-\nu^2)} = -\frac{\pi^2 E}{1-\nu^2}\left(\frac{d}{b}\right)^2 \quad (11)$$

Such a stress will be reached at a critical twist given by (5′) with $\sigma_p = 0$. Equations (5′) and (11) give:

$$w = 2\pi\sqrt{6/(1-\nu^2)}\Big/\frac{b}{d} \quad (12)$$

and for $\nu = 1/3$

$$w_{cr} = 16.3\Big/\frac{b}{d} \quad (12')$$

For the two tapes with b/d equal to 78 and 63, which were used in the photoelastic experiments, the critical twists w_{cr} according to eq (12′) should be 0.21 and 0.26, respectively. Instead, the buckling twist was found to be between 0.156 and 0.188 for the first and between 0.156 and 0.208 for the second. Thus, as might be expected, the computed critical twists and critical stresses exceed the experimental values. The difference in the twists is about 30% and in the stresses about 70%. The transverse compressive stress σ_y is too small to influence buckling appreciably. Its only effect could be a decrease by σ_y of the critical longitudinal stress σ_z.[2] The experimental critical stress of the tested tapes was about 700 psi ($E = 4.8 \times 10^5$ psi), whereas at the critical twist the transverse stress σ_y was well below 10 psi.

Photoelastic Effects in Nonuniform Stress Fields

Since, in general, the stress field is not uniform over the tape thickness (Fig. 4), the problem cannot be strictly treated as one of plane photoelasticity. The effect of variation of intensity and orientation of the stresses on polarized light has been studied by Mindlin and Goodman[3] but, as a simplifying approximation, one can refer to the earlier work of Drucker and Mindlin[4] on the effect of rotation of stresses of constant intensity, and also of Mindlin[5] on the effect of a stress gradient without rotation. It is shown that, in the absence of rotation, even the strongest gradient possible in an ordinary photoelastic material does not alter in any detectable amount the total birefringence as calculated for the average stress. This conclusion remains valid even for the more-sensitive epoxy resin used, the thin tape (approx. 0.01 in.), and the resulting higher-than-ordinary gradient of stress and birefringence. Thus all the points with zero or negligible rotation will show a birefringence proportional to σ_z. As indicated earlier and shown in Fig. 4, these are the points of zero stress σ_z, the tape edges, and the regions with high σ_z close to the edges and also, in the absence of axial pull, near the tape axis. For large axial pull, the rotation will be negligible throughout the tape.

In the instance of constant rate of rotation and retardation,[4] the ordinary and extraordinary components of light are expressed with sufficient accuracy by a complicated trigonometric function of the initial amplitudes, the photoelastic quantities, the ratio R of twice the rotation to the phase retardation, and the quantity S, where:

$$S = \sqrt{1 + R^2} \quad (13)$$

It is true that the results simplify considerably for rays of integer wavelength retardation. Then the state of polarization with respect to the principal stresses at incidence is identical to the state at exit with respect to the rotated principal stresses. Methods similar to those of ordinary photoelasticity are possible, with only the need of correction by a factor of S^{-1}. However, in the tape the rate of rotation is variable and Mindlin and Goodman's eq[3] should be used.

As an approximation, one may find the total relative retardation by integrating Drucker and Mindlin's[4] results for the variable rotation and stress intensity through the tape. The result is far less than one wave length. In effect, the superposition of the highest stresses from twist and axial pull produces about half a fringe at the tape edges and considerably less elsewhere. Accordingly, no simplifications were possible as for integer wave length retardations.

Usually, the relative retardation can be multiplied by repeated passages of the polarized light through the model. In the present problem, however, the multiple passages introduce additional rotational effects because, in the backward travel, the direction of rotation is reversed and R changes sign. In the expressions for the components of vibration, the terms containing S do not change with direction of passage, but those in R do. The results are more complicated than in single passage and no simple correction factor is applicable even if the accumulated retardation is of integer wave length. However, when the rotation is negligible or zero, the multiple passage should give results directly proportional to the stress σ_z. Obviously, this can always be achieved when the axial pull is sufficiently strong, so that the method of multiple passages is promising for this instance. It is of great interest that the results were unexpectedly found to be directly proportional to σ_z, even when the rotation was considerable.

Photoelastic Tests with Multiple Reflections

The method of multiple reflections, first used in photoelastic studies by D. Post,[6] is schematically explained in Fig. 5. In addition to the regular components of an ordinary point-source polariscope (light source U; collector lens V_1 producing a parallel beam of light; polaroid polarizer Q_1 and analyzer Q_2; collector lens V_2) the system uses also two partially reflecting mirrors M_1, M_2 one on each side of the tape model. The mirrors are at a small angle α to each other so that, after each double reflection between them, a new parallel beam of light emerges to the right. But with each double reflection between mirrors, the polarized rays pass two more times through the model. Ray r_3 has traversed the model three times; ray r_5, five times; ray r_7, seven times. Passage of the same ray occurs at distinct points lying very close to each other. If the magnitude and direction of the principal stresses do not vary through the model or at the consecutive points of passage, the relative retardation of each ray will be that of the original ray r_1 multiplied by the number of passages. Large relative retardations may be easily reached. In the tape tests, the angle α was formed by tilting the mirrors about a horizontal axis as shown in Fig. 5. Then the consecutive points of passage of the same ray through the tape are spread in the longitudinal direction of the tape and their state of stress is identical.

The parallel beams of rays with the same number of reflections are easily separated. They are at consecutive angles 2α and form distinct images of the point source on the focal plane T of lens V_2. The distance between consecutive images is $2\alpha F_2$, where F_2 is the focal distance of lens V_2. A suitable external diaphragm or, preferably, the stop of the camera lens (brought at or close to the focal plane T) easily isolates the rays with the required number of passages. To obtain a photoelastic image of suitable size, the focal lengths of the lenses must have the proper relations to the negative size.[7] Also the image separa-

Fig. 8—Photoelastic photographs after 7 passages through tape. Thickness d = 0.0112 in.; width b = 0.705 in. b:d = 63

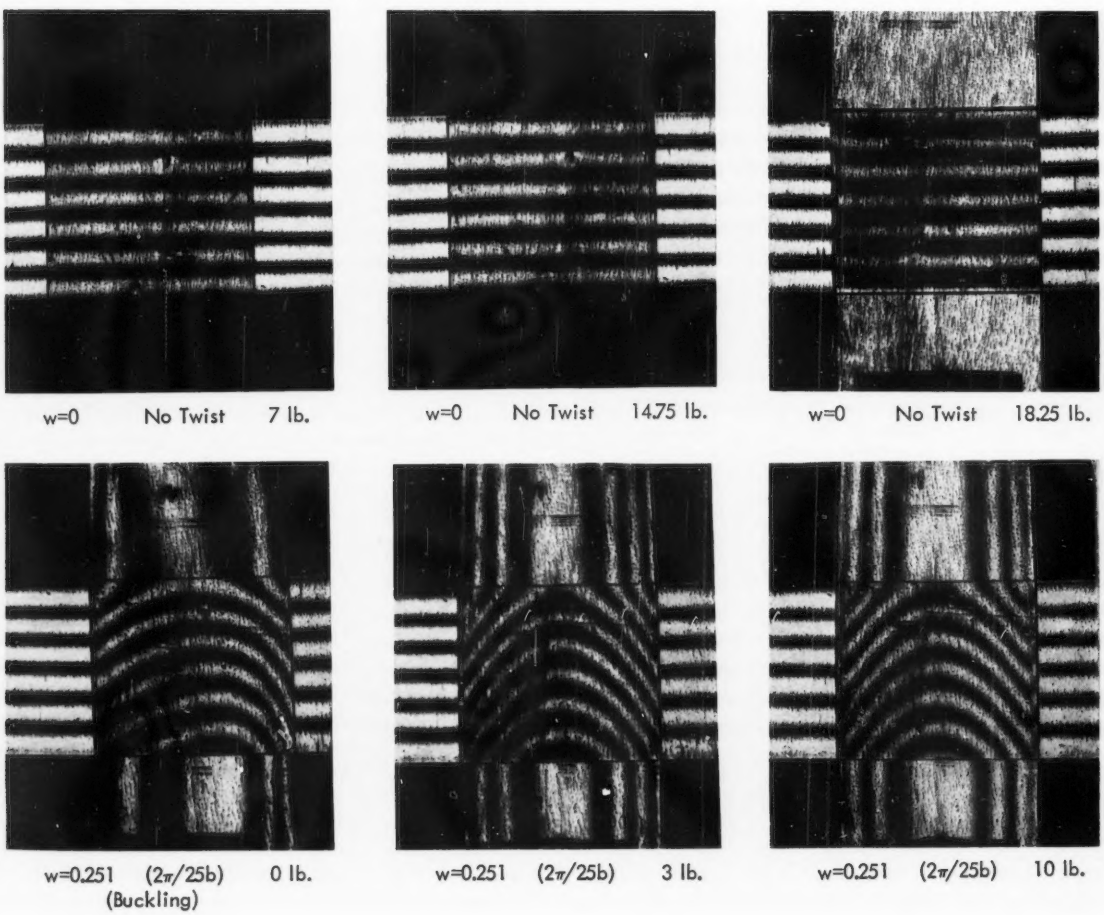

TABLE 2—OPTIMUM REFLECTIVITY AND INTENSITY FOR VARIOUS NUMBERS OF PASSAGES

Passages, i	Reflectivity, $m_{i,\,opt}$	Relative intensity $A_i,\ m/A_o$ For values of m					
		opt.	0.500	0.667	0.700	0.750	0.800
3	0.500	0.0625	0.0625	0.0576	0.0441	0.0351	0.0256
5	0.667	0.0220	0.0156	0.0220	0.0216	0.0197	0 0164
7	0.750	0.0111	0.0039	0.0075	0.0106	0.01111	0.0105
9	0.800	0.0067	0.0010	0.0027	0.0052	0.0062	0.0067
13	0.857	0.0032	...	0.0004	0.0012	0.0020	0.0027
17	0.889	0.0019	...	...	0.0003	0.0006	0.0004
21	0.910	0.0012	...	...	0.0001	0.0002	0.0005

tion $2\alpha F_2$ must exceed the size of the source image at the focal plane T or, in general, must be larger than the diameter of the cone of rays converging through the lens stop.

Of course, the intensity of the various parallel beams decreases fast with the number of reflections. Under ideal conditions of reflectivity m and transmission 1-m of each mirror and no other losses, the relative intensity of the beam with i passages will be ($i = 3, 5, 7, \ldots$)

$$A_i/A_0 = (1 - m)^2\, m^{i-1}$$

The optimum reflectivity varies with the number of reflections and can be easily found to be:

$$m_{i,\,opt} = (i - 1)/(i + 1) \qquad (i = 3,5,7, \ldots)$$

and the relative intensity of the light emerging after i passages:

$$A_{i,\,opt}/A_0 = 4(i - 1)^{i-1}/(i + 1)^{i+1}$$

The optimum reflectivity and intensity for various numbers of passages are given in Table 2.

The intensity drops extremely fast with the number of passages, but this is the price at which larger retardations are achieved. The tests presently described were done with mirrors of about 70% reflectivity and 30% transmission. With a 100-w zircon concentrated light source, a 5461 Å monochromatic interference filter, and 30-in. focal length of condenser and collector lenses, the exposure time needed for the seventh passage with Microfile Panchromatic film was 2 min.

Experimental Procedure

To avoid the very high diffusion produced by unwanted multiple reflections on the faces of the tape, the tape and mirrors were immersed in silicone oil of neighboring refractive index. The equipment constructed for pulling axially and twisting the tape and for adjusting the tilt of the mirrors is shown in Fig. 6. The tape ends are clamped in split end blocks B allowing good alignment. The end blocks are pinned to heads H_1, H_2 which are screwed into the fixed and movable cross bars of a small straining frame, but can be turned about the tape axis to provide any amount of twist. The lower head has a ball joint J which is lightly clamped between conical sockets at the lower end of a long tank of 2-in. square cross section, so that the lower head can be twisted while the tank remains immovably supported by the straining frame (support not shown). The upper part of the tank is wider and has glass windows W. Inside the windows are the partially reflecting mirrors M held in brass frames. Each frame is supported at three points, through fine adjusting screws. Corresponding screws of the two frames are in alignment and have opposite threads so that a common rotation moves the mirrors in opposed directions. The screws pass through rubber seals and the tank is filled with silicone oil.

The model tape was cast of cold setting epoxy resin C-4[8] to a thickness of 0.0112 in. and a width of 1 in. For the first tests, the width was trimmed to 0.875 in. and later to 0.705 in. giving a width-to-thickness ratio b/d of 78 and 63, respectively. Measurements of the optical and mechanical constants showed the existence of a pronounced creep in this epoxy resin of an older type. The variation of the stress-optical coefficient C_σ was quite strong, was higher and lasted longer under constant load than at constant strain, and was affected by temperature changes even of a few degrees. Fortunately, the modulus E varied in a similar way, so that the ratio E/C_σ, needed in the calculations, showed a much smaller change with time. Between 2 and 60 min of loading, the value of E/C_σ changed from about 5350 to 5000 fringes $\times$ ϵ/in. under constant load, and approximately also at constant strain.

A beam-compensation method was used. A horizontal C.R. 39 beam subjected to pure bending was placed just outside the tank on the camera side. The displacement of the parallel beam fringes from their normal position gave directly the retardation which was accumulated on the multiple passages through the model. This procedure would be exact if throughout the tape thickness the direction of the principal stresses were constant and parallel to those in the beam, as happens for the regions near the edges of the tape, and for the regions of zero average stress. The approximation should be particularly good at high applied axial loads which produce large stresses σ_z. Unexpectedly, the fringes appeared very clearly over the whole width of the tape in almost all tests, even with low or zero applied load, and the photoelastically calculated

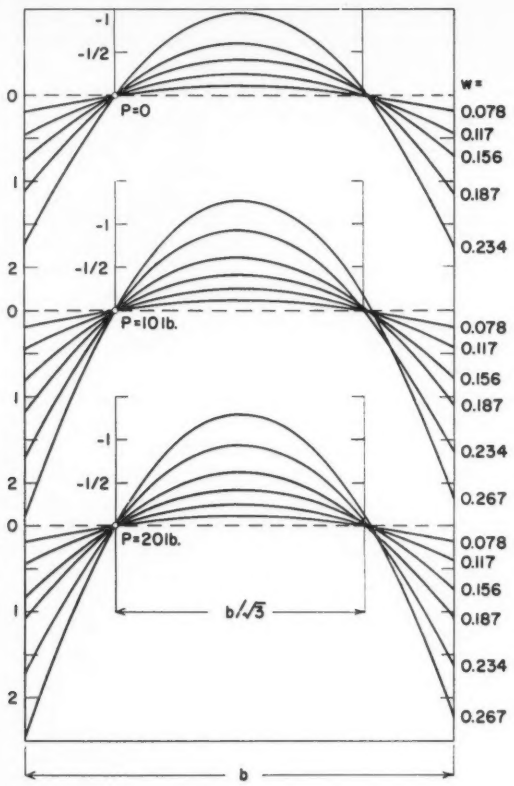

Fig. 9—Shape of photoelastic curves at various twists and axial loads. b:d = 78

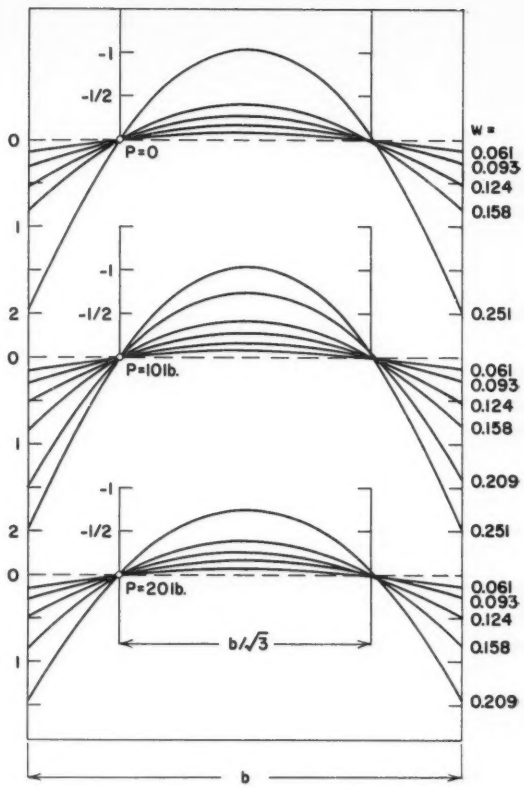

Fig. 10—Shape of photoelastic curves at various twists and axial loads. b:d = 63

stresses agree extremely well with the σ_z stress distribution of the preceding analysis. This seems to indicate that the total rotational effects are much smaller than was originally expected.

Tests Results

Photographs of the fringe pattern after seven passages through the 0.0112-in. thick tape were taken at twists up to $w = 0.267$ (one turn in 23.2 widths) and at the axial pulls from 0 to 20 lb at each twist. At the higher twists, some pull had to be applied to prevent buckling. Typical photographs are shown in Figs. 7 and 8, for tapes with a ratio b/d equal to 78 and 63, respectively. The tape is seen on the upper third and lower quarter of each picture, and the superimposed bent-beam compensator is in the middle, protruding on both sides of the tape. The curved fringes of the beam compensator, referred to the lines obtained by joining the straight beam fringes showing beyond the tape, provide directly the variation of birefringence in the tape.

The ratio of the full height of the curve segment for the entire width b to the height of the segment for $b/\sqrt{3}$ (see inset of Fig. 11) was calculated for all fringes. It was found to be remarkably close to 3 for all twists and axial pulls, thus showing that the fringes are very closely parabolic. Furthermore, it was found that the depth f of the parabolic segment changes with the twist w but is almost completely unaffected by variations in axial pull. These parabolas grouped by the value of the applied load are shown in Figs. 9 and 10 for the two tapes of width 0.875 and 0.705 in. It should be made clear that all curves of the same nominal load do not pass through the same point at $b/\sqrt{3}$ of the width where σ_{z0} is zero, though they pass very close to it. In Figs. 9 and 10 the curves were shifted vertically so as to pass through the same point of zero σ_{z0} to the left of the axis (left end of $b/\sqrt{3}$ width), but were not altered in any other respect.

The only significant quantity varying parabolically across the width of the tape is the average stress σ_{z0} or the average strain ϵ_{z0}. Since they result from a twist which remains constant during the test the strain ϵ_{z0} is constant and the stress σ_{z0} suffers relaxation and decreases with time. Accordingly, it would appear preferable to write the basic photoelastic relation in terms of average principal strains in the plane of the wave front:

$$N = 7d\ (\epsilon_{z0} - \epsilon_y)/C_\epsilon \qquad (14)$$

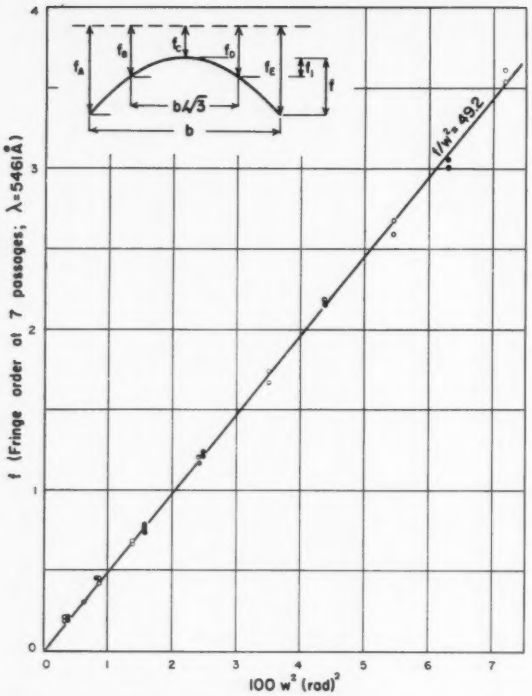

Fig. 11—Plot of height of parabolic fringe vs. square of twist

where

$$C_\epsilon = (1 + \nu)\, C_\sigma/E \qquad (15)$$

and $7d$ is the optical path of seven passages through the tape. Since the average stress σ_y is effectively zero throughout the tape, it follows that $\epsilon_y = -\nu\epsilon_{z0}$ and with (15)

$$N = 7(1 + \nu)\epsilon_{z0}d/C_\sigma = 7\epsilon_{z0}dE/C_\sigma \qquad (16)$$

But the quantity E/C_σ, known also as figure of merit, varies much less than C_σ during creep or relaxation, and ϵ_{z0} is constant. This is the great advantage of (16) over the corresponding stress optical relation which involves the strongly varying σ_{z0} and C_σ. The difference f of fringe order between edge and axis of the tape can be written in terms of the corresponding difference $\Delta\epsilon_{z0}$ of the strains

$$f = 7d\Delta\epsilon_{z0}E/C_\sigma$$

With (4′) giving $\Delta\epsilon_{z0} = {}^1/_8\, w^2$, it follows:

$$f = {}^7/_8\, w^2Ed/C_\sigma$$

or

$$f/w^2 = {}^7/_8\, d(E/C_\sigma) \qquad (17)$$

With an average value of E/C_0 equal to about 5100 fringes $\times$ ϵ/in. and $d = 0.0112$ in., eq (17) gives

$$f/w^2 = 50.0 \text{ fringes/(radian)}^2$$

As can be seen in Fig. 11, the experimental values of f/w^2 are all very close to the theoretical, except perhaps for very small twists where the measured quantities are small and the relative error large. The results of f against w^2 for both tapes fall remarkably well on a straight line through the origin, with slope 49.2 fringes $\times$ ϵ/in.

The complicated situation arising from creep under mixed boundary conditions is apparent in this problem. The axial pull was constant during each test; hence, as far as σ_p is concerned, the tape was creeping under constant load with a resulting increase of birefringence with time. On the contrary, the constant applied twist resulted in relaxation of the tape under constant strain ϵ_{z0} and γ_{yz}, with a corresponding decrease in the birefringence due to them. Even with linear laws of mechanical and optical creep and relaxation, the intensity of the resulting birefringence at each point changes with time and the principal optical directions tend to come closer to the longitudinal tape direction (z-axis). However, the long duration of each test allowed the fast changes to take place and the phenomenon to reach relative steadiness and uniformity. The complete phenomenon is not easily described. As an approximation supported by the experimental results, it can be said that the depth of the parabolas is due to constant straining, which is characterized by small and rapid relaxation resulting in small errors. On the contrary, the parallel displacement of the fringes is due to a constant σ_p and is subject to more pronounced and longer creep, resulting in the greater position errors of the parabolas.

Conclusion

The photoelastic results show no indication of any unusual effect at the points with strong rotation or any difference of behavior between points with strong or weak rotation. The shape of the fringes matches extremely well the parabolic distribution of the σ_{z0} stresses or ϵ_{z0} strains. It can be concluded also that the approximate analysis of the stresses in the twisted tape is substantiated by the experimental results. The reason for the absence of appreciably rotational effects will be the subject of further study.

References

1. *Timoshenko, S., "Strength of Materials," Van Nostrand, Vol. II 3rd ed., 286–291 (1956).*
2. *Timoshenko, S., "Theory of Elastic Stability," McGraw-Hill (1936).*
3. *Mindlin, R. D., and Goodman, L. E., "The Optical Equations of Three-Dimensional Photoelasticity," Jnl. Applied Phys., 20, No. 1, 89–95 (January 1949).*
4. *Drucker, D. C., and Mindlin, R. D., "Stress Analysis by Three-Dimensional Photoelastic Methods," Ibid., 11, No. 11, 724–732 (November 1940).*
5. *Mindlin, R. D., Jnl. Applied Mech., 8, A187 (1941).*
6. *Post, D., "Isochromatic Fringe Sharpening and Fringe Multiplication in Photoelasticity," Proc., SESA, XII, No. 2, 143–356 (1955).*
7. *Mylonas, C., "The Optical System of Polariscopes as Used in Photoelasticity," Jnl. Sci. Instr., 25, 77–87 (March 1948).*
8. *D'Agostino J., Drucker, D. C., Liu, C. K., and Mylonas, C., "Epoxy Adhesives and Casting Resins as Photoelastic Plastics," Proc., SESA, XII No. 2, 123–128 (1955).*

Influence of Breadth in Bars with Reinforced Circular Holes Under Tension

Photoelastic investigation of stress distribution in epoxy-resin bars includes various proportions of circular reinforcements and different widths of bars

by Heihachi Shimada

ABSTRACT—This paper reports stress distributions in epoxy-resin bars with reinforced circular holes under tension. The holes were reinforced by bonding aluminum rings to the bars inside the holes. The stress distributions were determined photoelastically.

Various proportions of circular reinforcements and different widths of bars were investigated under pure tension. Stress distributions were determined in the epoxy-resin part of the bar, and the maximum shear stresses were given special attention. The relation between maximum shear stress and the width of the bar was determined, and the ranges for which the theoretical solution for an infinite bar approximates that for a finite bar were defined.

Nomenclature

$1/\lambda$	$= b/R_2$.
b	= half the width of the bar.
d	= width of the reinforcement.
h	= thickness of bar.
n	$= R_2/R_1$.
R_1	= inner radius of the reinforcement.
R_2	= outer radius of the reinforcement.
p	= uniform axial stress.
ν	= poisson's ratio.
μ	= modulus of rigidity of epoxy resin.
μ_1	= modulus of rigidity of aluminum.
τ_m	= maximum shear stress at the edge of the reinforced hole.
σ_x, σ_y	= normal stresses, (x, y) coordinates.
$\sigma_r, \sigma_\theta, \tau_r\sigma_\theta$	= stress components of (r, θ) coordinates.
r, θ	= polar coordinates with origin at the center of the hole.

Heihachi Shimada is associated with Department of Mechanical Engineering, Tohoku University, Sendai, Japan.

Paper was presented by title at the 1959 SESA Annual Meeting held in Detroit, Mich., on October 21–23.

Introduction

The problem of reinforced circular holes is one that occurs frequently in the design of access holes or openings on airplane wings and fuselages for passing piping and electrical wiring to the various compartments. Much time has been devoted to the analysis of such openings. Timoshenko[1] developed an approximate analysis for reinforcement around a circular hole in a tension field. Sezawa and Kubo,[2] Sobrero[3] and Gurney[4] continued this work. Reissner and Morduchow[5] developed a general solution for the reinforcement of a circular hole for various type of loadings. The Taylor Model Basin[6] published the results of an experimental study of the influence of reinforcements for various types of openings subjected to uniform tension. Heller[7] experimentally tested various types of circular holes in bending with shear. Theoretical investigations for holes in infinite plates were discussed in references 8, 9, and 10.

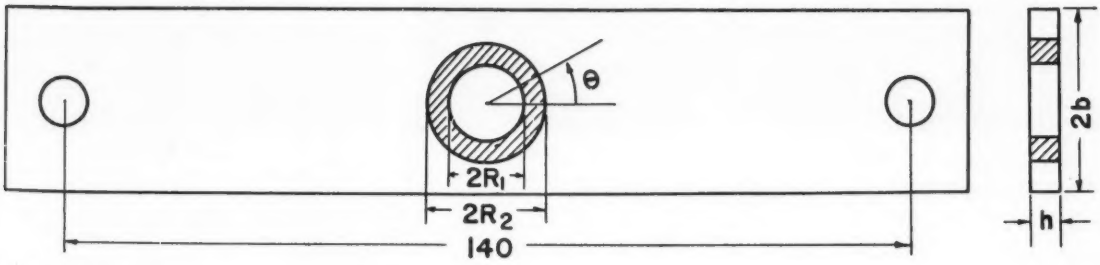

Fig. 1—Test piece

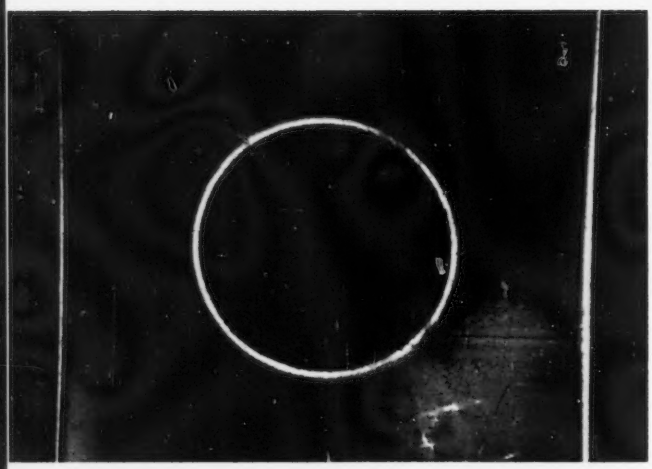

Fig. 2—Isochromatic fringes of the test piece under no load

The experimental investigations conducted previously used the same material for the reinforcement and for the plate or web. This paper is devoted to the effect of a reinforced circular cutout in a "finite bar," which was made of epoxy resin with the hole reinforced with an aluminum ring, subjected to pure tension. The observations were made in a simple polariscope. It was the purpose of this paper to study data from photoelastic experiments with composite models, which had a systematic variation in the ratio of the diameter of the hole to the width of the bar and a systematic variation in the degree of reinforcement. This study included a check on the mathematical solution which is limited to the small circular hole.

Model Construction and Test Procedure

The resin used for the bar was epoxy resin KT-102 (made in Japan). The reinforcements were made of aluminum, and the aluminum was bonded to the epoxy resin with Araldite 121, which sets at room temperature.[11] Very small initial stresses were introduced by bonding. This is shown in Fig. 2. The shapes and dimensions of the models used are shown in Fig. 1 and in Table 1 and 2. To eliminate the error of each test piece, two procedures were followed. The first procedure was selected to investigate the influence of the width of the bar in models with the same reinforcement. After the first test, the width of the specimen was reduced by machining. Thus, the specimen was tested first with maximum width and, then, with successively smaller widths. The second procedure was selected to determine the influence of varying degrees of reinforcement in models of the same width. In this case, the specimen was tested first with a solid circular plate filling the hole completely. Then tests were conducted with successively thinner circular rings for reinforcement.

Figure 3 shows a part of the isochromatic fringe pattern of the test pieces. The retardations were

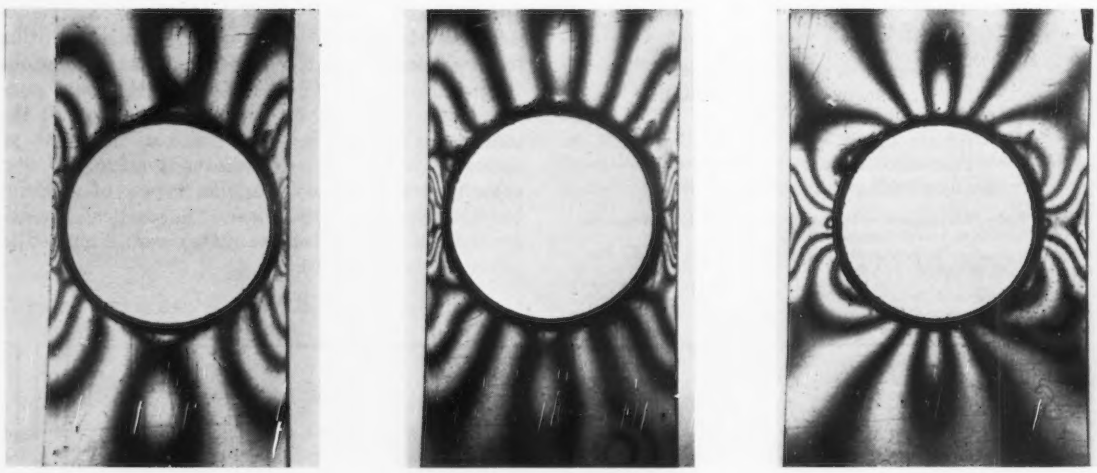

$1/\lambda = b/R_2 = 1.07$ $1/\lambda = b/R_2 = 1.14$ $1/\lambda = b/R_2 = 1.43$

Fig. 3—Isochromatic fringes of the first procedure at n = 1.067

TABLE 1—DIMENSIONS AND CONSTANTS OF MODELS

No.	R_1, mm	R_2, mm	$n = R_2/R_1$	h, mm	2b, mm	μ, kg/mm²	μ_1, kg/mm²
1	6.50	7.50	1.076	5.83	40.00, 30.00, 24.01, 20.00, 16.00, 15.50	122	2700
2	4.50	5.00	1.111	5.82	35.00, 30.00, 24.00, 18.00, 12.00, 11.00	122	2700
3	4.50	5.00	1.111	5.85	20.00	120	2690
4	3.50	4.00	1.143	5.87	20.00	120	2690
5	3.00	3.50	1.166	5.85	30.00, 20.00, 18.00, 12.00	120	2690
6	2.50	3.00	1.200	5.82	30.00, 24.00, 18.00, 12.00, 8.00, 7.00	122	2690
7	5.00	6.00	1.200	5.91	30.00, 20.00	121	2690
8	4.00	5.00	1.250	6.06	30.00, 20.00, 11.00	121	2690
9	3.00	4.00	1.333	5.96	20.00	120	2690
10	5.00	7.00	1.400	6.03	20.00	121	2690
11	3.00	5.00	1.667	6.02	30.00, 20.00, 16.00, 12.00	121	2690
12	4.00	7.00	1.750	5.98	20.00	121	2690
13	2.00	4.00	2.000	5.82	20.00, 12.00, 10.00	118	2690
14	0	4.00	∞	5.80	40.00, 32.00, 24.00, 16.00	124	2690
15	0	6.00	∞	5.83	20.00	124	2690
16	0	9.00	∞	5.78	20.00	124	2690

TABLE 2—DIMENSIONS AND CONSTANTS OF MODELS

No.	R_1, mm	R_2, mm	$n = R_2/R_1$	h, mm	2b, mm	μ, kg/mm²	μ_1, kg/mm²
17	0, 0.50, 1.00, 2.00	4.00	∞, 8, 4, 2	6.02	40.00	124	2690
18	0, 0.50, 1.00, 2.00	4.00	∞, 8, 4, 2	6.03	32.00	122	2690
19	0, 0.50, 1.00, 2.00	4.00	∞, 8, 4, 2	6.00	24.00	122	2700
20	0, 0.50, 1.00, 2.00	4.00	∞, 8, 4, 2	6.01	16.00	124	2690
21	0, 0.75, 1.50, 3.00	6.00	∞, 8, 4, 2	6.04	20.00	124	2690
22	0, 1.125, 2.25, 4.50	9.00	∞, 8, 4, 2	6.00	20.00	121	2690

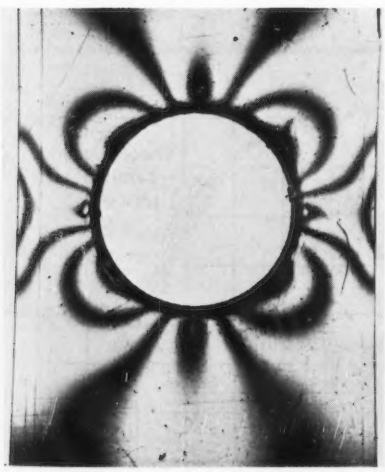

$1/\lambda = b/R_2 = 1.71$

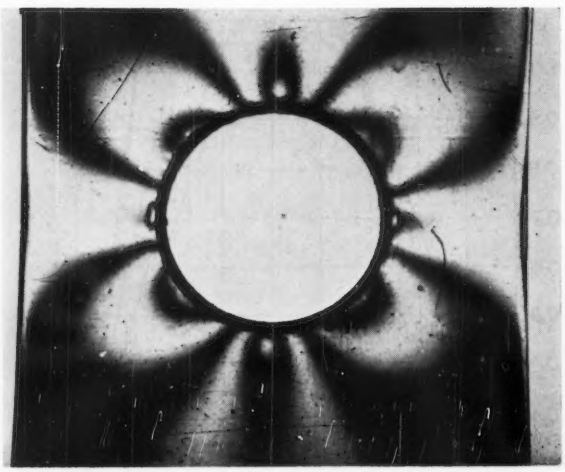

$1/\lambda = b/R_2 = 2.14$

measured from the isochromatic fringes. Fractional measurements were made by the Tardy method where necessary. The experiments were conducted with specimens designed so that the conditions in the "test" area were not influenced by the end-loading conditions.

Stresses in Tension Bars with Reinforced Holes

Figures 4(a) and 4(b) show the values of the ratio τ_m/p around the reinforced hole at the boundary in the epoxy resin for a series of n and $1/\lambda = b/R_2$. In this case $\mu/\mu_1 = 1/22$. In these figures, the broken lines give the theoretical values for an infinite bar with the same size reinforced hole. This solution is from Sawin.[10] At $n = 1.11$, when $1/\lambda$ decreased, the maximum value of τ_m increased and the point of maximum value of τ_m moved nearer $\theta = 90$ deg. At $n = 2$, when $1/\lambda$ decreased, the maximum values of τ_m did not change and the location of the maximum value of τ_m did not change. It is seen that the behavior of τ_m at the boundary of the reinforced hole changes with n.

Figure 5 shows a part of the stress distribution in the epoxy resin. In this figure, the "x" and the broken line give the theoretical values for an infinite bar with the same reinforcement.

Influence of Breadth of Bar

To study the influence of the width of the bar, the maximum values of τ_m/p around the reinforced hole boundary, shown in Fig. 6, are considered. Again $\mu/\mu_1 = 1/22$. This figure shows the experimental maximum values of τ_m for a series of values n from 1.067 to ∞ for various values of $1/\lambda$. The values for $1/\lambda = \infty$ are theoretical. For $n \geqq 1.25$, the maximum values of τ_m are almost constant over the full range of $1/\lambda$. For $n < 1.25$, the maximum value of τ_m increases as $1/\lambda$ approaches 1.

Figure 7 shows the location of the maximum values of τ_m. It can be seen that the location is constant in the same cases for which the value of τ_m is constant in Fig. 6.

Influence of the Breadth of the Reinforcement

Figure 8 shows the maximum values of τ_m/p for a series of values of $1/\lambda$ for values of $1/n$ from 0 to 1. The values for $1/n = 1$ are known values. For $1/n \leqq 0.80$ ($n \geqq 1.25$), τ_m/p is the same line, because as shown in Fig. 6, τ_m/p is independent of λ when $n \geqq 1.25$. However, for $1/n > 0.80$, the maximum τ_m/p increases as $1/\lambda$ decreases.

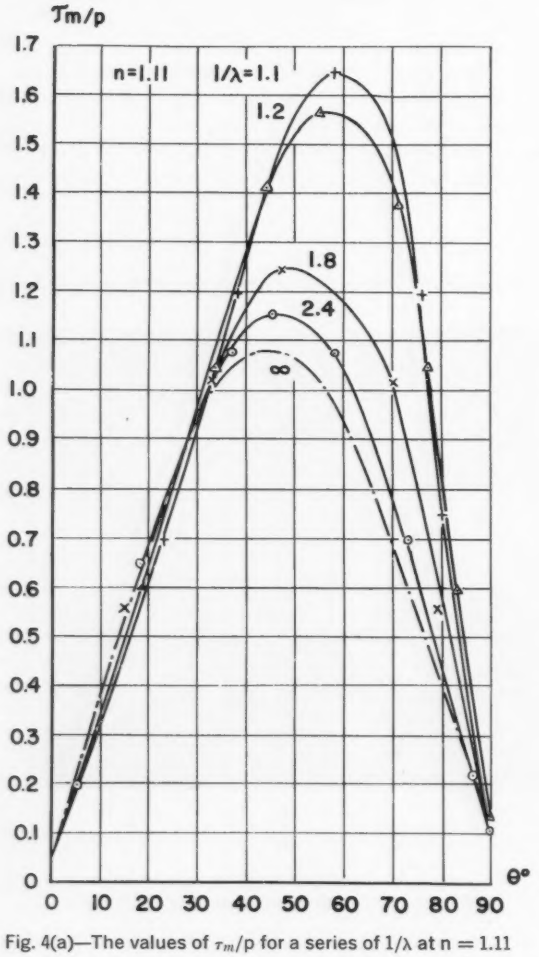

Fig. 4(a)—The values of τ_m/p for a series of $1/\lambda$ at n = 1.11

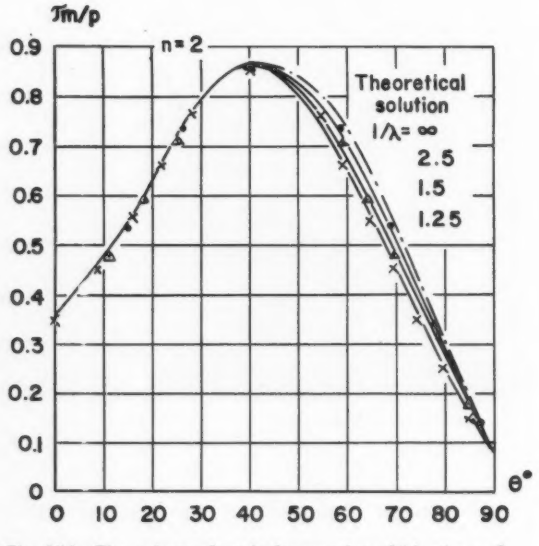

Fig. 4(b)—The values of $\tau m/p$ for a series of $1/\lambda$ at n = 2

Conclusion

Stresses were studied photoelastically in bars with reinforced circular holes for which the reinforcing material had a higher modulus of rigidity than the photoelastic material. In this experiment, the influence of the width of bar was studied, and it was established that the width of the bar influenced the maximum shear stress when $n < 1.25$. When $n \geqq 1.25$, the stresses in bars with the reinforced circular hole used here were the same as those given by the theoretical solution for an infinite plate.

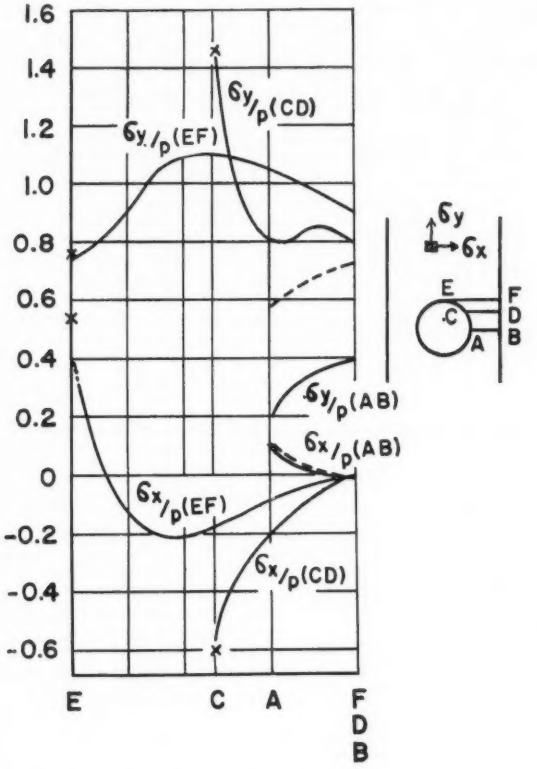

Fig. 5—Normal stresses in epoxy resin

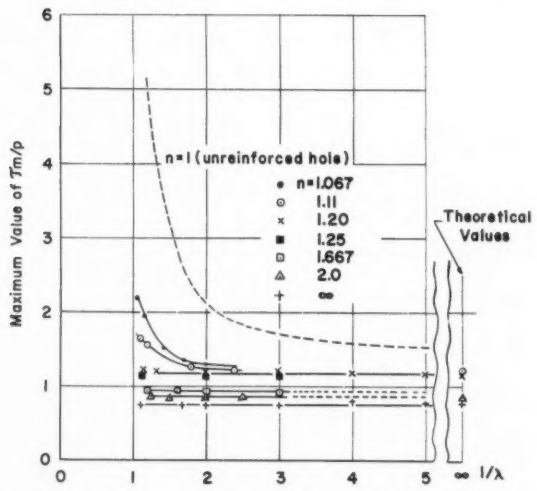

Fig. 6—Maximum values of τ_m/p for $1/\lambda$ (influence of the breadth of bars)

Acknowledgments

The author wishes to express his thanks to Prof. Emeritus S. Higuchi of the Tohoku University for his advice and encouragement. Appreciation is also expressed to Prof. F. Numachi for his generous support and to Prof. O. Tamate for useful discussion.

Continued

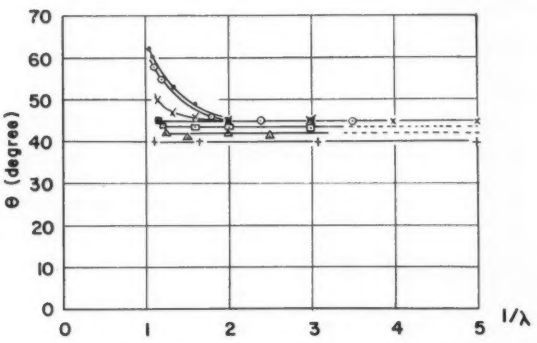

Fig. 7—Point of the maximum values of τ_m/p for a series of n

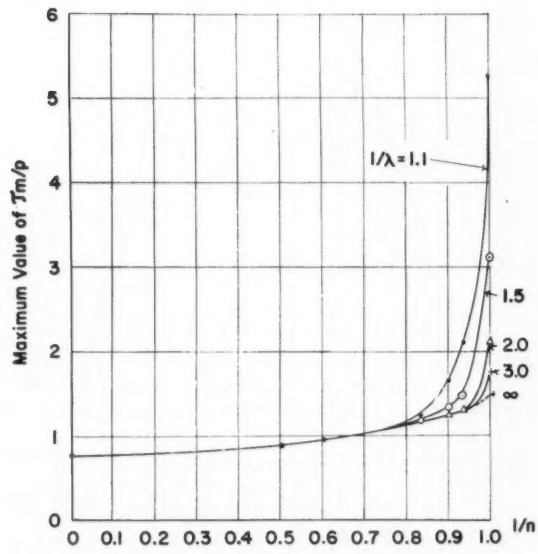

Fig. 8—Maximum values of τ_m/p for $1/n$ (influence of the breadth of reinforcement)

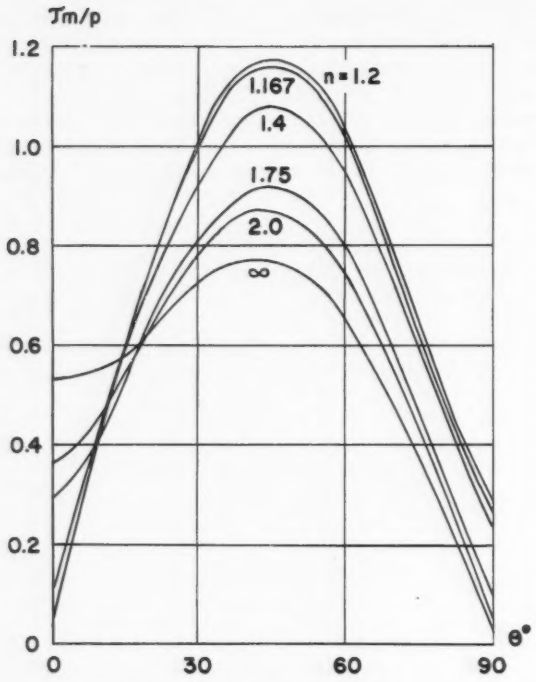

Fig. 9—Theoretical values of τ_m/p around the bonding boundary

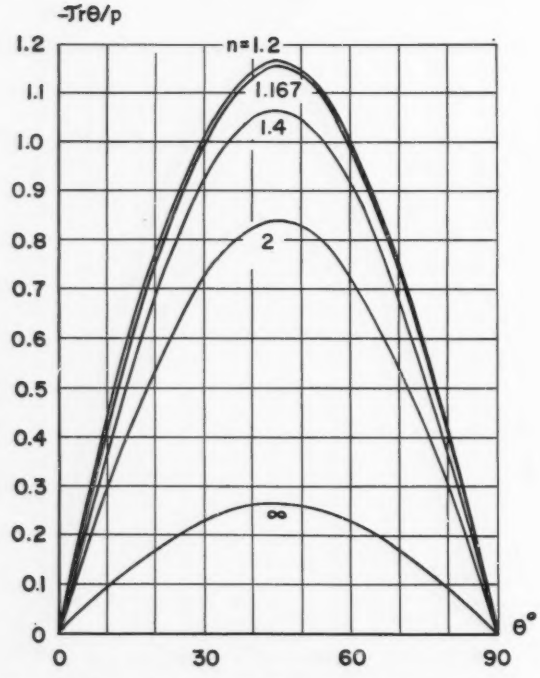

Fig. 10—Theoretical values of $\tau_{r\theta}/p$ around the bonding boundary

Continued

References

1. Timoshenko, S., "On the Stresses in a Flat Plate with a Circular Hole," J. Franklin In t., 197 (1924).

2. Sezawa, K., and Kubo, K., "Stresses in Plate with Flanged Circular Hole," Tokyo Impe. Univ. Aero. Res. Inst. Rep., 7 (1932).

3. Sobrero, L., "Sollecitazioni Elastiche di un Sistema Piano con Foro Rinforzato," Memorie della Classe di Scienze Fisiche, Matematiche e Naturali, 10, No. 4 (1939).

4. Gurney, C., "An Analysis of the Stresses in a Flat Plate with a Reinforced Circular Hole under Edge Forces," Aero. Res. Comit. R&M, No. 1834, London (1938).

5. Reissner, H., and Morduchow, M., "Reinforced Circular Cutouts in Plane Sheet," Nati. Advi. Comit. Aero. Tech. Note, No. 1852, Washington (April 1949).

6. "The Effect of Openings on the Ultimate Tensile Strength of Flat Plates," U. S. Exp. Model Basin, Rep. No. 446, Washington (March 1938).

7. Heller, S. R., "Reinforced Circular Holes in Bending with Shear," SNAME Trans., 60 p. 124 (1952).

8. Levy, S., McPherson, A. E., and Smith, F. C., "Reinforcement of a Small Circular Hole in a Sheet under Tension," J. Appl. Mech., 15, 160 (June 1948).

9. Beskin, L., "Strengthening of Circular Holes in Plates Under Edge Loads," ASME Trans. (1944).

10. Sawin, G. N., "Spannungserhöhung am Rande von Lochern," p. 254, Veb Verlag Technik, Berlin (1956).

11. Shimada, H., "Photoelastic Investigation of Stresses in Composite Models with Notches and Holes," Brit. J. Appl. Phys., 91, No. 1 (1958).

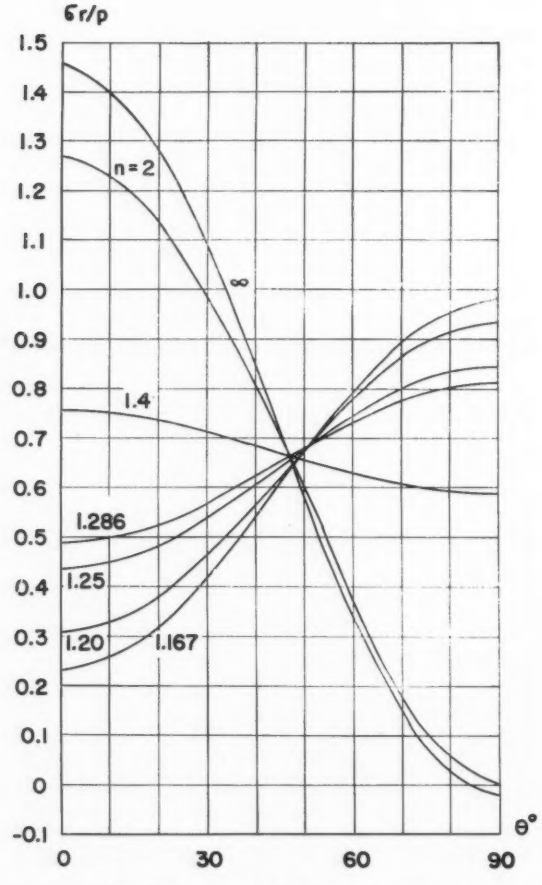

Fig. 11—Theoretical values of σ_r/p around the bonding boundary

APPENDIX

The following theoretical solution for a reinforced circular hole in an infinite plate under tension was given by Sawin.[10]

$$\sigma_r = \frac{p}{2}\left[\left(1 - \frac{1}{2}\beta_{-1}\cdot\frac{R_2^2}{r^2}\right) + \left(1 - 2\alpha_{-1}\cdot\frac{R_2^2}{r^2} - \frac{3}{2}\beta_{-3}\frac{R_2^4}{r^4}\right)\cos 2\theta\right],$$

$$\sigma_\theta = \frac{p}{2}\left[\left(1 + \frac{1}{2}\beta_{-1}\cdot\frac{R_2^2}{r^2}\right) - \left(1 - \frac{3}{2}\beta_{-3}\cdot\frac{R_2^4}{r^4}\right)\cos 2\theta\right],$$

$$\tau_{r\theta} = -\frac{p}{2}\left(1 + \alpha_{-1}\cdot\frac{R_2^2}{r^2} + \frac{3}{2}\beta_{-3}\cdot\frac{R_2^4}{r^4}\right)\sin 2\theta\Big],$$

$$\beta_{-1} = 2 - \frac{2(1+\kappa)}{2\left(\frac{\mu}{\mu_1} - 1\right) - n^2\left[\left(\frac{\mu}{\mu_1} - 1\right) - \left(1 + \kappa_1\frac{\mu}{\mu_1}\right)\right]},$$

$$\beta_{-3} = -2 + \frac{2(1+\kappa)}{D_1}\left[\left(\frac{\mu}{\mu_1} - 1\right)(4n^6 - 7n^4 + 4n^2 - 1) + n^4(n^4 - 1)\left(1 + \kappa_1\frac{\mu}{\mu_1}\right)\right]$$

$$\alpha_{-1} = 2 - \frac{2(1+\kappa)}{D_1}\left[\left(\frac{\mu}{\mu_1} - 1\right)(3n^6 - 6n^4 + 4n^2 - 1) + n^6(n^2 - 1)\left(1 + \kappa_1\frac{\mu}{\mu_1}\right)\right]$$

$$D_1 = \left(\kappa + \frac{\mu}{\mu_1}\right)n^2\left[\left(\frac{\mu}{\mu_1} - 1\right)(3n^4 - 6n^2 + 4 + n^6\left(1 + \kappa_1\frac{\mu}{\mu_1}\right)\right] + \left(\kappa_1\frac{\mu}{\mu_1} - \kappa\right)\left[\left(\frac{\mu}{\mu_1} - 1\right) + n^6\left(1 + \kappa_1\frac{\mu}{\mu_1}\right)\right]$$

$$\kappa = \frac{3 - \nu}{1 + \nu}, \quad \kappa_1 = \frac{3 - \nu_1}{1 + \nu_1}.$$

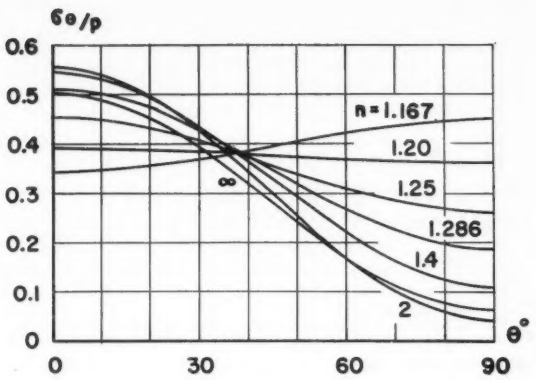

Fig. 12—Theoretical values of σ_θ/p around the bonding boundary

For reinforcement with aluminum, $\kappa = 1.94$, $\kappa_1 = 2.08$, $\mu/\mu_1 = 1/22$.

The distributions of stresses around the reinforced hole in the epoxy resin are shown in Figs. 9, 10, 11, and 12.

On the Transverse-strain Sensitivity of Foil Gages

The conditions under which the transverse-strain sensitivity of a foil gage filament may assume small positive or negative values are discussed in this technical note

by J. H. Meier

Introduction

The end loops of flat-grid wire strain gages cause some transverse gage sensitivity; it can readily be calculated from the grid configuration.[1, 2] Foil gages are designed with extra-large end connections having low resistance in order to reduce transverse-strain sensitivity. Yet, many foil gages have some transverse sensitivity; in some cases, it even is negative.[3] The cause of the transverse sensitivity in foil gages must thus be different from the cause in flat-grid wire gages and it must be suspected that individual foil-gage elements, which are parallel to the gage axis, have transverse sensitivity in themselves.

J. H. Meier is associated with General Engineering Laboratory, General Electric Co., Schenectady, N. Y.

Nomenclature

- σ = stress; positive if tensile.
- ϵ = strain; positive if elongation.
- ν = Poisson's ratio of filament material.
- E = modulus of elasticity of filament material.
- φ = transmission efficiency of transverse strain from base material to element of foil gage.
- ρ_0 = specific resistance of unstrained filament material.

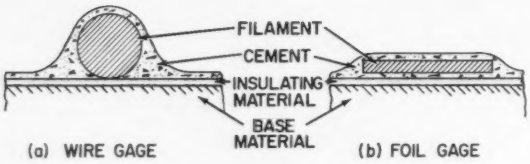

Fig. 1—Cross section through individual strain-gage elements

ρ = specific resistance of filament material while under strain.
R = resistance.
ΔR = change in resistance due to strain; positive if increasing.
V = volume.
ΔV = change in volume; positive if increasing.
m = factor defined by hypothesis of eq 5.

Subscripts:
a refers to direction of the filament axis.
n refers to direction transverse to the filament axis.
p refers to direction perpendicular to the surface.
s refers to shape.
v refers to volume.

Analysis

Consider an individual wire filament (Fig. 1a): The axial strain ϵ_a is imposed near the very ends by shear stresses in the bond. In a uniform stress field, the bond does not transmit any strains from the base material to the wire over most of the length. On the other hand, transmission of transverse strain from the base material to the wire would require "squeezing" of the filament all along its length; however, the bond is not nearly stiff enough in relation to the wire. Transverse deformation of the wire is thus dictated by axial strain and Poisson's ratio, i.e.,

$$\epsilon_n = -\nu\epsilon_a \tag{1}$$

Similarly, the strain in the direction perpendicular to the surface is

$$\epsilon_p = -\nu\epsilon_a \tag{2}$$

The change in shape thus accounts for a strain sensitivity of a wire filament as defined by

$$(\Delta R/R)_s = \epsilon_a - \epsilon_n - \epsilon_p = \epsilon_a(1 + 2\nu) \tag{3}$$

Filaments of commercial wire gages have a strain sensitivity of about 2.0, i.e.,

$$\frac{\Delta R/R}{\epsilon_a} \sim 2.0 \tag{4}$$

As a matter of fact, in many cases, the strain sensitivity of the wire is deliberately selected as 2.0 in order to obtain the same gage factor in the elastic and in the plastic range.

Since in the elastic range $(1 + 2\nu) \sim 1.6$, it must be concluded that the specific resistance of the filament must change due to strain. The effect of this change in specific resistance is to account for the difference in the actual strain sensitivity of the filament and $(1 + 2\nu)$. In the plastic range, however, the gage factor of all filaments approaches 2.0 which indeed corresponds to $(1 + 2\nu)$ for the plastic range. The mechanism of the change in specific resistance of the filament in the elastic range has not been explained. An explanation fitting the circumstances would be to relate the change in specific resistance to the change in volume by the hypothesis:

$$\rho = \rho_0(1 + m\Delta V/V) = \rho_0\{1 + m(\epsilon_a + \epsilon_n + \epsilon_p)\} \tag{5}$$

For a single wire filament the contribution to strain sensitivity from the volume change alone would thus be given by

$$(\Delta R/R)_v = \epsilon_a m(1 - 2\nu) \tag{6}$$

The total sensitivity of the filament can thus be expressed as

$$\frac{\Delta R/R}{\epsilon_a} = \frac{(\Delta R/R)_s}{\epsilon_a} + \frac{(\Delta R/R)_v}{\epsilon_a} = 1 + 2\nu + m(1 - 2\nu) \tag{7}$$

For $m = 1$, $(\Delta R/R)/\epsilon_a$ becomes 2.0. Hence, if the hypothesis of eq 5 does hold, m must be in the vicinity of 1.0 for the most common wire-gage filaments.

Now consider an element of a foil gage under transverse strain ϵ_n in the base material (Fig. 1b); in order to establish transverse sensitivity we set $\epsilon_a = 0$. Transmission of the transverse strain ϵ_n from base material to filament may not be perfect, because the cement has to "squeeze" the filament all along its length. Transmission of transverse strain would be expected to be much better, however, than in the case of a wire filament. Let us assume a transverse strain $\varphi\epsilon_n$ imposed on the filament, where φ is the bonding efficiency for transverse strains.

The filament is in a state of plane stress and the stresses corresponding to the strains $\epsilon_a = 0$ and ϵ_n are

$$\sigma_a = \varphi\nu\epsilon_n E/(1 - \nu^2) \tag{8}$$

and

$$\sigma_n = \varphi\epsilon_n E/(1 - \nu^2)$$

From these stresses and the fact that $\sigma_p = 0$, the filament strain in the direction perpendicular to its plane is calculated as

$$\epsilon_p = -\varphi\nu\epsilon_n/(1 - \nu) \tag{9}$$

The change in shape thus accounts for a filament sensitivity defined by:

$$(\Delta R/R)_s = -\varphi\epsilon_n(1 - 2\nu)/(1 - \nu) \tag{10}$$

and the change in volume is responsible for

$$(\Delta R/R)_v = m\varphi\epsilon_n(1 - 2\nu)/(1 - \nu) \tag{11}$$

From the total of eqs 10 and 11, the filament sensitivity to transverse strains can thus be calculated as

$$\frac{\Delta R/R}{\epsilon_n} = (m - 1)\varphi(1 - 2\nu)/(1 - \nu) \tag{12}$$

For $m = 1$, the transverse-strain sensitivity would be expected to be zero. However, for small deviations of m from 1.0, the transverse-strain sensitivity of a foil gage filament may assume small positive or negative values.

References

1. Baumberger, R., and Hines, F., "Practical Reduction Formulas for Use on Bonded Wire Strain Gages in Two-Dimensional Stress Fields," Proc., SESA, Vol. II, No. I, *113–147 (1944).*

2. Handbook for Experimental Stress Analysis, *John Wiley and Sons, pp. 408–411 (1950).*

3. Stein, Peter, "Transverse Sensitivity Effects on Transducers," Strain Gage Readings, *2, N. 6, p. 38 (February–March 1960).*

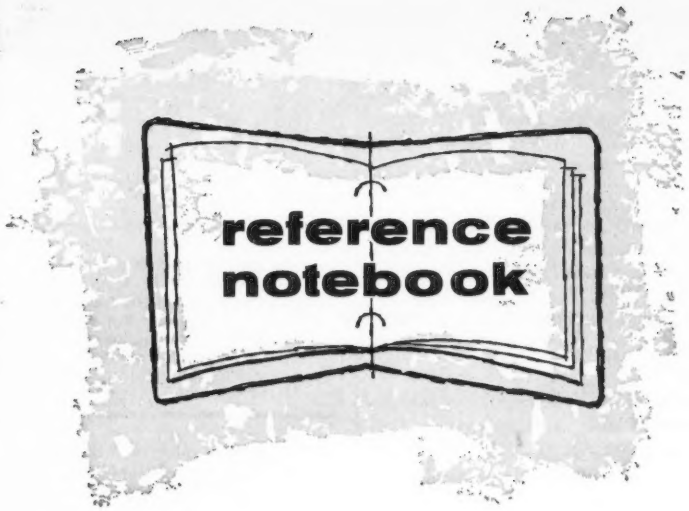

SELECTED BIBLIOGRAPHY

Brittle Coatings

*Chronological Compilation From 1932 to February 1961**

Continued from page 20A of June 1961 issue of Experimental Mechanics

Evans, F. G., Lissner, H. R., and Pedersen, H. E.
"Deformation Studies of the Femur Under Dynamic Vertical Loading." *The Anatomical Record*, Vol. 101, No. 2, 1948, pp. 225–241.

Halgren, J. A., Sheridan, S. A., and Goodman, B.
"Practical Applications of Stress Analysis at I.H." *The Iron Age*, March 1949, pp. 77–80.

Pedersen, H. E., Evans, F. G., and Lissner, H. R.
"Deformation Studies of the Femur Under Various Loadings and Orientations." *The Anatomical Record*, Vol. 103, No. 2, 1949, pp. 159–185.

Almen, J. O.
"Fatigue Weakness of Surfaces." *Product Engineering*, 1950, pp. 118–140.

Hetenyi, M.
"Brittle Models and Brittle Coatings." *Handbook of Experimental Stress Analysis*, Chap. 14, 1950, pp. 636.

Franck, R. J.
"How to Develop Cast Products." *Foundry*, June 1951.

Ellis, Greer
"Brittle Coatings for Stress Analysis." *The Tool Engineer*, June, July 1951.

Durelli, A. J., and Okubo, S.
"Heat Treated Brittle Coating Increases Sensitivity." *Product Engineering*, Dec. 1951.

Tokarcik, A. G., and Polzin, M. H.
"Quantitative Evaluation of Residual Stresses by the Stresscoat Drilling Technique." *Proc. Soc. Exp. Stress Analysis*, Vol. 9, No. 2, 1951, pp. 195–207.

Evans, F. G., Pedersen, H. E., and Lissner, H. R.
"The Role of Tensile Stress in the Mechanism of Femoral Fractures." *The Jour. of Bone and Joint Surgery*, Vol. 33-A, No. 2, 1951, pp. 485–501.

Stokey, W. F.
"Elastic and Creep Properties of Stresscoat." *Proc. Soc. Exp. Stress Analysis*, Vol. 10, No. 1, 1952, pp. 179–186.

Eisenhardt, G. H., and Walsh, W. L.
"Stress Analysis of a Pipe Wrench." *Proc. Soc. Exp. Stress Analysis*, Vol. 10, No. 1, 1952, pp. 227–234.

Durelli, A. J., and Tsao, C. H.
"Discussion of Paper Entitled Quantitative Evaluation of Residual Stresses by the Stresscoat Drilling Technique" (Vol. 9, No. 2, pp. 195). *Proc. Soc. Exp. Stress Analysis*, Vol. 10, No. 1, 1952, pp. 237–242.

Schmittner, W. G.
"Determination of Centrifugal Stresses in a Turbosupercharger Impeller by Means of Stresscoat." *Proc. Soc. Exp. Stress Analysis*, Vol. 10, No. 2, 1952, pp. 9–22.

Mould, R. E.
"The Behavior of Glass Bottles Under Impact." *Journal of the American Ceramic Society*, 1952, pp. 230–235.

Fisher, J. C.
"Why Metals Are Weak." *General Electric Review*, July 1953, pp. 15–18.

Durelli, A. J., and Okubo, S.
"Influence of Strain Gradient on Brittle Coating Sensitivity." *Product Engineering*, Jan. 1953.

Polzin, M. H.
"Performance Evaluation of a Magnesium Alloy Truck Wheel." *Proc. Soc. Exp. Stress Analysis*, Vol. 11, No. 1, 1953, pp. 65–80.

Durelli, A. J., and Tsao, C. H.
"Use of Brittle Coating Data in Stress Analysis." *Proc. Soc. Exp. Stress Analysis*, Vol. 11, No. 1, 1953, pp. 181–196.

Hartman, J. B., and Benner, R. E.
"Stress Analysis in Design." *Machine Design*, March 1954, pp. 135–148; April 1954, pp. 186–196; June 1954, pp. 144–150; July 1954, pp. 139–146.

Durelli, A. J., and Okubo, S.
"Crack Density Studies in Stresscoat." *Proc. Soc. Exp. Stress Analysis*, Vol. 11, No. 2, 1954, pp. 153–160.

Various Magnaflux Stresscoat Instruction Manuals (1937–1954).

Durelli, A. J., and Phillips, E. A.
"Criteria for Selecting Experimental Stress Analysis Methods." *Product Engineering*, January 1955.

Magnaflux Corporation
"Principles of Stresscoat, a Manual for Use with the Brittle Coating Stress Analysis Method." 1955.

Durelli, A. J., Okubo, S., and Jacobson, R. H.
"Study of Some Properties of Stresscoat." *Proceedings of the Society for Experimental Stress Analysis*, Vol. 12, No. 2, 1955, pp. 55–76.

R. H. Herrmann,
"Nondestructive Testing Aids Casting Design." *Foundry*, March 1955.

Plan Now to Attend

First International Congress and 1961 Exposition

November 1-3

Hotel New Yorker New York, N. Y.

* This chronological bibliography is based on a compilation prepared by the Magnaflux Corp., subsidiary of General Mills, Chicago, Ill.

Patton, W. G.
"Stress Analysis Takes Guesswork Out of Product Performance." *Iron Age*, September 1955.

Beckham, J. W.
"Use of Experimental Stress Analysis as a Casting Design Tool." *AFS Transactions*, Vol. 63, 1955.

Holliday, F. R.
"Stress Tests Helped Design Chrysler's Die-Cast Aluminum Torque Converter Housings." *SAE Journal*, October 1955, pp. 17–20.

Magnaflux Corporation
"Correction Before Rejection Cuts Scrap Losses." *Magnafacts*, Vol. 4, No. 1, 1956, pp. 6–7.

Gray, Allen G.
"What You Can Do About Metal Fatigue." *Steel, Jan. 16, 1956*, pp. 68–72.

Durelli, A. J., Jacobson, R. H., and Okubo, S.
"Further Studies of Properties of Stresscoat." *Society for Experimental Stress Analysis*, Vol. 13, No. 1, 1956, pp. 35–53.

Staats, H. N., and Baranowski, S. J.
"Calibrated Porcelain Enamel Coatings." *The American Ceramic Society Bulletin*, Vol. 35, No. 4, April 15, 1956.

Durelli, A. J., and Dally, J. W.
"Some Properties of Stresscoat Under Dynamic Loading." *Proceedings of the Society for Experimental Stress Analysis*, Vol. 15, No. 1, 1957, pp. 43–56.

Ward, D. J., and Grotto, L. A.
"Analyzing Tractor Design for Stresses." *SAE Journal*, October 1957.

Eckert, E. J.
"Aids for Designing Better Tractor Parts." *SAE Journal*, January 1958, pp. 28–29.

Stern, F. B.
"A New Method for Measuring High-Temperature Stresses with Strain-Sensitive Ceramic-Base Coatings." *Machine Design*, May 29, 1958, pp. 147–149.

Dally, J. W., Durelli, A. J., and Parks, V. J.
"Further Studies of Properties of Stresscoat Under Dynamic Loading." *Proceedings Society for Experimental Stress Analysis*, Vol. 15, No. 2, 1958, pp. 57–66.

Durelli, A. J., Phillips, E. A., and Tsao, C. H.
"Introduction to the Theoretical and Experimental Analysis of Stress and Strain." McGraw-Hill, New York, 1958.

Ravitch, L. H.
"Some Applications of Stress Analysis Techniques in Improving Casting Designs." *General Motors Engineering Journal*, Vol. 5, No. 4, October-November-December 1958, pp. 22–27.

Durelli, A. J., Dally, J. W., and Riley, W. F.
"Stress and Strength Studies on Turbine Blade Attachments." *Proceedings of the SESA*, Vol. XVI, No. 1, 1958, pp. 171–182.

Design Engineering
"Stresscoat Spray for Stress Analysis." November 1958, pp. 59–61.

Hiltbold, Von F.
"Spannungslackanalyse von Bauteilen." *Schweizer Archiv für angewandte Wissenschaft und Technik*, Issue 2, Vol. 24, 1958.

Stern, F. B.
"Ceramic Coatings for Experimental Stress Analysis." ASTM Special Technical Publication No. 230, 1958, pp. 97–105.

Magnaflux Corporation
"Redesign Provides Lighter Products of Aluminum at Alcoa's Cleveland Development Division, Stress Analysis with Stresscoat Gives Quick Answers." *Magnafacts*, Vol. 7, No. 2, 1959, pp. 4–5.

Beckham, J. W.
"Redesign of Trailer Castings Offers Greater Strength, Lighter Weight." *Trailer/Body Builders*, November 1959.

Dally, J. W., and Durelli, A. J.
"Stress Analysis of a Reactor Head Closure." *Proceedings of the SESA*, Vol. XVII, No. 2, 1960, pp. 71–86.

Steidel, R. F., Jr., and Makerov, C. E.
"The Tensile Properties of Some Engineering Materials at Moderate Rates of Strain." *ASTM Bulletin*, July 1960, pp. 57–58.

Allen, L. B.
"Determination of the Effect of Annealing on Residual Molding Stresses." *SPE Journal*, July 1960, pp. 713–716.

Durelli, A. J., Dally, J. W., and Morse, S.
"Experimental Study of Large-diameter Thin-wall Pressure Vessels." EXPERIMENTAL MECHANICS, February 1961, pp. 33–42.

You'll find
READER INFORMATION CARD
on Page 17A

A Note to AUTHORS

- All papers and technical notes should conform to style requirements set forth in the manual "An SESA Paper" and the "Authors' Check List." Obtain your copies from SESA Headquarters, 21 Bridge Square, Westport, Conn.
- All papers and technical notes must be reviewed and accepted by the Papers and Proceedings Committee in order to qualify for publication.
- Authors must provide a statement that their articles have not been previously published nor submitted for publication elsewhere.
- One original and two copies of the manuscript, complete and carefully typed with double spacing and wide margins, are to be sent to: Roscoe Guernsey, Chairman, Papers and Proceedings Committee, General Electric Co., Bldg. 37, Room 669, Schenectady 5, N. Y.
- Authors should state their affiliation, title or position and mailing address.
- All papers, but not necessarily technical notes, must be presented at a Society Meeting either orally or by title.
- If at all possible, length of text should not exceed 4000 words; a technical note should not contain more than 750 words.
- Illustrations must be clearly drawn in ink and should not be larger than $8\frac{1}{2}$ x 11 in. "Guided" lettering should be used at all times and should be large enough to be legible when reduced. Photographs must be sharp, glossy prints. A separate list of captions for all figures must be typed with double spacing. The figure number and author's name should appear on the back of each illustration.
- Reprints may be ordered from SESA Headquarters.

sesa news

Technical Variety Featured at Philadelphia Spring Meeting

Well Organized Activities Contribute to Success

From the welcoming address by Acting-president Irwin Vigness on Wednesday morning to the parting farewells on Friday evening, SESA meeting-goers experienced a varied technical program studded with enough social and educational activities to completely fill the three-day Spring Meeting at Philadelphia, Pa. The May 10–12 affair was run quietly and efficiently by the Delaware Valley Section at the Benjamin Franklin Hotel.

Technical sessions were held each morning and afternoon except Thursday afternoon when the plant tours were made. The numerous other activities included a seminar introducing the use of computers, two plant tours, a cocktail social hour and a banquet complete with dinner, some unusual entertainment and a most interesting guest speaker. Among the special activities were the authors' breakfasts held each morning to help organize the presentations of the day, the meetings of the standing committees, the Standing Committee's Dinner and the meeting of the Executive Committee. Educational exhibits were on view continually in the busy registration area. Two attractive tours were arranged as part of the Ladies' Program. In detail, all the events added up to a valuable and pleasant opportunity to hear and to meet the leaders in the field of experimental mechanics, to make new acquaintances and to greet old friends.

Starting point and information center for activities at the 1961 Spring Meeting was the registration area located in the exhibits foyer next to auditorium. Henry Cook is signing in William Pittman of Baltimore, Md.

Technical Sessions Offer Variety

The main event of the Spring Meeting was the series of five technical sessions, each one consisting of four original contributions made by the authors. In general, outstanding papers were presented in a number of varied applications ranging from fundamental investigations to practical tests. Some of these covered new developments in techniques, in instruments and instrumentation; the evaluation of instrumental accuracy; the study of different physical effects and conditions: residual stress, internal strain, fatigue, thermal fatigue, elasticity, plasticity; analyses of machine and structural components; and others not readily classifiable. While variety proved to be an attractive feature in itself, efficient programming and good acoustics also helped to make the

First event of the day, the authors' breakfasts were held each morning. Typical group shows speakers with local and national officers before the opening session

Acting-president Irwin Vigness greeted the opening-day audience with "Words of Welcome." He also reported on recent important developments within the Society

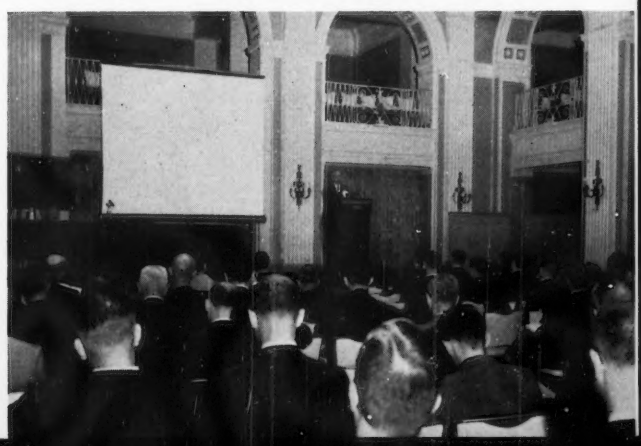

When SESA friends get together, the topic may be stress analysis, or—the weather! Left to right are Treasurer William M. Murray, Clarence Smith, Honorary Member Frank Tatnall, George West, Meeting Chairman Stewart Sennet and Acting-president Vigness

Many may wonder what kind of tale Chairman Roscoe Guernsey was telling the Papers and Proceedings Committee to warrant such undivided attention. However, the group reviewed acceptance standards and many other details

sessions a success. A welcome pause came each morning in the form of coffee breaks.

One of the featured attractions aroused considerable interest among the members present. This was the theme session devoted to "Experimental Mechanics at High Temperature." Present day emphasis on problems relating to high-speed aircraft, rockets, satellites and to nuclear engineering and design, have focused attention on high-temperature measurements and testing. As a result, the timely theme session was very popular.

Seminar Introduces Computer Fundamentals

A valuable addition to the meeting program was the Wednesday evening seminar introducing the use of computers to those unfamiliar with their operation. While engineering students are today being introduced to these machines, many earlier graduates never had this opportunity to take advantage of their possibilities. The one-evening seminar represented a distinct service to these men. Two speakers presented the basic philosophy, the fundamentals of programming and the type of problems to which the two kinds—digital and antilog—are best suited. The actual solution of a specific problem was then discussed using slides. Paul Sage of General Electric's Missile and Space Vehicle Department discussed the digital computer and Keith Parthemore of DuPont's Mechanical Research Laboratory presented the antilog type.

Representatives from various sections met to discuss affairs of the Local Sections Committee. Left to right they are M. M. Lemcoe, G. A. Butz, Chairman C. R. Smith, F. S. Bogardus, J. G. Willmot, C. W. Bert, G. W. West

Plant Tours Visit Unusual Installations

Two places of unusual interest were visited Thursday afternoon when enthusiastic groups were led on guided tours of the Eddystone Power Station of the Philadelphia Electric Co. and the Space Sciences Laboratory of the General Electric Co. Some of the members present were well aware of the intricate engineering problems that

Excellent turnout helped to make Standing Committees' Dinner a great success. Committeemen received official thanks for their work during past year

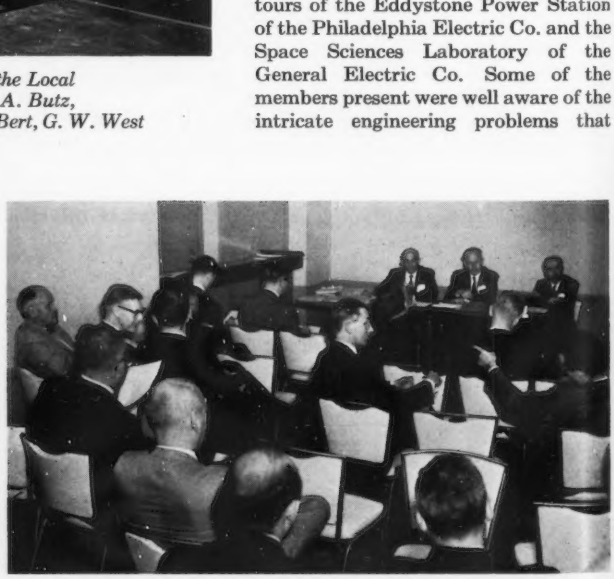

Hard-working Executive Committee heard reports from standing committees, deliberated over SESA policies until early morning hours, then reconvened later. Shown is J. C. New making a point while Executive Secretary Bonney Rossi, Acting-president Vigness and Treasurer Murray listen at table

Evening seminar on computers aroused considerable interest. R. J. Stone, chairman of the event, is shown introducing Keith Parthemore of DuPont's Mechanical Research Laboratory and Paul Sage of General Electric's Missile and Space Vehicle Division

Happy group ready to embark on one of the two plant tours Thursday afternoon, May 11. Both tours proved popular and informative

had to be solved to make the Eddystone Station the world's outstanding high-temperature and high-pressure power generating steam plant. For those who were not, the trip proved to be a real education in the latest design problems of power engineering. The G.E. tour was very popular, having been completely sold out the day before. Only 40 persons of citizenship status were permitted to view the advanced techniques employed in man's conquest of space.

Social hour just before banquet on Thursday evening was a good time to make or renew personal contacts. Doing just that are, from left, Past-president B. J. Lazan, Honorary Member M. M. Frocht, Executive Secretary Rossi and Past-president E. Wenk, Jr.

Social Hour Precedes Banquet

After the plant tours, the cocktail hour in the Betsy Ross Room seemed quite appropriate, putting everyone in just the right mood of gaiety to enjoy the banquet. With appetites thus sharpened, the banquet dinner was relished by all. Frank Tatnall, well known as the first Honorary Member of the SESA, acted as Master of Ceremonies and, as usual, turned in a superb performance. Acting on a bright idea the day before, he managed to persuade some of the ladies present to bedeck themselves in costumes of the Gay Nineties and to present songs and dances of the period. With the addition of Clarence Smith, top-hatted and caned, the effect was hilarious—as it was intended to be. After a short monologue and a few other extemporaneous skits, the speaker of the evening, Francis F. Bradshaw, was introduced.

Dr. Bradshaw Reviews Management Crisis

A long-time student as well as a

Banquet featured several notable events—including an excellent dinner—to make the occasion one to remember. Seated at head table are (l to r) Executive Secretary Rossi, Mrs. Sennet, Delaware Valley Section Chairman L. Moffett, Acting-president Vigness, Master of Ceremonies Tatnall, Guest Speaker Francis Bradshaw, Meeting Chairman Sennet, Mrs. Vigness, Treasurer Murray, Mrs. Moffett, and J. Scott, banquet chairman

Strictly amateur chorus of the spontaneous "Gay Nineties Revue" was inspired by Mr. Tatnall. Performers are (l to r) Mrs. C. C. Perry, Mrs. S. Sennet, Clarence Smith, Mrs. B. Anderson, Mrs. J. Hovanesian

professional consultant in business management, Dr. Bradshaw is presently chairman of the board of the management consulting firm, Richardson, Bellows, Henry & Co. of New York City. The title of his address was "Influences of the Cold War on Relations Between Technical People and Management." In a most interesting and original approach, Dr. Bradshaw indicated the weaknesses in the management functions of Western economic culture and suggested some ways in which the deficiencies could be corrected.

Women's Program Provides Diversion

While members and guests were busily engaged in technical activities, their wives found time to leave the Hotel on a junket of their own. On Wednesday, the ladies took a trip around historical Philadelphia, visiting Independence Hall, Betsy Ross House and other places of early American fame. On Thursday, after a "brunch," the group embarked on a tour of Longwood Gardens, the world-famous estate of the late P. S. DuPont. Located in nearby Chester County, Longwood, with its arboretum, flower gardens, fountains, pools and immense conservatory, proved to be an enjoyable experience even though activities were somewhat restricted by bad weather.

The attractive Lafayette Room was placed at the disposal of the ladies during their stay. Each morning, a coffee-hour was held prior to starting off on the trip for the day.

Local Arrangements Committee

The committee responsible for the success of the meeting was under the direction of Chairman Stewart Sennet. Lou Moffett was vice chairman, while Bruce Sutton handled general arrangements. Other members were H. W. Cook, publicity and membership; H. M. Owens, technical sessions; J. Scott, banquet; R. Stiles, plant tours; A. Shore, educational exhibits; J. Stone, seminar; and P. Swartz, finance. The women's activities were conducted by Mrs. S. Sennet, Mrs. L. Moffett and Mrs. B. Sutton.

Mr. Tatnall as MC produced several amusing skits from his "bag of tricks." Here he is in a serious moment listening to Guest Speaker Bradshaw. Dr. Bradshaw gave an enlightening talk on management problems

Delaware Valley Section members and wives who took part in running the 1961 Spring Meeting. Standing (l to r): P. Swartz, J. Scott, R. Stiles, B. Sutton, H. Owens, A. Shore, S. Sennet, L. Moffett, L. Mains, H. Cook, and J. Walmsley. Seated: C. Moyer, Mrs. Sennet, Mrs. Moffett, F. Tatnall and R. Stone

International Congress Program to Include Special Stress-analysis Lectures

Specially prepared lecture sessions on stress-analysis techniques, aimed at fulfilling a twofold purpose, will play a prominent part in the program of the First International Congress on Experimental Mechanics, to be held November 1–3 at the Hotel New Yorker, New York City. Scheduled for Wednesday evening, November 1, two lecture-discussion periods will be conducted concurrently.

One session is intended for undergraduate engineering students and for graduates who need to review fundamentals. The purpose is to help interested individuals to take a step beyond the elementary college course and to open the door to a better understanding of the theory and application of modern stress-analysis techniques. Topics under discussion will include wire strain gages, photoelasticity and brittle coatings. No fee will be charged, but those attending must be registered for the Congress. Students from local colleges are welcome and may attend by registering in advance at a nominal fee, presently set at one dollar.

The other session will cover some advanced phases of modern stress analysis embodied in the application of the new types of gages, including high-temperature and semiconductor gages. One or more outstanding speakers will be engaged to discuss various experiences investigators have had in connection with the use of these gages. In presenting the subject matter, emphasis will be placed on the most recently developed information, not as yet widely circulated. As in the elementary session, no extra fee will be charged, but the attendees, both members and nonmembers, must be duly registered for the Congress.

The First International Congress on Experimental Mechanics will feature as its main event a series of morning and afternoon technical sessions. Each session will be devoted to the presentation of papers by authors who have made some significant contribution in the field of stress analysis or in experimental mechanics. This year a number of investigators from other nations have accepted invitations to discuss their original findings or to report on the type of work being done in their respective countries.

The Metropolitan New York Section members, the hosts for this year's Congress, are now in the process of arranging the details for a complete program of technical and social activities. Some of these include such events as a banquet featuring a foreign dignitary who will bring an important message from abroad, an attractive ladies program, authors' breakfasts, committee meetings, and a full exposition of equipment, materials and instruments used in the field.

section reports

Hudson-Mohawk

Semiconductor Strain Gages

On Apr. 27, 1961, the *Hudson-Mohawk* Section held its sixth and last meeting of the 1960–61 season. The meeting took place in the Freshman Dining Hall at Rensselaer Polytechnic Institute in Troy. Chairman Robert E. Weigle presided. Fifty members and guests attended.

Following a pleasant and well-attended dinner, Dr. Weigle turned the meeting over to Charles S. Duckwald to conduct the election of the officers and the advisory board for the 1961–62 season. Nominated and elected were: John P. Purtell, Watervliet Arsenal—chairman; Thomas Slot, General Electric Co.—vice-chairman; Daniel Post, Rensselaer Polytechnic Institute—secretary; Louis H. Estabrook, General Electric Co.—treasurer; Robert E. Weigle, Watervliet Arsenal, Gabriel Horvay, General Electric Co., Lewis T. Assini, Rensselaer Polytechnic Inst., Samuel Levy, General Electric Co.—Advisory Board.

After the election, D. J. DeMichele introduced the speaker, Warren P. Mason, who spoke on "Recent Developments in Semiconductor Strain Gages." Dr. Mason heads the Mechanics Research Group of the Mathematical Research Department, Bell Telephone Laboratories, Murray Hill, N. J.

In his talk, Dr. Mason discussed the piezoresistive properties of certain semiconducting materials and how these properties have been utilized in strain gages. It was noted that this type of gage is attractive because of its high gage factor compared to conventional gages. The effect of doping of the crystal, temperature and crystallographic orientation of the sensitivity was discussed. Finally some examples were given of the application of semiconductor elements to practical strain measurement problems. Among these were force transducers, torque transducers, accelerometers and strain rosettes. A lively question period followed the talk, indicative of the great interest created in these simple devices.

(Reported by T. Slot for the Hudson-Mohawk Section)

Milwaukee

Strain-gage Techniques

The April meeting of the *Milwaukee* Section was held at the ESM building on Apr. 27, 1961. Thirty-four members were present. This was the final meeting of the 1960–61 year.

The Treasurer's report was presented and approved. Officers for the 1961–62 year were nominated as follows: Chairman—Quentin W. Hein, The Falk Corp.; Vice-chairman—Donald E. Niles, Outboard Marine Research; Secy-Treas.—Robert A. Johns, Belle City Malleable Iron Co.; Director (2 yr)—William Bloedorn, Chain Belt Co. A unanimous ballot was voted.

Bill Bloedorn, retiring chairman, presented the annual Chairman's report. Of prime interest was the announcement that the 1962 annual meeting of the National Society will be held in Milwaukee. Bill was elected Chairman of the Preparations Committee to prepare for the meeting.

James Dorsey, chief engineer of the Strain Gage Division of Baldwin-Lima-Hamilton, spoke on "New Developments in Strain-gage Techniques." He described the types of strain gages available at present and listed precautions which must be observed in their use. He made particular mention of wound gages, temperature compensation, semiconductors, foil gages, and monofilament gages. During the discussion period following the talk, he described methods of gaging highly extensible rubber-like materials. The large number of questions and comments were an indication of the interest shown in Mr. Dorsey's excellent presentation.

(Reported by D. E. Niles for the Milwaukee Section)

Bulletin

Three New Sections Approved

On May 10, 1961, the Executive Committee voted into membership in the SESA three new sections. They are named *Great Salt Lake*, *Pacific Northwest* and *Toronto-Hamilton*. The respective organizing representatives in these areas are Clifford S. Barton, Emmet E. Day and John S. Root.

PIEZORESISTIVE GAGES AT RPI

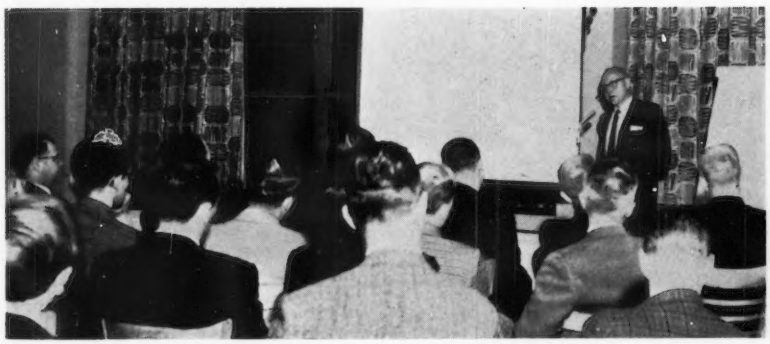

Warren P. Mason addresses the Hudson-Mohawk Section at its April 27 meeting. He spoke on "Recent Developments in Semiconductor Strain Gages"

from the campus

Talbot Laboratory, University of Illinois

ROARK TO RETIRE FROM UNIVERSITY OF WISCONSIN

A man who has given most of his adult life to the study of stress and strain applied to metal and concrete retires from the University of Wisconsin faculty this year.

The man is Raymond J. Roark, professor of engineering mechanics in the UW College of Engineering. He is a long time member of the SESA.

Prof. Roark started out as civil engineer, but his interest in the strength and safety of the structures he had to design as a civil engineer led him into the engineering-mechanics field. He joined the UW engineering-mechanics faculty as an instructor in 1913. After serving as a field artillery captain with U. S. forces in World War I, he returned to teaching. His 41-year teaching and research career at UW was interrupted only briefly by big-game hunting trips to Africa and Indo-China.

Many technical articles on Prof. Roark's research in the field of statics, dynamics, strength of materials and aerodynamics have been published in engineering journals.

Prof. Roark is also the co-author of a textbook, "Mechanics for Engineers: Statics and Dynamics," widely used for many years, and he is the sole author of what is called the engineers' stress-strain bible, entitled "Formulas for Stress and Strain." Three editions of this basic engineering handbook have been published since its first printing in 1938, and Prof. Roark is now working on a 4th edition to incorporate the results of research on present-day stress analysis problems in nuclear power and space technology.

MATERIALS UNDER THERMAL STRESSES

A short course, "Materials Under Thermal Stress" will be given August 27-September 1 by The Pennsylvania State University and will be under the direction of Joseph Marin, professor of engineering mechanics.

The object of the course is to present an intensive treatment of the present state of the art of thermal stress analysis and interpretation. The presentation will be based mainly on information developed within the last five years, some of which has not received general publication.

The course will be presented by S. S. Manson who is chief, Materials and Structures Division, NASA. Lectures will be given each morning while discussion and study will take place in the afternoon. Enrollment is limited.

For further information write to: Engineering Seminars, Conference Center, The Pennsylvania State University, University Park, Pa.

ACADEMIC YEAR INSTITUTES

The Institutes Section of the National Science Foundation was established to provide programs that will enable teachers to obtain a more complete and up-to-date knowledge of new developments in their particular subject-matter fields. Two types of institutes provide training during the academic year—namely, Academic Year and In-service Institutes. The former afford teachers the opportunity to spend a full year in study of subject matter, usually at the graduate level.

In-service Institutes are designed to establish supplementary training programs for some 9000 secondary school teachers of science and mathematics. Participants obtain additional knowledge of subject matter during or after school hours or on Saturdays.

During academic year 1960–61 there are 33 Institutes in operation granting support to approximately 1500 teachers. About 15,000 applications were received by the participating institutions for admission to the program. The budget for the Academic Year Institutes program exceeds nine million dollars a year.

JIM RYAN "AT HOME" AFTER 30 YEARS

James J. Ryan, professor in the Mechanical Engineering Department of the University of Minnesota, on May 22, celebrated the completion of 30 years of service on the staff. Many of his former students and friends visited his office and research laboratory where a special exhibit was arranged to display instruments he has invented and his automotive crash safety equipment.

"Jim" Ryan expressed his satisfaction over having had the opportunity, during the past 30 years, to be of service and thanked all those who have participated in his many activities.

SWRI STRAIN-GAGE CONFERENCE

Members of the 1961 "Strain Gage Techniques" course given under the joint sponsorship of the SESA and Southwest Research Institute, San Antonio, Tex., April 17–21. Standing at the rear are three of the lecturers: (left to right) Peter K. Stein, M. M. Lemcoe and William M. Murray

Three Short Intensive Courses on

STRAIN GAGES & PHOTOELASTICITY

at the DEPARTMENT OF ENGINEERING
UNIVERSITY OF CALIFORNIA AT LOS ANGELES

FOR WHOM INTENDED

These three courses have been designed to present an integrated program on theory and practice, including a review of fundamentals and discussions of some of the latest techniques, especially those suited to high and low temperature strain gage applications. Attention will also be given to instrumentation, which, in many cases, can be used equally well with other kinds of transducers.

The courses are intended primarily for those with a bachelor's (or higher) degree in engineering, physics, or metallurgy. However, in certain cases, experienced technicians without degrees can be expected to gain full benefit.

The material content of the courses, although presented largely from the point of view of the mechanical engineer, has been selected to provide maximum benefit for those who are already skilled in stress analysis but who may have little experience in electrical instrumentation, and likewise for electronics experts who may not be quite so familiar with certain aspects of stress analysis.

STRAIN GAGE LECTURE COURSE

August 21 - 25, 1961 (Monday through Friday)

The first of the two strain gage courses will consist of a series of lectures supplemented with illustrative demonstrations. Some of these lectures have been prepared especially for beginners and consequently are of an elementary nature; however, other lectures of a much more advanced character will also be included in the series. The latter group will contain detailed information, especially relating to high temperature strain gages, which will be useful to those who already possess considerable experience. The content of the course has been selected and organized for maximum benefit to designers, metallurgists, laboratory workers, laboratory supervisors, theoretical stress analysts, and others, who wish to advance their knowledge relating to the uses of strain gages and the techniques which are available for producing optimum results.

Both the theoretical and practical aspects of strain gages themselves, methods of installation, and allied equipment, will be presented in the lectures. Details of strain gage applications for measuring force, torque, bending, shear, and accelerations, will be discussed as well as simple electric circuits for automatic computation of quantities which depend upon the simultaneous observation of strains at more than one location.

The following will be included in the topics which are to be presented:

Basic theory of Wire, Foil, and Semi-Conductor strain gages
Details of gage characteristics
Techniques for installing gages
Mechanical and Electrical aspects of the gage system
Fundamental Laws of Measurement
Electric Circuits for strain gages
Dynamic and Static Strain Measurements
Computing Bridge circuits for direct measurement of quantities depending upon several strains
Stresscoat as an Auxiliary Tool
Measuring systems and instruments
Low-temperature applications of strain gages
High-temperature strain gages and their installation
Commercial Equipment
Rosette analysis and interpretation of observations

STRAIN GAGE LABORATORY COURSE

August 28 - September 1, 1961 (Monday through Friday)

For those who wish to gain personal experience in the installation of gages and the handling of equipment, a second course containing a series of laboratory experiments will be offered. The laboratory program is supplementary to the lecture course. It will consist of a set of projects, each containing one or more experiments, which have been designed to illustrate the topics taken up in the lecture course during the previous week. The following exercises will be included to provide practice in the practical applications of strain gage techniques:

Strain Gage Installation for normal and high temperature applications
Static observations with single and multiple gage bridges
Dynamic strain Measurements
Characteristics and checking of electrical equipment used with strain gages
Strain Rosette Analysis
Characteristics and handling of certain commercial equipment
Measurement of Force, Torque, Bending, and Moments at inaccessible locations

Since the benefits which can be obtained by attendance at the laboratory program depend to a large extent upon an understanding of the underlying theory, registration in the laboratory course will be limited to those who have attended the previous lecture course, or its equivalent in prior years.

INDUSTRIAL PHOTOELASTICITY

(Lectures & Laboratory)

September 5 - 9, 1961 (Tuesday through Saturday)

The course in Industrial Photoelasticity will review the fundamental theory and laboratory techniques related to the classical applications of polarized light for solving stress problems. In addition to this, discussions of some of the most advanced techniques, including Three-Dimensional Photoelasticity and Photoelastic Surface Coatings (PhotoStress), will also be presented.

The course will emphasize the ways in which photoelasticity can be used to solve industrial problems. Attention will also be given to the advantages and limitations of the method and its relation to other experimental techniques with which it may often be combined most effectively.

Tae material will be presented through lectures, demonstrations, and laboratory exercises. Consideration will also be given to the properties and selection of photoelastic materials as well as the specification of equipment required to set up a laboratory. This program has been designed especially for the engineer or metallurgist who has little or no previous knowledge of the subject.

TUITION

The tuition per registrant for each course will be as follows:—

Strain Gage Lecture Course	**$175.00**
Strain Gage Laboratory Course	**$175.00**
Industrial Photoelasticity	**$200.00**

FOR FURTHER INFORMATION, call or write,

ENGINEERING EXTENSION, DEPARTMENT OF ENGINEERING,
Room 6266, ENGINEERING-PHYSICAL SCIENCES BUILDING,
UNIVERSITY OF CALIFORNIA, LOS ANGELES, 24, CALIFORNIA

Telephone — GRanite 3-0971, Extension 369

1961 SESA EXPOSITION

in conjunction with

FIRST INTERNATIONAL CONGRESS ON EXPERIMENTAL MECHANICS

Hotel New Yorker • November 1–3

All on one floor . . . at New York's famous and popular hotel . . . lively exhibits of what's what in experimental mechanics . . . by the who's who in the industry.

Manufacturers of all types of engineering and scientific equipment used in this field are invited to exhibit.

Hundreds of engineers and scientists involved in instrumentation, measuring such mechanical quantities as stress, strain, load, displacement, acceleration, pressure, and vibration, will attend. These men are most directly concerned with specifying, buying and using equipment.

Choice booths now available to fit all budgets.

Be sure to attend!

FOR FURTHER INFORMATION WRITE:

SESA HEADQUARTERS
21 BRIDGE SQUARE
WESTPORT, CONNECTICUT

or circle No. 20 on Readers Information Card